Drought response of *Prunus serotina* in the Netherlands

MSc-Thesis

Paul van Duinhoven

January 2023

WAGENINGEN UNIVERSITY
WAGENINGEN UR

Drought response of *Prunus serotina* in the Netherlands

Paul A. van Duinhoven

January 2023

AV2023-05

FEM 80436

Supervision by:

dr.ir. Jan den Ouden

dr. Ute Sass-Klaassen

Forest Ecology and Forest Management Group

The Author declares

1) That his work is his own and
2) That he has adhered to The Netherlands Code of Conduct for Academic Practice

Contents

Summary

Due to climate change, the suitability of tree species in their current growth sites are subject to change. Since the suitability of present forest tree species are in decline as their climate envelopes shift elsewhere, forest managers in the Netherlands are looking for tree species whose climate envelopes better match the expected future climate.
Among their options is the naturalized exotic tree species *Prunus serotina*. This tree from north America is able to provide high-quality wood in favourable conditions and could be sufficiently adjusted to the expected increased frequency of drought events in the Netherlands.

This study aimed to establish the growth response of *Prunus serotina* to drought events through dendrochronology, and whether this response varied across gradients of soil moisture and shade competition. The hypotheses were that the resistance of *Prunus serotina* to drought is dependent on shade levels, whereas the recovery from drought events would be dependent on soil moisture.

80 *Prunus serotina* trees were sampled across four sites in the Netherlands. Two of these sites featured xeric soils and two of these site featured mesic soils. None of the sampled trees had access to groundwater. The twenty samples taken per site were subdivided among ten dominant and ten codominant trees. Forest basal area measurements, light measurements, DBH measurements and soil profiles were made additionally on these sites. Tree ring widths were measured and analysed for pointer years and their growth responses in selected drought years. Additionally, climate-growth relations were analysed for the full reconstructed growth histories of the sampled *Prunus serotina* trees. These analyses were performed grouped by canopy position and compared to each other. Growth responses to light and shade were analysed through the construction of linear and mixed models.

The results of the analyses showed that *Prunus serotina* are still affected negatively in their growth during drought years, but also benefit from rapid recovery from drought years, even after repetitive drought years. Resistance to drought during the drought year was not conclusively connected to shade gradients. The constructed models pointed towards an influential role for forest basal area competition and sometimes light in general growth, but there was no difference in the resistance response observed between canopy groups. Recovery after drought was observed to be higher on mesic sites than on xeric sites in a fairly clear dichotomy. A dichotomy that was observed more often, such as in less extreme growth-climate correlations on mesic sites.

This study reasserts the positive effect of soil moisture on *Prunus serotina* recovery capability, but fails to provide conclusive evidence on the relation between shade levels and drought resistance, due to mistakes in the sampling design, missing values and conflicting results.
Overall, this study established that *Prunus serotina* can indeed be suitable for an expected climate with an increased frequency of drought events, due to consistently rapid recovery.

1 Introduction

As a result of climate change, the average temperature is increasing worldwide at varied rates. With the temperature, the evapotranspiration that takes place in forested areas is also increasing. (Ouyang. 2021). In the Netherlands, the climate of the period between 1991 and 2020 saw an increase of two extra tropical days (where temperatures exceed 30 ºC) with respect to the previous period of 1981-2010 and the first recorded temperatures exceeding 40 ºC. In the same decades the precipitation deficit in the top 5% driest years had increased by up to 50 mm in comparison to the top 5% of the 1981-2010 period. (KNMI. 2022a). An increased incidence of extreme weather events in temperate areas, means that trees increasingly find themselves under drought stress (Krejza et al., 2021).

Tree species can be more or less resilient depending on their ability to resist drought events and their ability to recover from them. Species are resistant to drought when they are able to prevent the drought from causing damage, and have good recovery when their growth rates after the drought are no less than their pre-drought growth rates.

Responses of trees to resist drought include variation of leaf water potential by closing stomata or shedding leaves entirely (Ryan, 2011). Both these strategies impair the ability of trees to photosynthesize with the consequence that less assimilates are available for physiological processes including defence mechanisms and growth. Trees with a higher hydraulic safety margin, through species adaptation or site conditions, may outcompete trees with lower hydraulic safety margins. These trees are outcompeted because they need to sacrifice assimilation for hydraulic safety more quickly, resulting in them being outgrown and impairing their ability to recover from the reduced growth. In extreme cases this would eventually result in mortality of outcompeted trees through carbon starvation (Sevanto et al., 2014).

An absence of resistance strategies is risky however. Water-stress induced cavitation might destroy the water transport capacity of these trees by cavitation of water transport vessels, which would then cause a risk of death through desiccation. Resilient tree species would be more capable of returning to pre-drought growth rates, providing the damage suffered is not too extensive (McDowell et al. 2008). But when the drought-induced damage to water transport vessels is severe, it is often permanent, resulting in permanent radial growth reduction after the drought until it results in an eventual death (Cailleret et al., 2017).

Since the response of trees to drought events becomes an increasingly important factor for both their survival and growth, their response therefore also affects the functioning of the ecosystem they are a part of and their delivery of ecosystem services (Matthews et al., 2014; DeSoto et al., 2020).

Because the long lifespan of trees means that most trees have settled in or are offspring of trees that have settled in a climate of the past, current tree species composition may no longer be the best fitting species composition relative to their climate envelopes (Morin et al., 2018). In response to this and additional aspects causing stress, such as soil acidification, and given the current tree species composition in Europe, forest managers are looking for exotic provenances and species that would be suitable to integrate to European forests, in accordance with their current and expected climate envelopes, with which to enrich or replace the current species composition (Bussotti et al., 2015; Thuiller et al., 2006).

One exotic species that has already naturalized is the black cherry (*Prunus serotina)*. The black cherry is a pioneer tree species in the Rosaceae family native to North America. The subspecies *Prunus serotina serotina* mainly occurs in the eastern United States and south-eastern Canada. Additional subspecies occur in the southwestern United States, Mexico and Guatemala. It occurred sporadically in primary mixed forests, but became more prevalent in modern secondary forests thanks to its strong pioneer character (Hough, 1960).
When growing in forests, it sometimes occurs in monoculture, but more often grows alongside a wide variety of other light-demanding species, including -but not limited to-: *Robinia pseudoacacia , Betula lenta, Fraxinus americana, Juglans cinerea, Quercus coccinea, Abies balsamea, Populus tremuloides* and *Populus grandidentata*. The fast youth growth of Black cherry means it is usually able to outgrow these species in an even-aged stand where canopy positions become stratified by species (Marquis, 1990). More shade-tolerant species such as *Tilia americana, Acer saccharum* and a variety of bushes are able to continue growing underneath the dominant stratum of black cherry and become codominant if they originate from an older cohort. Black cherry is unable to settle underneath these other species due to its low shade tolerance, but black cherry is able to maintain its presence in older uneven-aged forests by exploiting gaps in the canopy caused by disturbances, such as disease. The vitality of black cherry appears to be impacted more by forest structure than abiotic conditions. (Auclair & Cottam, 1971; Auclair, 1975; Marquis, 1990).
The Black cherry often takes on poor growth forms in the wild, especially when sprouting through vegetative regeneration, but is nonetheless widely cultivated in North-America, due to the high quality of wood this species can produce when their growth form is favourable. The black cherry is capable of exceeding 30 m in height and 150 cm in diameter. It therefore is a tree of significant importance in the managed forests of North America (Hough, 1960). It grows best on mesophytic sites, being indifferent to varying levels of drainage, but suffers on waterlogged sites (Marquis , 1990). Black cherry is also a common species in unmanaged forests that nonetheless underwent change since European settlement. Because Black cherry seed is dispersed by animals such as birds, it is able to settle in forests that have become isolated through the years by fragmentation (Auclair & Cottam. 1971).

Black cherry was initially imported to Europe in 1623 for its aesthetic qualities and was eventually widely planted in the forests of the Netherlands and Belgium during the early twentieth century. This was an assisted settlement with the aims of improving wood production of the species it accompanied by improving litter quality to account for the nutrient poor sandy soils they were planted on (Nyssen, 2011; Vanhellemont et al., 2010). Black cherry has since fallen out of favour with most forest managers due to its potential to become invasive in forest ecosystems on nutrient-poor sandy soils, especially because it hampered the regeneration of other light demanding species such as Scots pine (*Pinus sylvestris*) (Nyssen, 2011; Vanhellemont et al., 2010). Attempts to eradicate black cherry from Dutch forests have proven largely unsuccessful and costly (Vanhellemont et al., 2010). The discussion on the desirability of black cherry in Dutch forests with regards to specific management goals has resurfaced in recent years (Nyssen et al., 2019; Nyssen et al., 2016).

Regardless of this discussion, the suitability of black cherry in the context of the shifting climate in Europe has yet to be established. In contrast, research on the drought response of black cherry has been performed in its native range of North America, where black cherry has shown itself to be susceptible to drought events during the years 1985 and 1995 (Abrams et al., 1998). The response of black cherry was, however, varied and appeared to depend on the evaluated ecotype and the

climate, soil and slope orientation of the sites (Abrams et al., 1992). Lasting growth reduction occurred on riparian sites and xeric ridges, whereas growth reduction was limited in mesic valleys and recovery occurred on barrens (Abrams et al., 1998).
The ecotypes in the European range of black cherry are unlikely to be specifically adapted to drought resistance, since genetic evaluation of black cherries in its European exotic range point towards multiple introductions from the Allegheny Plateau, where a humid continental climate reigns (Pairon et al., 2010). Annual rainfall is significantly higher on the Allegheny plateau, when comparing for example the values in 1990 at around 1000 mm per year (Marquis, 1990) than the around 750 mm per year in the Netherlands (CBS et al., 2020). While the yearly average temperature is similar at 10°C on the Allegheny Plateau versus 11°C in the Netherlands, the average July day temperatures are higher on the Allegheny plateau at 28°C, in comparison to 23°C in the Netherlands (KNMI., 2022a; Marquis, 1990).

In addition to the site and ecotype, drought responses of black cherries in North America seem to be sensitive to variations in exposure of individual trees to sunlight, wherein individuals exposed to full sunlight displayed a larger reduction in growth during drought (Abrams et al., 1992).

From literature it is known that the ecotypes of black cherries in Europe display good growth on sandy soils, outperforming most native pioneer species there (Closset-Kopp et al., 2011). It is also known that black cherry is able to survive for a long time in the understory of early pioneer forests and still responds to opening of the canopy up to 39 years of age (Auclair & Cottam., 1971).
It is not known, however, how this growth performance changes when experiencing drought stress in the European range and whether the response to drought stress is altered by this shade tolerance in the same manner as in North America.

The objective of this research is thus to investigate the growth response of black cherries in the Netherlands to drought stress across a soil moisture and shade gradient.

1.1 Problem statement

The growth response of *Prunus serotina* to drought during the growing season in the Netherlands is currently ambiguous.

1.2 Research questions

1) How does radial growth of *Prunus serotina* change during drought years in comparison to the preceding and following years?
    a) What is the difference in radial growth along a shade gradient during drought years?
    b) What is the difference in radial growth of *Prunus serotina* growing on sandy soils with different water holding capacities during drought years?

1.3 Hypotheses

1. Radial growth is significantly reduced during drought years. The resistance to radial growth reduction is dependent on biotic site factors, whereas recovery is dependent on abiotic site factors.

The expectation is that during drought years the radial growth of black cherries is significantly reduced in comparison to other years, as is the case in the native North American range of black cherry, with resistance to radial growth reduction being dependent on biotic factors such as competition-induced shade and recovery to pre-drought levels of radial growth being dependent on abiotic factors, such as soil moisture. (Abrams et al., 1998; Abrams et al., 1992).

a) Shaded individuals display significantly less radial growth reduction in comparison to fully exposed individuals.

The expectation is that there are significant differences in radial growth along a shade gradient for black cherries. This is based on observations in the native North American range of black cherry (Abrams et al., 1992) and the regulatory effects that a forest climate can have. The hypothesized cause for this difference is that dominant individuals of black cherry are exposed to a non-forest climate with reduced or no shade and therefore higher temperatures and evapotranspiration. While pioneer species are adapted to a non-forest environment, environmental extremes can still grow large enough in these environments to become the limiting factor for growth during drought events. Shaded individuals would therefore be at least partially protected from the heightened temperatures and evapotranspiration, giving them a temporary advantage during extreme droughts, requiring them to be less resistant to drought.

b) Radial growth is significantly lower on xeric sandy soils in comparison to mesic sandy soils.

The expectation is that the reduced capacity of xeric sandy soils to hold rainwater, due to a larger grain size than found in mesic sites, reduces the availability of soil moisture to the local black cherries. This gives the black cherries little headroom to react to droughts, decreasing the resistance to drought stress of these trees, making damage more likely, which can in turn make recovery to usual levels of radial growth more difficult (Desoto et al., 2020). North-American literature also states that black cherries are more vulnerable to drought on xeric sites in its native range, meaning that the black cherry is unsuited to extremes in soil moisture (Abrams et al., 1998; Marquis., 1990).

The combined relationships that result in the given hypotheses are displayed in figure 1. This conceptual model assumes that water availability is the single most limiting factor at play during a drought event, even though events from before a drought year could influence radial growth the subsequent year, such as bud development and carbon storage (Zweifel et al., 2006). SPEI is an indicative value of drought, where in this conceptual model positive values indicate humid conditions and negative values indicate drought conditions.

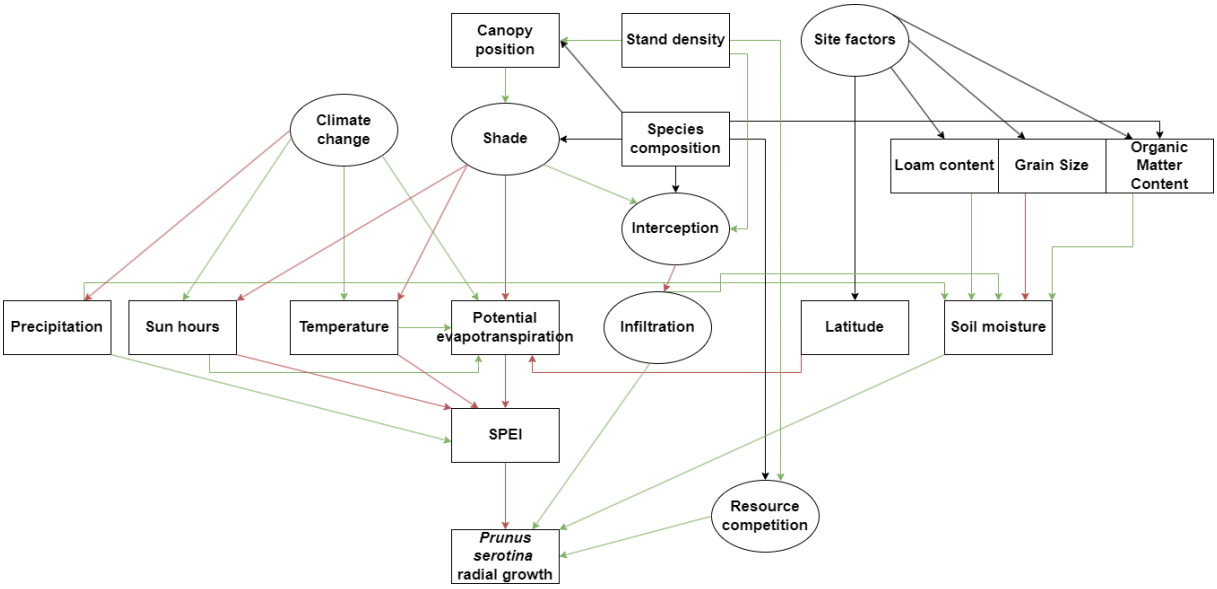

Figure 1: A conceptual model, displaying hypothesized relationships. Rectangular items are values that can be collected or calculated, whereas oval items are mechanisms. Green arrows display positive reinforcement whereas red arrows display negative reinforcement. Black arrows display relationships of which the direction depends on the influencing variable.

2 Methods

2.1 Object & Data

The research objects were stem discs and increment core samples of black cherries from four sites around the Netherlands, all of which were forests on sandy soils where black cherry occured both in shaded conditions and as exposed trees in the forest canopy. 80 trees were sampled in a clustered sampling design, where twenty trees were sampled per site from a total of four sites, of which two were located on xeric sandy soils and of which the other two were located on mesic loamy soils. On all sites, the groundwater was too deep for tree roots to reach. The soil moisture level of these sites could not be directly measured. One of the driving factors of soil moisture, soil grain size, was measured instead. This grain size was measured using a sand ruler. Two increment core samples were taken per tree on opposing radii. On the site Johannahoeve 2, stem discs were taken, on which two radii were measured.
Sampled trees were selected on-site on the basis of their crown exposure, as reference for the expected shade level, since sampling had taken place before the leaves of the forest had fully developed that year. Light measurements were therefore performed later, in June. Ten trees were sampled per canopy position per site. Sample tree selection was altered in Oerle, where trees sampled by earlier studies were avoided, as well as at Johannahoeve 2, where the sampling was part of a thinning experiment. There, trees were sampled randomly from the marked trees surrounding each future crop tree.

Core samples and stem discs were taken from black cherry individuals in the field at various sites. From the sample sites were also collected the site code, longitude, altitude, soil substrate, soil organic matter (OM) content, soil profile and the forest's basal area.
The site code was used to identify individual sites. The soil grain size, OM and loam content were used to determine a proxy for the level of soil moisture. A soil profile was made on a per-site basis for this purpose, as well as for a general characterization of the soil. The forest basal area was also measured for every measured tree to serve as a reference value on the density of the forest, which can serve as a reference for the intensity of competition effects. An estimation of the shade level was made on a per-tree basis, rather than a per-site basis.

The samples were taken from a height of about 30 cm, in order to also sample the earliest rings which formed when the sampled tree had not yet reached a height of 130 cm. 30 cm was sufficiently high above the wide base of the tree.
From these objects the measurement of ring widths with a precision of 1/100 mm give insight in the diameter at the sample height throughout the life history of the sampled tree. The diameter at 130 cm was measured as well.

Other data gathered were time series data on the precipitation and temperature, gathered from records of weather stations made publicly available by the Royal Netherlands Meteorological institute (KNMI., 2022b).

2.2 Study sites

The investigated black cherries originate from four sites in the centre southeast of the Netherlands. At all sites the groundwater table was too deep for the roots of the cherries to reach. The soils of these sites were also all of a sandy material basis, though different soil processes and history differentiate these soils.

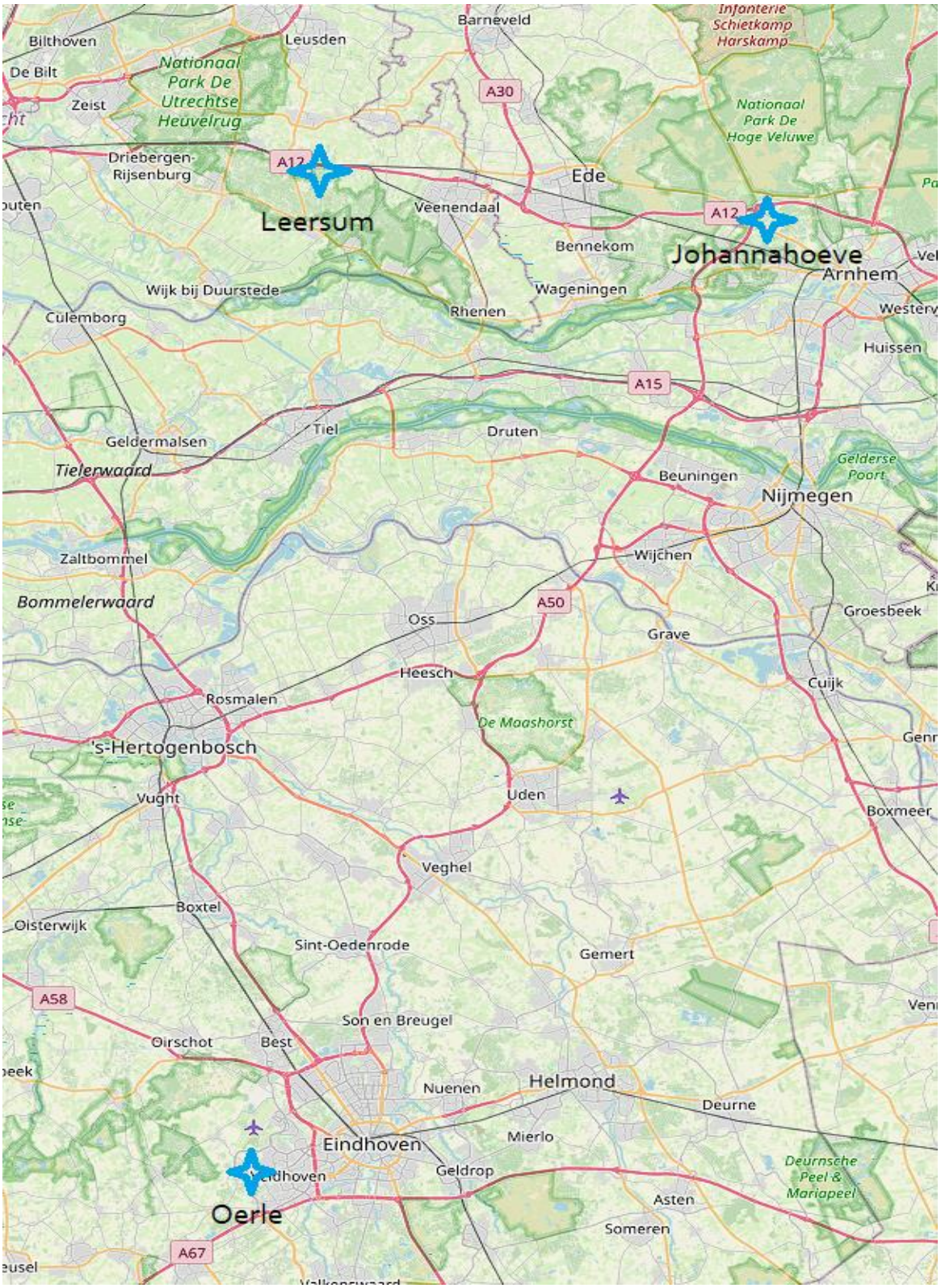

Figure 2:A map showing the locations of the study sites. The rough locations are marked by a blue star. Background layer provided by OpenStreetMap

The stand of Johannahoeve 1 was situated near the southern edge of the Veluwe area. A satellite image is provided in appendix 2. The site itself was a former patch of farmland abandoned some time between 1931 and 1956 (Het Kadaster., 2022). The soil still had a large quantity of organic material during sampling as a consequence. The stand was younger than surrounding stands with Scots pine (*Pinus sylvestris*) in the mix. The investigated black cherries appeared to be even-aged, likely stemming from a clearcut around the year 1978. The black cherries shared the stand exclusively with *Betula* species. These grew a little taller than the black cherries and were unlikely to be much, if any, older than the black cherries.

The stand of Johannahoeve 2 was situated in the same forest as Johannahoeve 1, but had a different history, given the presence of Scots pine and Pedunculate oak *(Quercus robur),* besides the usual birch (*Betula spp.)*. The size of these trees suggest they might have stemmed from between 1931 and 1956, before which the site was farmland and/or a heather field (Het Kadaster., 2022). The black cherries might have been added to these forests and later cut, after which the individuals resprouted. Despite the different history, the soil was very similar to that of Johannahoeve 1.

The stand of Oerle was situated near Eindhoven and Veldhoven. A satellite image is provided in Appendix 3. The area has been a forest since before the 20th century (Het Kadaster., 2022). The forest featured stands that were not mono-aged. The stands were also diverse. Tree species close enough to contribute to the basal area measurements nearby the black cherries included Scots pine, birch, oak, Japanese larch *(Larix kaempferi)* and white pine *(Pinus strobus)*. The soil was loamy and showed little traces of organic matter content.

The stand of Leersum was a line of black cherries growing on the forest edge bordering the A12 motorway. A satellite image is provided in Appendix 4. The black cherries faced a clearing between it and another line of trees, which included another two of the sampled cherries. All but these two faced the same way, towards the clearing, which used to be a parking space connected to the motorway until, at the earliest, 1989 (Het Kadaster., 2022). The soil was entirely black, indicating a high organic matter content, likely inherited from former agricultural use.

Table 1: A summary of site characteristics and characteristics of the sampled trees. Soil code retrieved from Okx (2015). Altitude provided by Rijkswaterstaat (2018).

Code	Region	Location	Ahn3 (masl)	Soil code	M50	Soil moisture	Other species than black cherry
J1	Veluwe	Johannahoeve 1	30	Hd21	75 – 600	Xeric	Birch
J2	Veluwe	Johannahoeve 2	32	Hd21	75 – 600	Xeric	Birch, Scots Pine, Oak
O	Eindhoven	Oerle	24	zEZ55	75 – 210	Mesic	Birch, Scots Pine, Oak, Japanese Larch, White Pine.
L	Utrechtse Heuvelrug	Leersum	8	zEZ51	16 - 300	Mesic	Birch, Scots Pine, Oak, Rowan

The general soil profile, as sampled in the field, was summarized in Figure 3. Both Johannahoeve sites had similar podzol soils with relatively large grains. Oerle had a sandy soil with less podzolization and more loam content. Leersum had a humic podzol with a large OM content throughout the profile. The maximum depth of infiltration was still visible enough to demarcate regardless.

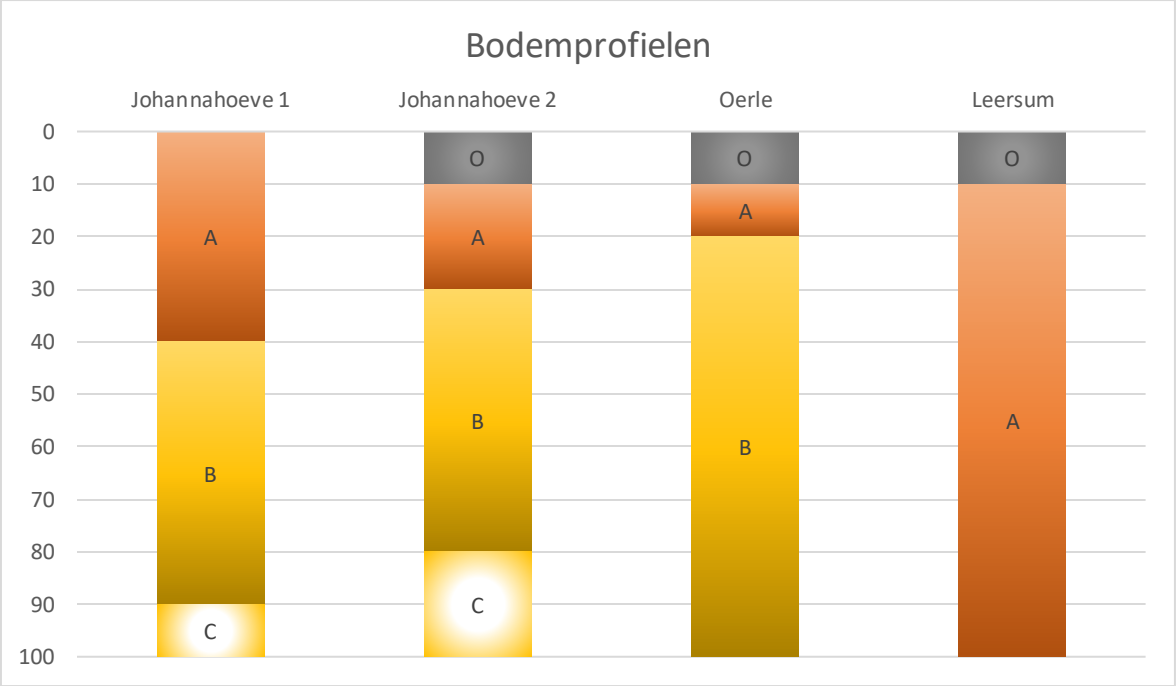

Figure 3 The soil profiles up to a meter deep, taken at each site. O represents the organic on top of the mineral layer. A represents the mineral layer where accumulation of organic material takes place. B represents the mineral layer where infiltration of organic material takes place. C represents an unaltered mineral layer.

2.3 Sample processing

Ring width-data was gathered using a Lintab digital positioning table in combination with TSAP-win software, which are both products of Rinntech-Metriwerk GmbH. Preparation of stem discs for this analysis was done by smoothening the surface of the samples with utility knives and sandpaper and by marking the smoothened surface with chalk to enhance the contrast of cell walls.
Increment core samples were prepared by gluing them to a dedicated sample holder and cutting them with a microtome after the glue has dried for a day. The increment bores were also prepared with sandpaper and chalk to increase the contrast of wood vessels. Measurement of the samples was done on two radii, as free as possible of reaction wood, to take into account imperfections in the roundness of the tree. In the case of core samples, two were taken per sampled tree at angles approaching 90 degrees to account for imperfections in roundness and reaction wood. All measurements were performed in the direction from the bark to the pith.
After ring width measurements, quality checks were performed using Cofecha software (Holmes., 1983; Grissino-Mayer., 2001). A low correlation of ring-width measurements to the mean series of trees of the same sampling site indicated possible measurement errors, such as missing rings or duplicate measurements, and provided suggestions where these errors could be by indicating what changes could have potentially higher correlations to the mean curve, to assist in correcting these errors or new better measurements.

2.4 Data Handling

Ring-width chronologies were detrended using a ten-year smoothening spline in R, after which the two measurements per tree were averaged to create a mean chronology for every sampled tree. This was performed again to gain master chronologies on a per-sampling-site basis and canopy position basis.

The detrending attempts to remove the influence of the tree age on the chronologies, meaning the remaining variation in ring width size should be the result of environmental and biotic conditions specific to that growth year. The detrending therefore also eliminates the structural decline of the codominant chronologies in comparison to the dominant chronologies. Differences in sites become visible when responses in specific years are compared. Likewise, chronologies deviating from the trend stand out more for comparisons within the site.

The basal area increment (BAI) at 30 cm height was calculated from these detrended master chronologies. The mean value of this BAI, for each individual tree, became the response variable in the statistical analysis. DBH was used instead of the BAI for analyses where the repeated measurements of each growth year would cause pseudoreplication.

Three-month SPEI-values were calculated to represent historical drought conditions. It was calculated from the collected values of precipitation and temperature from the KNMI (2022b), as well as the latitude using the Hargreaves calculation method. Calculations were performed using R software by R core team and R foundation for Statistical Computing (R Foundation., 2021) the accompanying SPEI package for this software, by Beguería et al. (2014)

2.5 Data analysis

Statistical analysis was performed by correlating climate variables, which include SPEI, temperature and precipitation as dependent variables, to the ring-width series using the dplR and treeclim packages in R (Bunn & Korpela., 2020; Zang & Biondi., 2015). The results were tested for significance and are visualized in histograms and correlograms using the treeclim and corrplot packages (Wei & Simko., 2021).

The Lloret indices of resistance, recovery and resilience were calculated manually. The associated recovery periods were calculated using the pointRes (van der Maaten-Theunissen et al., 2022) and dendRoLab packages (Buras, 2022; Buras et al, 2022). These packages were also used to identify pointer years. These were used alongside drought years identified by July three-month SPEI-values below -1. The Lloret indices were displayed in boxplots for comparison between sites and between canopy positions.

DendRoLab was also used to perform unconstrained ordination on the detrended ring-width series, in order to infer whether their variance was different depending on their location.

Linear and mixed models were created in R to investigate correlation between the tree DBH as the dependent variable and forest basal area and light as independent variables. The site was added as a factor where applicable.

The variables that are used in this research and their relations to each other are given in a conceptual model diagram in figure 4

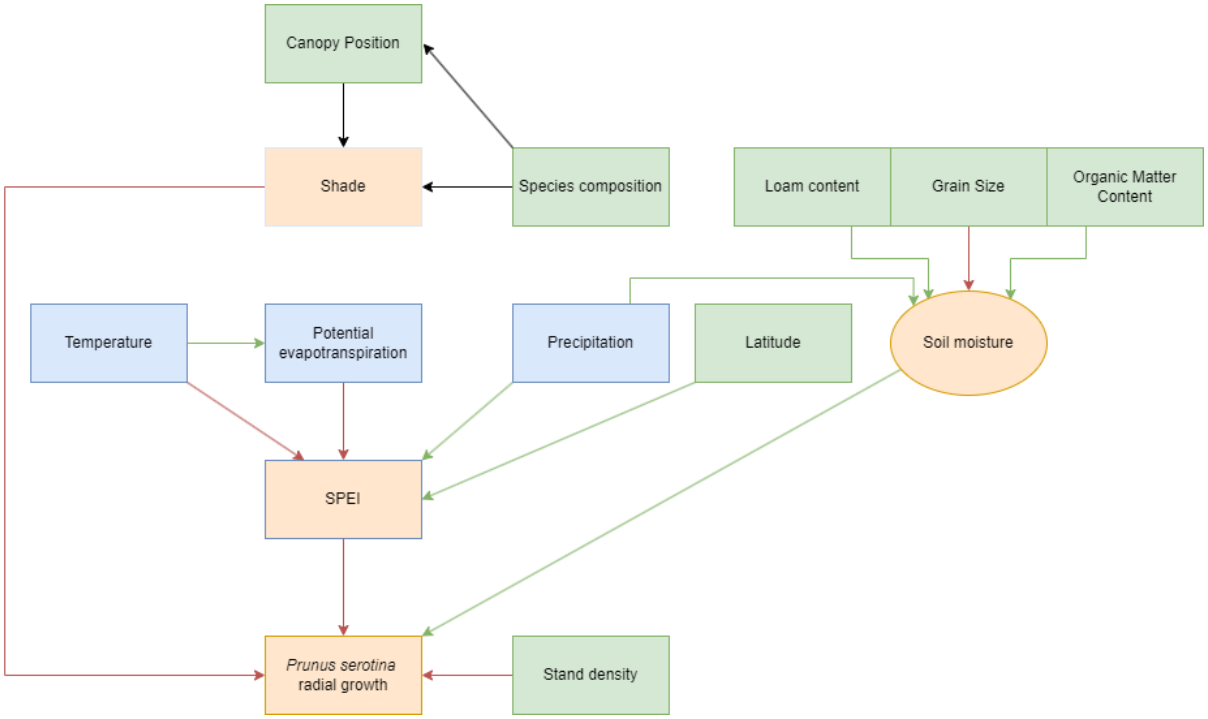

Figure 4: Simplified conceptual model of the variables used. Orange variables relate directly to the research questions. Green variables are measured in the field. Blue variables are retrieved from the Royal Netherlands Meteorological institute. Soil moisture, loam- and OM content are the only variables that could not be measured, and were thus inferenced.

3 Results

3.1 Ring width chronologies

The ring width measurements yielded the chronologies of figure 5. Peaks and drops in ring width growth that affected the whole site are visible in specific years, though life events of individual trees and site-specific events meant that these peaks and drops are not present in every sample. The series of individual trees became increasingly divergent towards their youngest years, where canopy positions had not been established yet. As time progressed, the dominant chronologies showed greater ring growth than the codominant chronologies more consistently. The direction of yearly variation typically remained the same regardless of canopy position.

The average ring growth was generally higher, at 3 to 4 mm/year in Leersum and Oerle than in Johannahoeve, at around 2 mm/year. Within Johannahoeve, site 1 displays the highest average ring growth.

The largest ring width was observed in Oerle, at 17.46 millimetres. This tree, O-14, curiously declined from such high growth to only 0.53 millimetres in 2021.

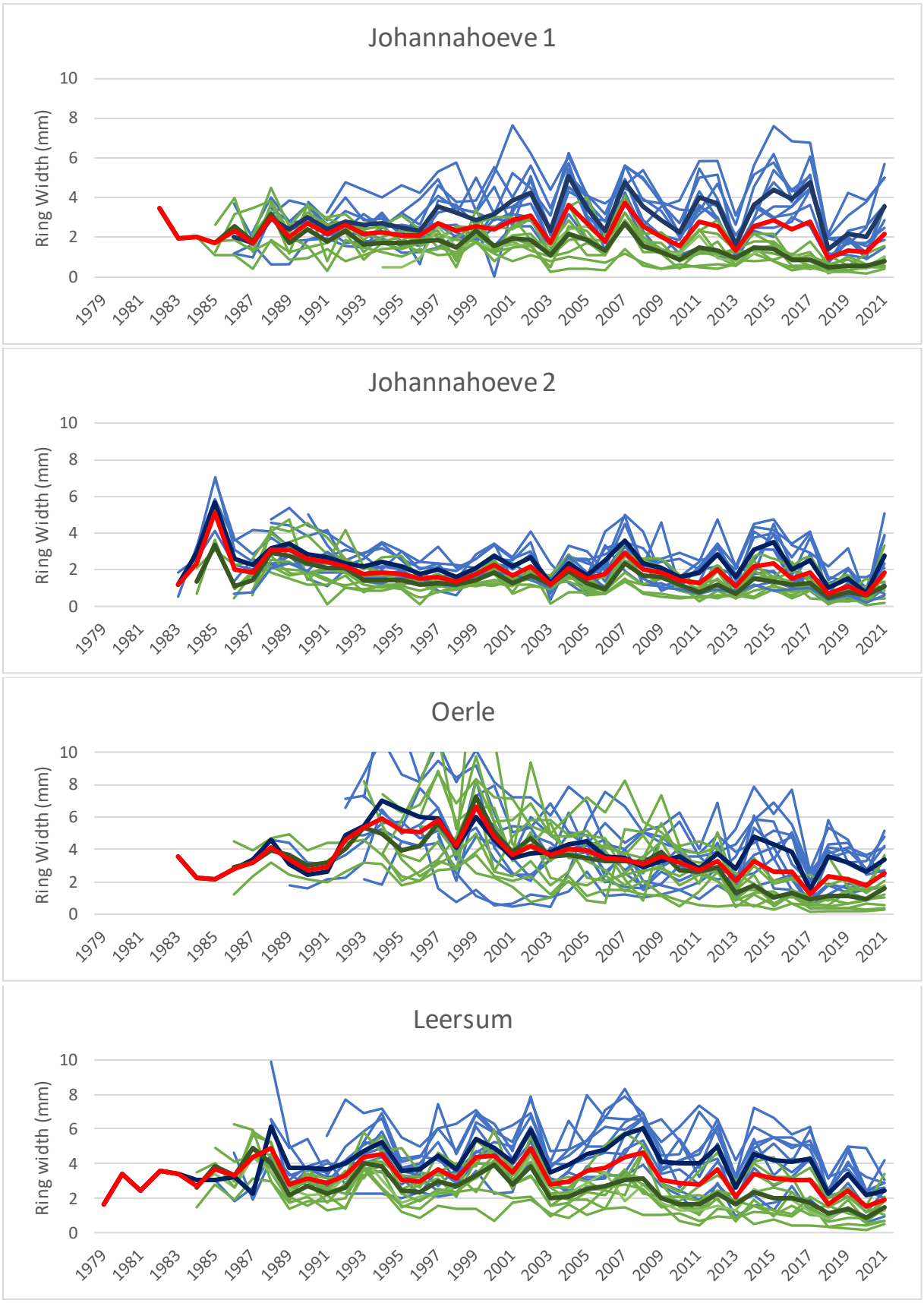

Figure 5: Mean chronologies per tree of the raw ring width measurements across the four sites. Dominant chronologies are displayed in blue. The mean dominant chronology is displayed in a darker shade of blue. Codominant chronologies are displayed in green. The mean codominant chronology is displayed in a darker shade of green. The mean site chronology is displayed in red. Note that the y-axis scale in the graph of Oerle exceeds the y-axis limits, due to very high growth in some individuals of up to 17 mm/year during this period.

The detrended versions of these same chronologies in Figure 5, are given in Appendix 1. The most extreme growth spurt, relative to normal growth in its site, was reached by a codominant tree (J1-20) in Johannahoeve 1, at a value of 2.32 in the year 2008. This site also saw the most extreme decline in growth, compared to normal growth for the site, at a value of 0.01, reached by a dominant tree in 2000. During the drought period from 2018 to 2020, the Johannahoeve sites deviated more from their respective normal growths than the trees in the Oerle and Leersum sites did for theirs.

It appears from the chronologies that most trees sprouted during or close to the year 1978. For Johannahoeve 1, it is plausible that black cherry was introduced to this site that year, considering the site's history. Nevertheless, the use of core sampling meant that the pith of the tree was often missed, making it impossible to precisely date the arrival of black cherries on these sites. Estimations of the sprouting years, based on chronologies that reached the pith and the expected height growth of sprouts, are given in table 2. Cherries appear to be present somewhat earlier in Oerle and Leersum, the latter of which included a sampled tree of which the pith at 30 cm dated to 1979. On the other hand, rotten cores caused some trees to be unsuitable to provide insights beyond recent years. The worst such case is the tree O-12, which provided no readable rings beyond 1998.

With the growth added cumulatively in Figure 7 it becomes visible where radial growth was maintained and how this adds up with time. Leersum profited the most of continually high growth and has thus accumulated more basal area, as can also be seen from the DBH measurements in table 2. Like the DBH measurements, Johannahoeve and then Oerle follow with generally higher accumulated basal area. Johannahoeve 1 is hardly visible, hidden behind the cumulative curves of the codominant trees, which are present in every site, and trees of which measurements started accumulating later due to missing rings, which are mostly present in Oerle and Leersum.

Finally the detrended measurements were combined in the site-specific chronologies of figure 6. Rather than a real ring width value, these chronologies display the ring width index (RWI). This index shows how much the ring widths of that year deviated from an average growth year on the same site. After the detrend, most of the variation is equal for both canopy positions. Variation between canopy positions that remain is focused on the years 1999, 2016 and 2017 for Johannahoeve 1, 2006 for Johannahoeve 2, 2005 and 2015 for Oerle and 1986, 1987 1993. The canopy positions displayed different growth during these years, but returned to more or less equal growth outside of these years.

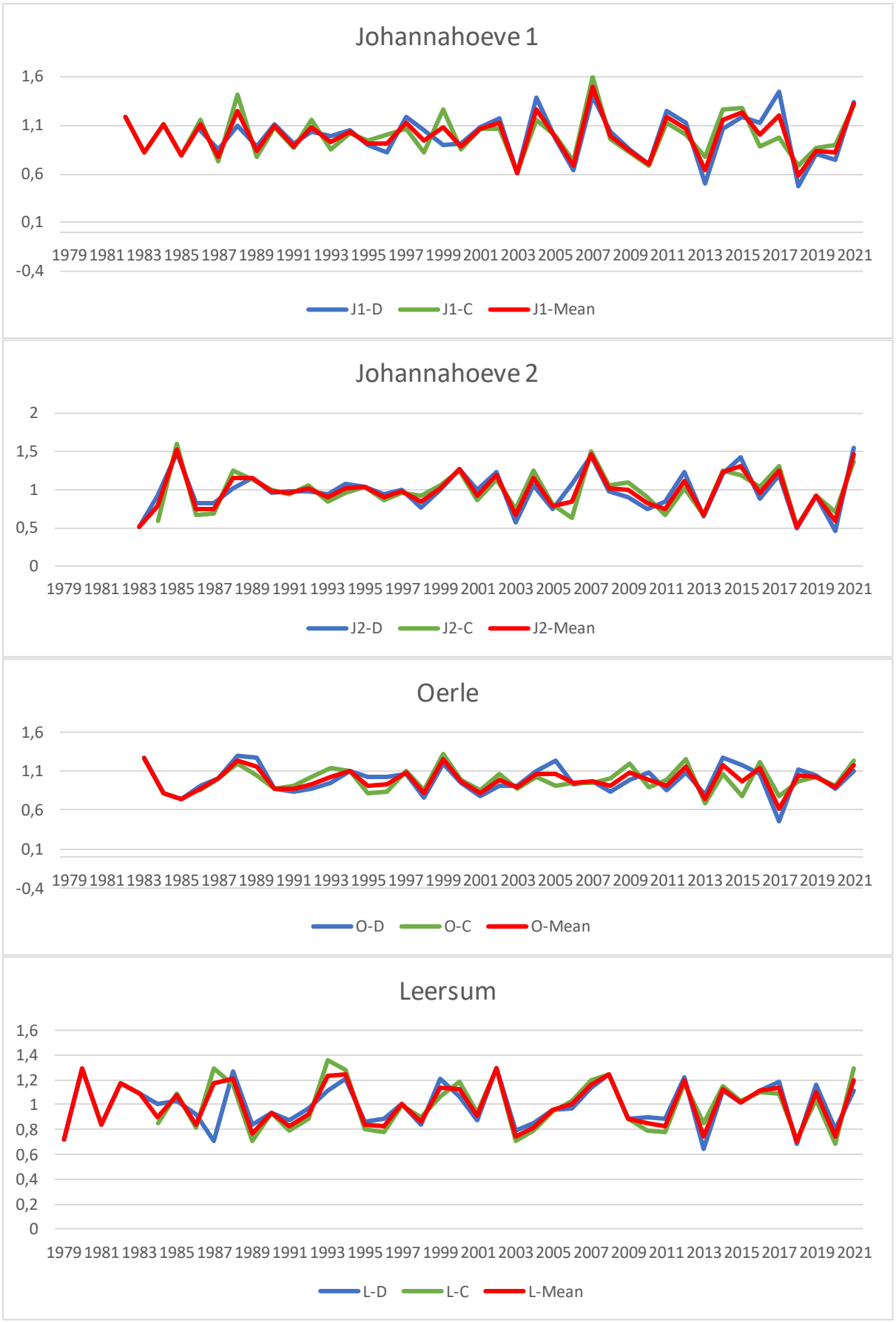

Figure 6: Dominant, codominant and mean chronologies divided per site. The dominant chronologies (-D) are displayed in blue, the codominant chronologies (-C) are displayed in green and the mean chronologies are displayed in red.

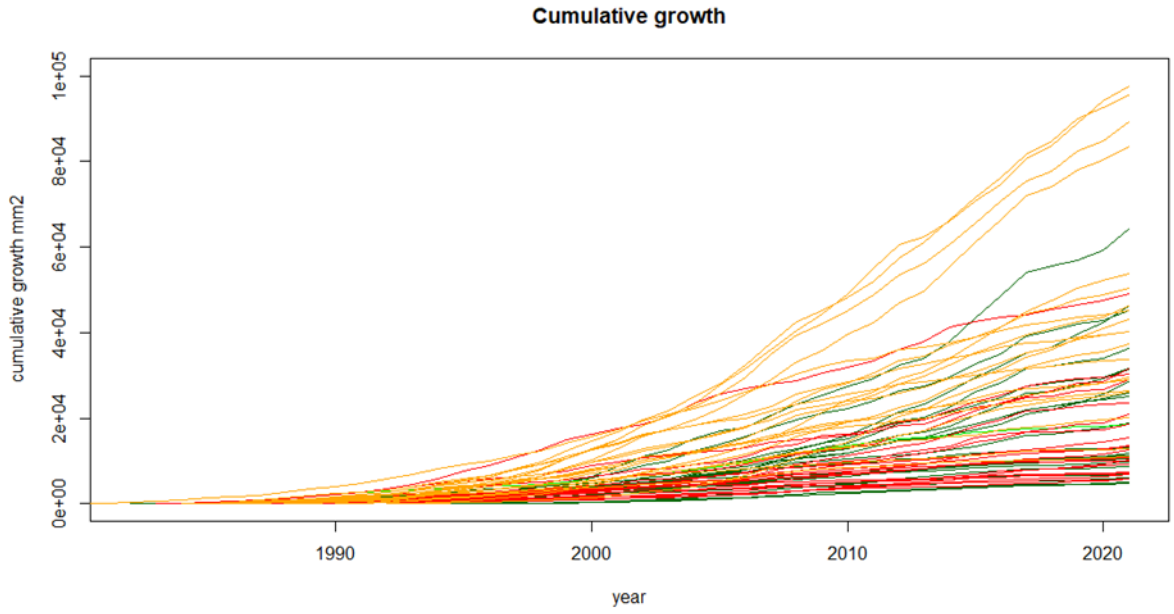

Figure 7: Cumulative growth curves, colour-coded by site. With Johannahoeve 1 in dark green, Johannahoeve 2 in light green, Oerle in red and Leersum in orange. Note that the x-axis displays the year, rather than years since sprouting. This means that curves with missing rings start later and therefore underestimate the accumulated basal area in 2021, which is better represented by the DBH in table 2.

Table 2: Other characteristics of sampled trees per site.

Code	Oldest sampled year	Estimated stem year	Average DBH of dominant group (cm)	Average Height of dominant group (m)	Average basal area (m^3/ha)	Average DBH of codominant group (cm)	Average Height of codominant group (m)
J1	1982	1980	23,0	NA	19,5	11.53	NA
J2	1983	1982	16,90	15,73	24,6	11.36	11.62
O	1983	1981	28,62	19,23	14,7	21.27	16.42
L	1979	1977	31,53	15,13	29,5	22.06	13.19

3.2 Pointer years

Besides manually choosing years with known droughts, or choosing them based on criteria such as SPEI-values or precipitation shortage, it was also possible to infer what years were of special interest to the investigated black cherries by identifying what years saw abnormally large changes in yearly growth compared to surrounding years. The Bias-adjusted Standardized Growth Change (BSGC) identified growth values outside of a 90% confidence interval and tested their significance at an α of 0.05. In the default settings used to obtain these identifications, deflection periods - the time during which growth remains abnormal after a disturbance year- could be detected, should they exist.

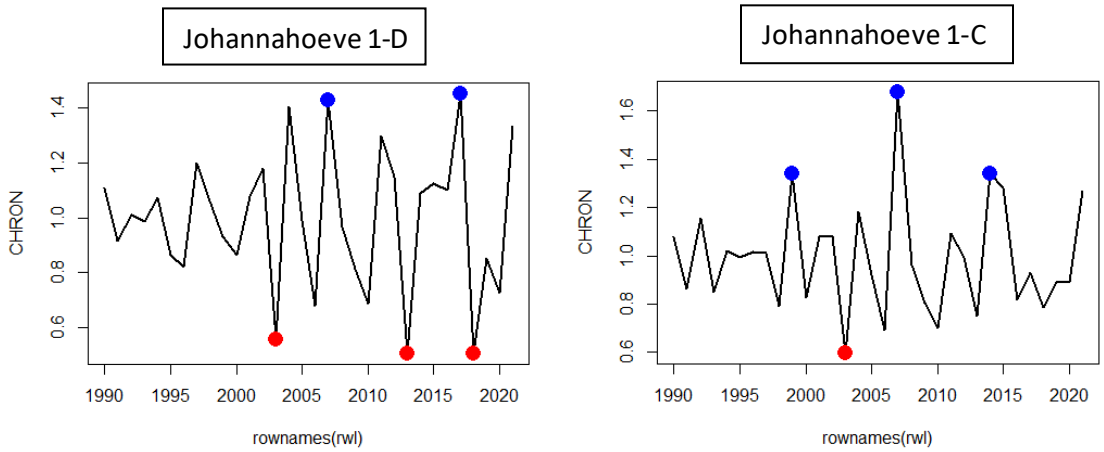

Figure 8: Pointer years as identified by BSGC for the dominant (left) and codominant (right) trees in Johannahoeve 1.

In the first site evaluated, Johannahoeve 1, the co-dominant trees suffered a negative pointer year in 2003 and a positive one in 1998, 2007 and 2014. The dominant trees also had 2003 as a negative pointer year. Additionally, 2013 and 2018 were labelled by this method as negative pointer years. 2007 and 2017 were labelled as positive pointer years. Despite the method's ability to detect deflection periods, during which growth speeds are affected by events in earlier years, None of the pointer years had such periods. Diameter growth in the following year being is marked as independent of pointer years.

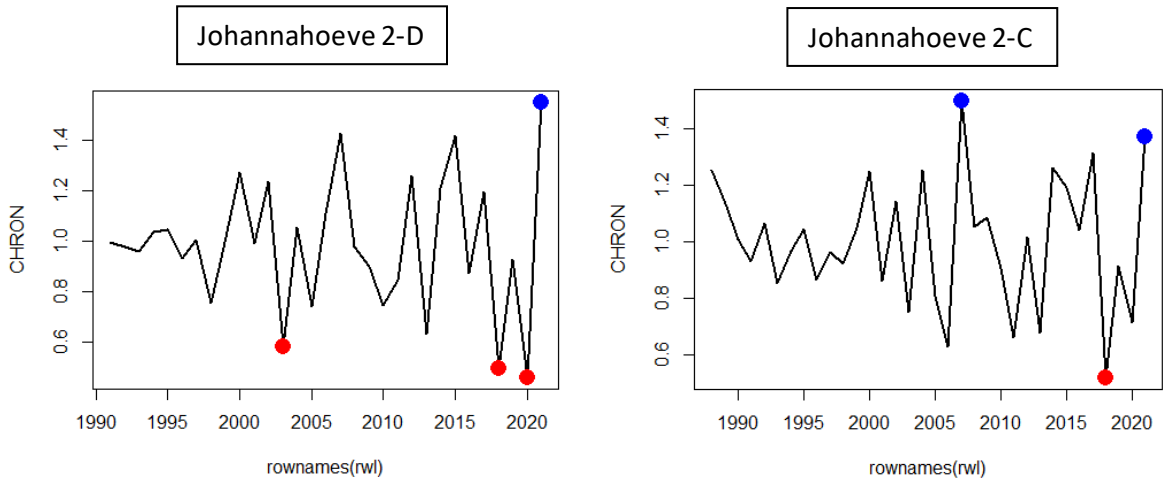

Figure 9: Pointer years as identified by BSGC for the dominant (left) and codominant (right) trees in Johannahoeve 2.

In the same evaluation in Johannahoeve 2, the year 2003 was experienced as a negative pointer year by the dominant trees. 2007 was experienced as a positive pointer year by the codominant trees. 2018 was experienced as a negative pointer year by both dominant trees and by codominant trees. Additionally, both canopy positions experienced 2021 as a positive pointer year. Dominant trees experienced 2020 as a negative pointer year as well. Again, none of the pointer years experienced a deflection period of any sort. The BSGC likely saw the period of reduced growth from 2018 to 2020 as two separate events with a year of recovery in between.

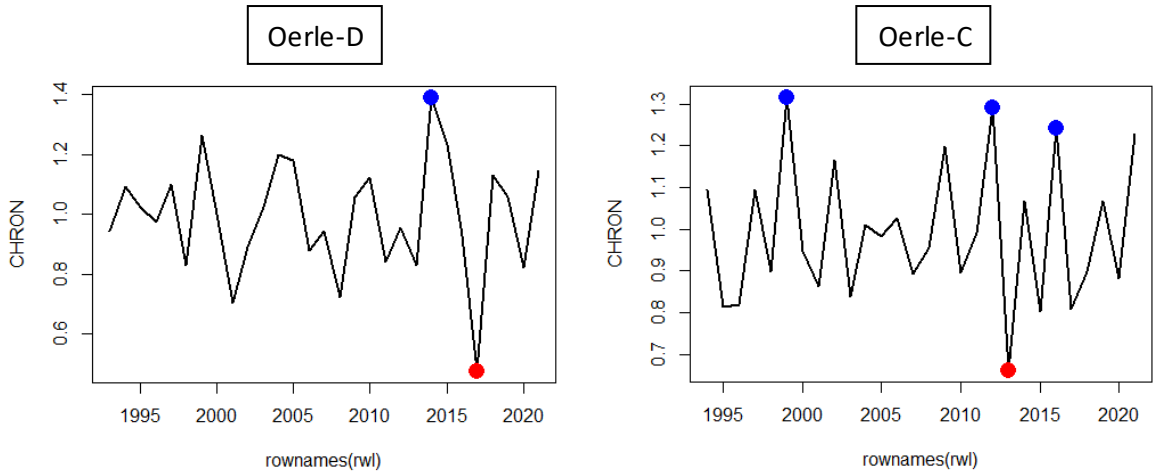

Figure 10: Pointer years as identified by BSGC for the dominant (left) and codominant (right) trees in Oerle.

The identification of pointer years in Oerle in figure 10, saw only one negative pointer year for each social group: 2017 for the dominant group and 2013 for the codominant group. The dominant group had only 2014 as a positive pointer year. The codominant had pointer years in 1999, 2012 and 2016. Again, none of these pointer years showed a deflection period.

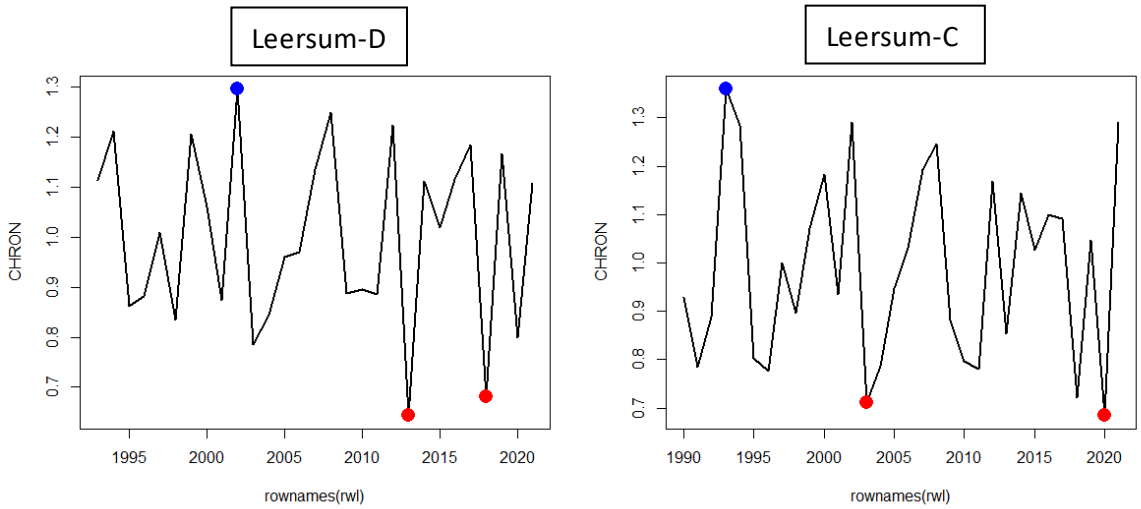

Figure 11: Pointer years as identified by BSGC for the dominant (left) and codominant (right) trees in Leersum.

For Leersum, in figure 11, positive pointer years were seen only in the older rings, those being 2002 and 1993 for the dominant and codominant trees respectively. While 2003 was classified as a negative pointer year for the codominant trees, the year was not classified as such for the dominant trees, likely due to the method's rule *rm.succ* being enabled, which prevented pointer years being identified immediately after a pointer year of the opposite direction in an attempt to reduce bias. The dominant and codominant groups of cherries appeared to disagree whether 2018 or 2020 is the main negative pointer year of the 2018-2020 period. Deflection periods have again not been identified. Pointer years across all sites and canopy positions are summarized in Table 3.

Table 3: Pointer years statistically identified by BSGC. Positive pointer years are marked by a plus (+). Negative pointer years are marked by a minus (-). Pointer years are given for both sites and subgroups of site and canopy positions.

Year	J1-D	J1-C	J2-D	J2-C	O-D	O-C	L-D	L-C	J1	J2	O	D
1993							+					
1999						+		+			+	
2002								+				+
2003	-	-	-					-	-			
2004												
2007	+	+		+					+	+		
2012						+						
2013	-					-			-		-	
2014					+							
2016						+						
2017	+				-						-	
2018	-		-	-			-		-	-		-
2020			-					-				
2021				+						+		

3.3 Resistance, recovery and resilience

While statistically calculated pointer years gave some insight into growth dynamics in the life history on each site, they did not provide a causal relationship as to what is the driving influence behind abnormal growth speeds. To evaluate what years warrant further investigation, the calculated three-month SPEI values, given in table 4, were consulted to identify years with abnormal moisture conditions.

Table 4: July three-month SPEI-values in years from 1980 to 2021. Years are only shown where the values drop below -1 in at least one site. A redder color emphasizes lower values, indicating dry conditions. A bluer color emphasizes higher values, indicating wetter conditions.

Year	Johannahoeve & Leersum	Oerle
1983	-1,17186	1,543759
1986	-1,44294	-0,34657
1989	-1,8919	1,393246
1990	-1,20383	1,51223
1992	-1,37761	-1,13002
1994	-1,06079	0,912824
1999	-1,23142	1,476759
2001	-1,14863	0,768466
2003	-1,8133	-1,15584
2006	-2,1236	0,2522
2008	-1,20322	0,644811
2009	-0,49213	-1,60308
2010	-1,23655	-0,94246
2015	-0,86104	-1,42945
2017	-1,02347	-1,96263
2018	-2,42273	-1,19999
2019	-1,04453	-1,39256
2020	-1,26488	1,14313

The years 2003, 2017 and 2018 were identified as negative pointer years both by the BSGC method, summarized in table 3, and SPEI drought index, as summarized in table 4. The growth decline in these years were thus likely at least partially a result of water deficits. With the identification of these years, it became possible to calculate resilience indices using pointRes, such as Lloret indices and recovery period lengths associated with those drought years (Van der Maaten-Theunissen et al., 2020). These indices could then be compared between sites and canopy positions.

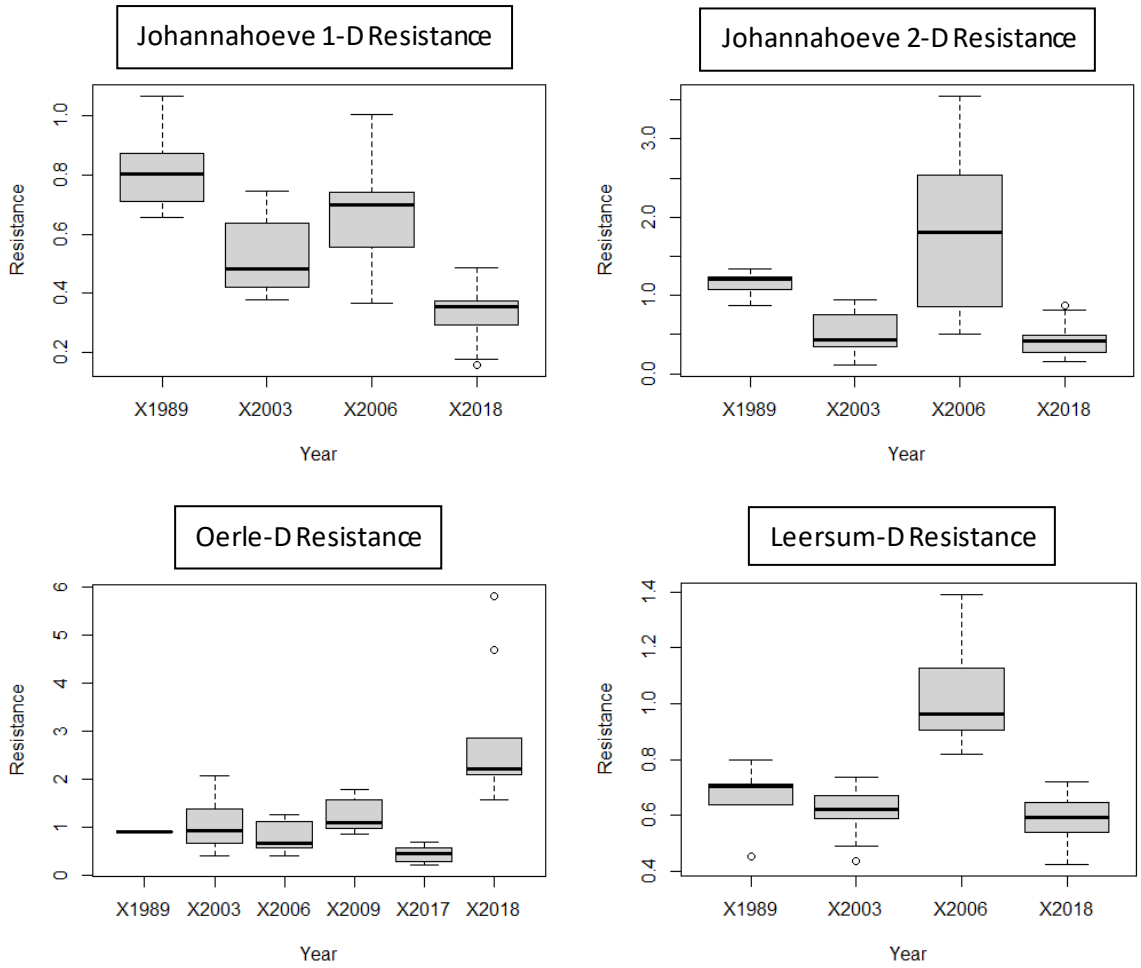

Figure 12: Resilience indices displayed across four boxplots in one plot per site. Sites are ordered clockwise from the top-left: Johannahoeve 1, Johannahoeve 2, Leersum, Oerle. A higher resistance index indicates better growth. A resistance index of 1 indicates no growth change. Take note that the Y-axes do not share identical scaling.

The resistance indices, the ratios between the growth before and during the drought year, in figure 12, show that dominant black cherries suffered growth reduction during drought years, but not exclusively so. Despite being located close to each other, the black cherries of Johannahoeve 2 fared much better during the 2006 drought than their counterparts in Johannahoeve 1 even exceeding pre-drought growth. Oerle saw different responses to drought due to other weather conditions, hence the inclusion of the years 2006, 2009 and 2017. When the resistance values were subjected to two-sample t-tests, all sites differed significantly from each other, with the exception of Johannahoeve 2, which had an insignificant difference in mean resistance values with both Oerle and Leersum.

Table 5: P-values of two-sample t-tests, comparing the mean resistance values of dominant trees by site. Green P-values represent significantly different means, whereas red P-values represent insignificantly different means, at an alpha of 0.05.

Two-sample T-test	Johannahoeve 1	Johannahoeve 2	Oerle	Leersum
Johannahoeve 1		0.003281	1.935e-05	0.002627
Johannahoeve 2	0.003281		0.1211	0.07424
Oerle	1.935e-05	0.1211		0.0007493
Leersum	0.002627	0.07424	0.0007493	

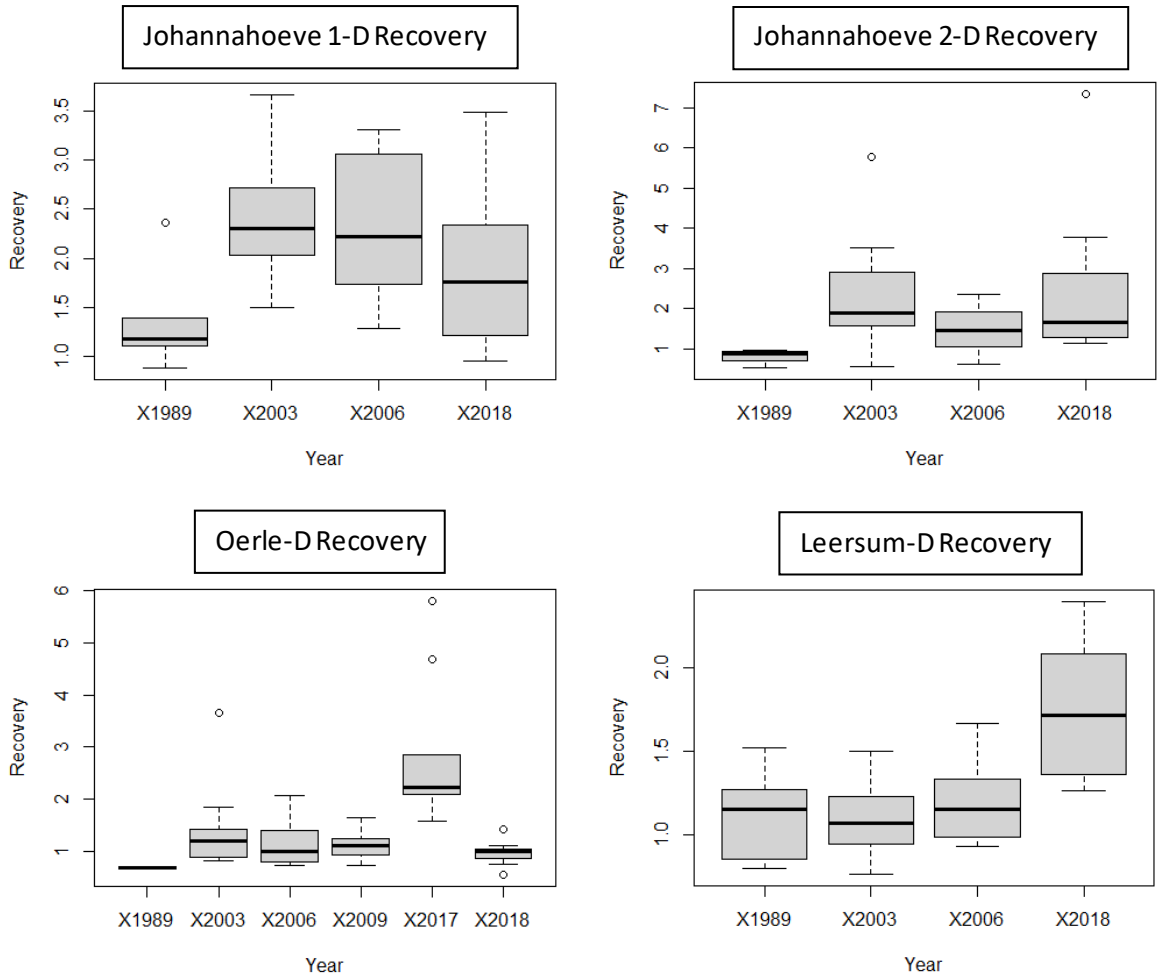

Figure 13: Recovery indices displayed across four boxplots in one plot per site. Sites are ordered clockwise from the top-left: Johannahoeve 1, Johannahoeve 2, Leersum, Oerle. A higher recovery index indicates a larger ratio between drought and post-drought growth.

Regardless of the growth reduction experienced during drought years, most black cherries were able to recover quickly, as indicated by the recovery indices, the ratio between growth during and after the drought, in figure 13. The growth rate in the year immediately after the 2003 drought was often double that of the rate during the 2003 drought in both Johannahoeve sites. Recovery after 2006 was lower, but still high at 1.5 times the growth rate during the drought. Recovery was lower overall in Leersum and Oerle, but still present. Recovery after the local 2017 drought was exceptionally high in Oerle. Mean recovery in Oerle was different from Johannahoeve 1. Leersum was different from both Johannahoeve sites. All other compared means differed insignificantly.

Table 6: P-values of two-sample t-tests, comparing the mean recovery values of dominant trees by site. Green P-values represent significantly different means, whereas red P-values represent insignificantly different means, at an alpha of 0.05.

Two-sample T-test	Johannahoeve 1	Johannahoeve 2	Oerle	Leersum
Johannahoeve 1		0.2852	0.001644	4.255e-06
Johannahoeve 2	0.2852		0.1894	0.041
Oerle	0.001644	0.1894		0.3642
Leersum	4.255e-06	0.041	0.3642	

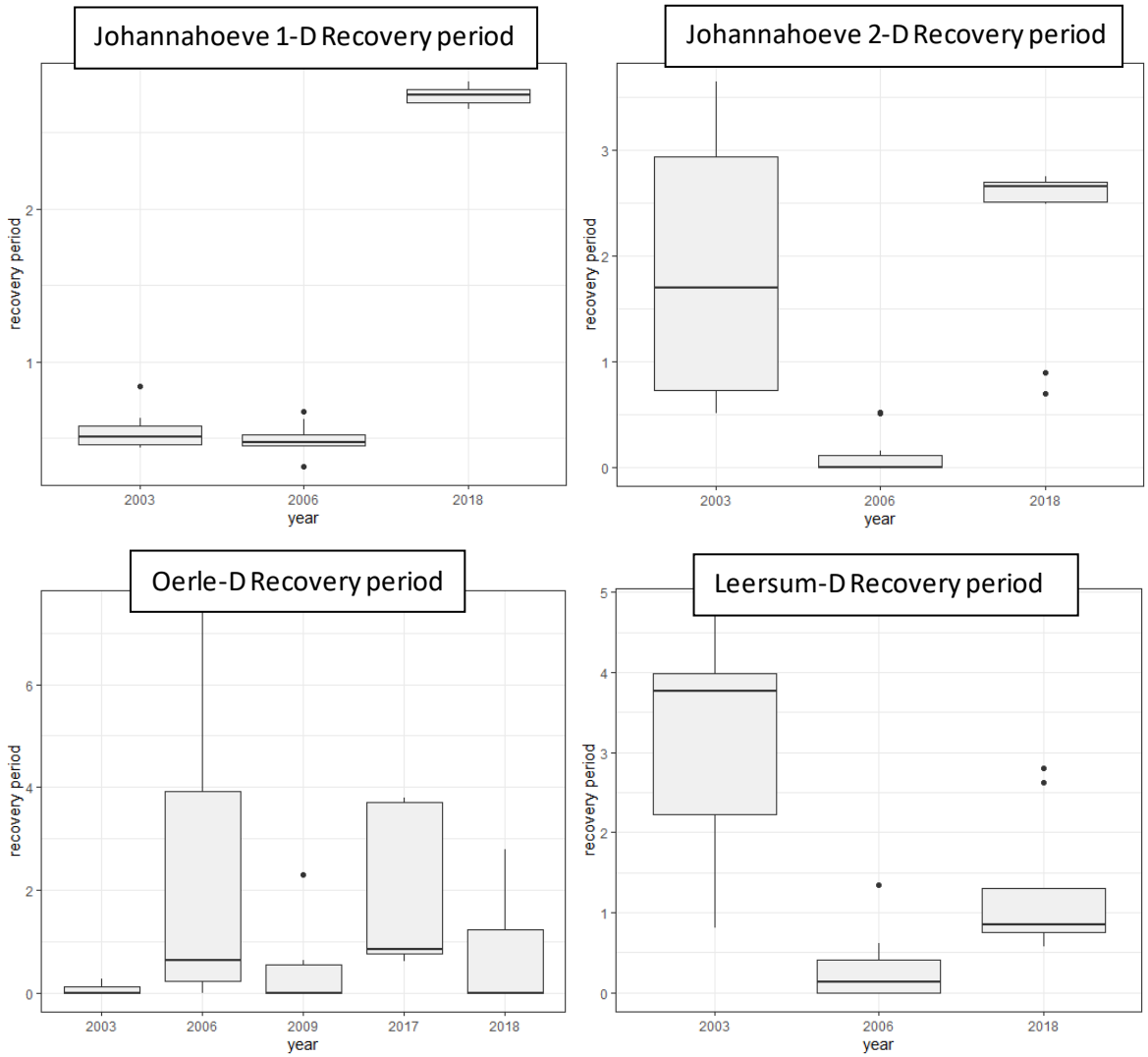

Figure 14: Boxplots indicating the length of the recovery periods according to pointRes. A recovery period of zero means the preceding year was not experienced as a negative year for the individual. A recovery period of 1 means the pre-drought growth rate was attained.

Unlike the BSGC method, pointRes was able to identify a recovery period after drought years, as seen in figure 14, but these seemed to rarely exceed one year, unless the drought years were followed up by more drought years, as is the case for 2018 and for Oerle 2017. This might also include the recovery periods in Johannahoeve 2 and Leersum after the 2003 drought, where recovery periods were significantly longer, but also varied within these stands. The high medians of the year were not incidents experienced by individual trees. When these trees had not attained their 2002 growth rates by 2005, their recovery period would be extended by the 2006 drought.

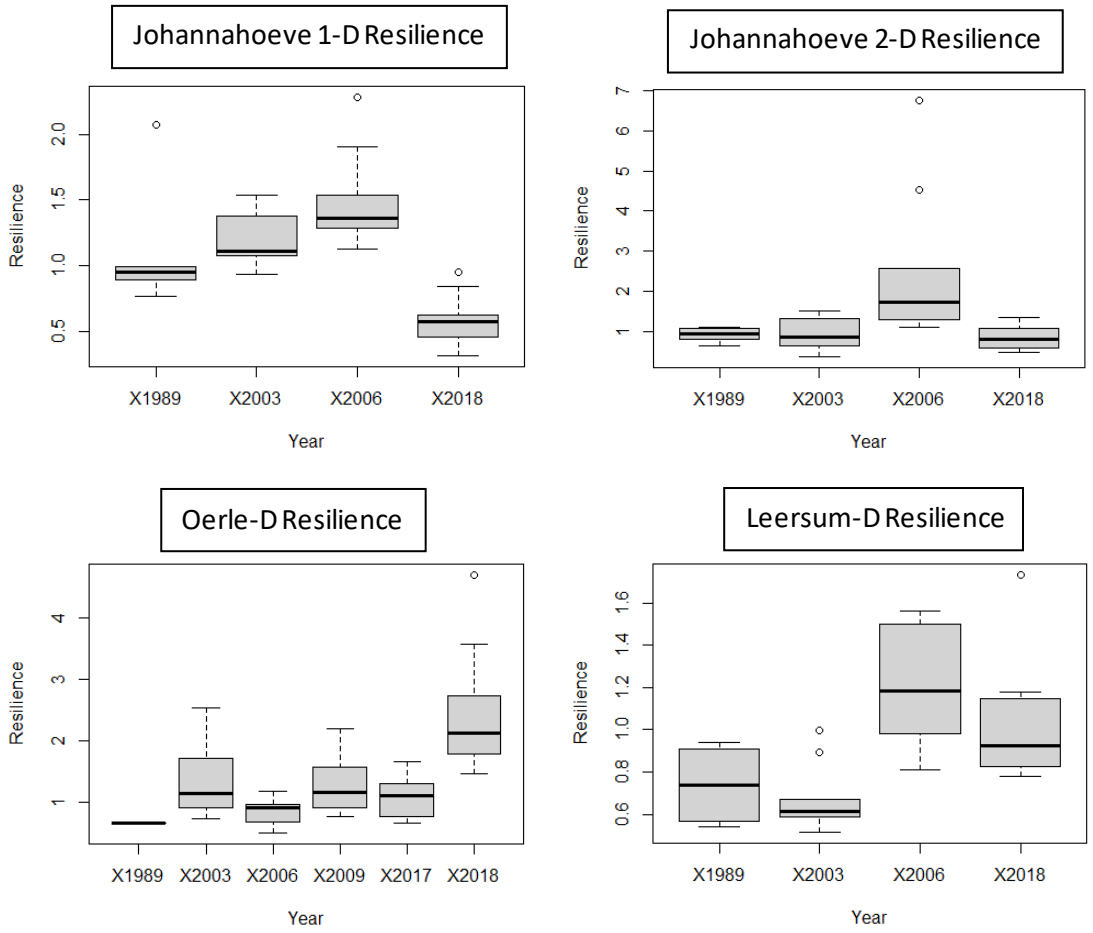

Figure 15: Boxplots of the resilience indices. A higher resilience index indicates a better ability to return to pre-drought levels.

The resilience indices, the ratio between growth before and after a drought, of figure 15 indicated that the black cherries there were not just able to recover their growth entirely to their pre-drought levels, but they frequently exceeded them too; displaying stronger growth than usual after a drought. Exceptions to this were Johannahoeve 1 and Oerle after the 2006 drought, Leersum after the 1989 and 2003 droughts and 2017. The resilience of the black cherries in Oerle appeared to be lower than their counterparts in the other sites. The mean resilience values of Oerle differed significantly from the mean resilience values of Johannahoeve 1 and Leersum. All other compared means differed insignificantly.

Table 7: P-values of two-sample t-tests, comparing the mean resilience values of dominant trees by site. Green P-values represent significantly different means, whereas red P-values represent insignificantly different means, at an alpha of 0.05.

Two-sample T-test	Johannahoeve 1	Johannahoeve 2	Oerle	Leersum
Johannahoeve 1		0.3027	0.02293	0.08831
Johannahoeve 2	0.3027		0.6604	0.06139
Oerle	0.02293	0.6604		0.0002006
Leersum	0.08831	0.06139	0.0002006	

3.3a Canopy positions

The Lloret indices were calculated on a yearly basis under the assumption that year-specific events caused the differences in these indices between sites. In this study, the indices were calculated for co-dominant individuals too, in order to infer if possible effects of year-specific events were distributed evenly. The Boxplots are displayed in appendix 5 to 8.

In general, there were only minimal differences in the Lloret indices between the canopy positions. The codominant groups appeared to have a slightly higher resistance and also longer recovery periods, but differences were small. Where differences in resistance and recovery periods were large, they were not structural across all sites. Johannahoeve 2 did not conform to the trend of the other sites and sees lower resistance values for all codominant trees, but not to an equally large degree for every year. Resilience is effectively equal between the canopy positions everywhere.

When the Lloret indices of the dominant groups were tested against the means of the codominant group by a two-sample T-test, the differences were insignificant on all sites for every index.

Table 8: P-values of two-sided two-sample T-tests comparing the mean lloret indices between the dominant and codominant group of the site. The cells are coloured red to indicate that the values are insignificant at an α of 0.05.

Two-sample T-test	Johannahoeve 1	Johannahoeve 2	Oerle	Leersum
Resistance	0.07248	0.06424	0.3786	0.6589
Recovery	0.3858	0.6856	0.1014	0.881
Resilience	0.3764	0.5348	0.07092	0.8109

3.4 Climate correlations

Variation in abiotic conditions through time on the sites could be determined by variation in climatic conditions. The various components of this climate could be correlated to the detrended ring width series. These yielded correlation coefficients on a monthly basis, going from June in the previous year, to September of the evaluated year. These coefficients were then gathered for both the entire life history in plots and in moving window correlograms for specific months. The correlograms give insight in how the coefficients change throughout the years.

3.4a Johannahoeve 1

The black cherries in Johannahoeve 1 appear sensitive to climatic conditions in the late summer and in the winter. Every climatic condition correlated with ring widths significantly in the month July for both figure 16 and 17. Ring widths were larger in years with cooler and wetter July months. High winter temperatures also correlated to larger ring widths, as did precipitation in January. Precipitation only started correlating significantly from 1987 onwards, as can be seen in figure 17. This figure also shows that SPEI values correlated in the winter months of January to March until 1988, but no longer afterwards.

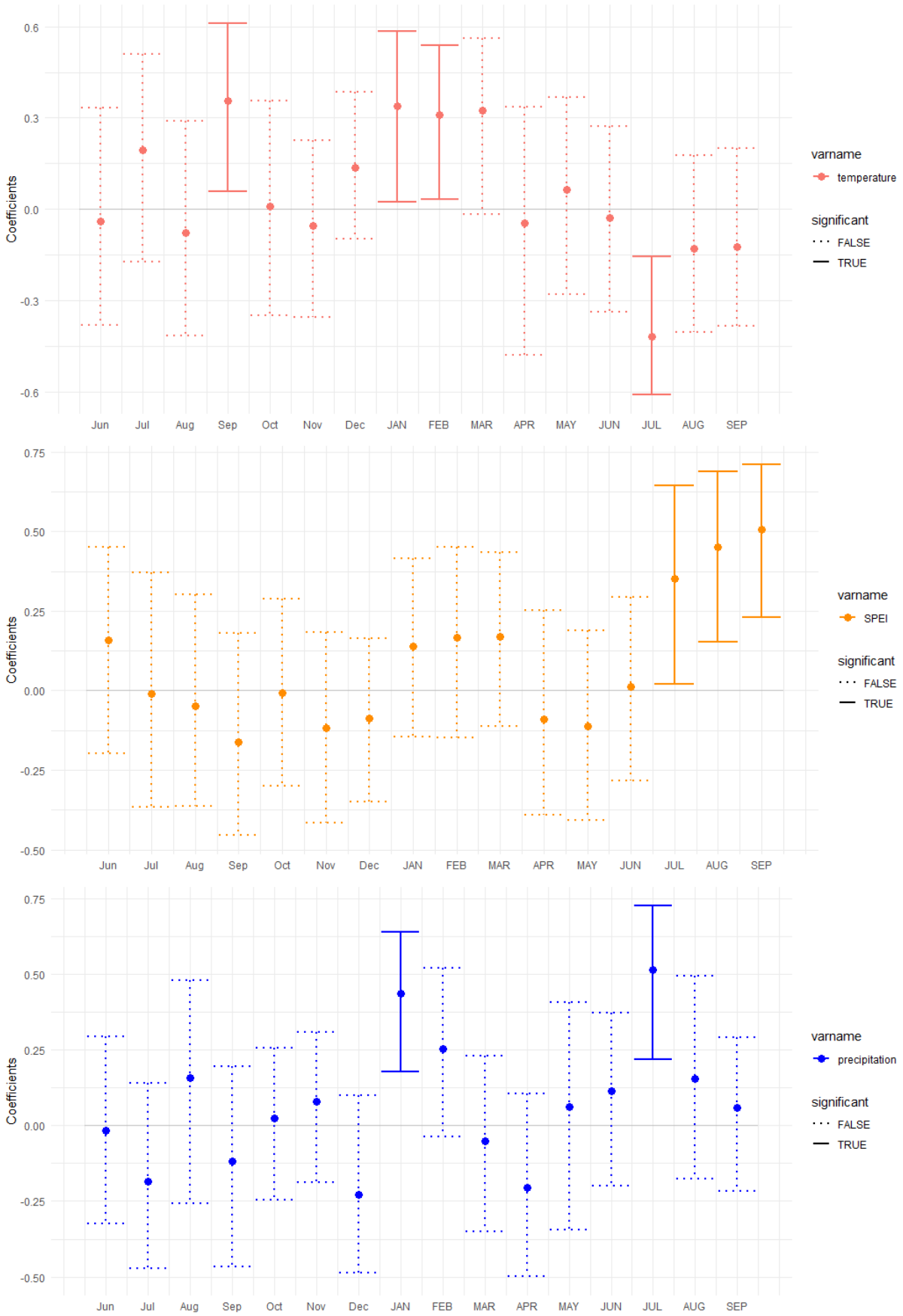

Figure 16: Plots of the correlation values between temperature (red), SPEI (orange) and precipitation per month with the ring-width series of Johannahoeve 1.

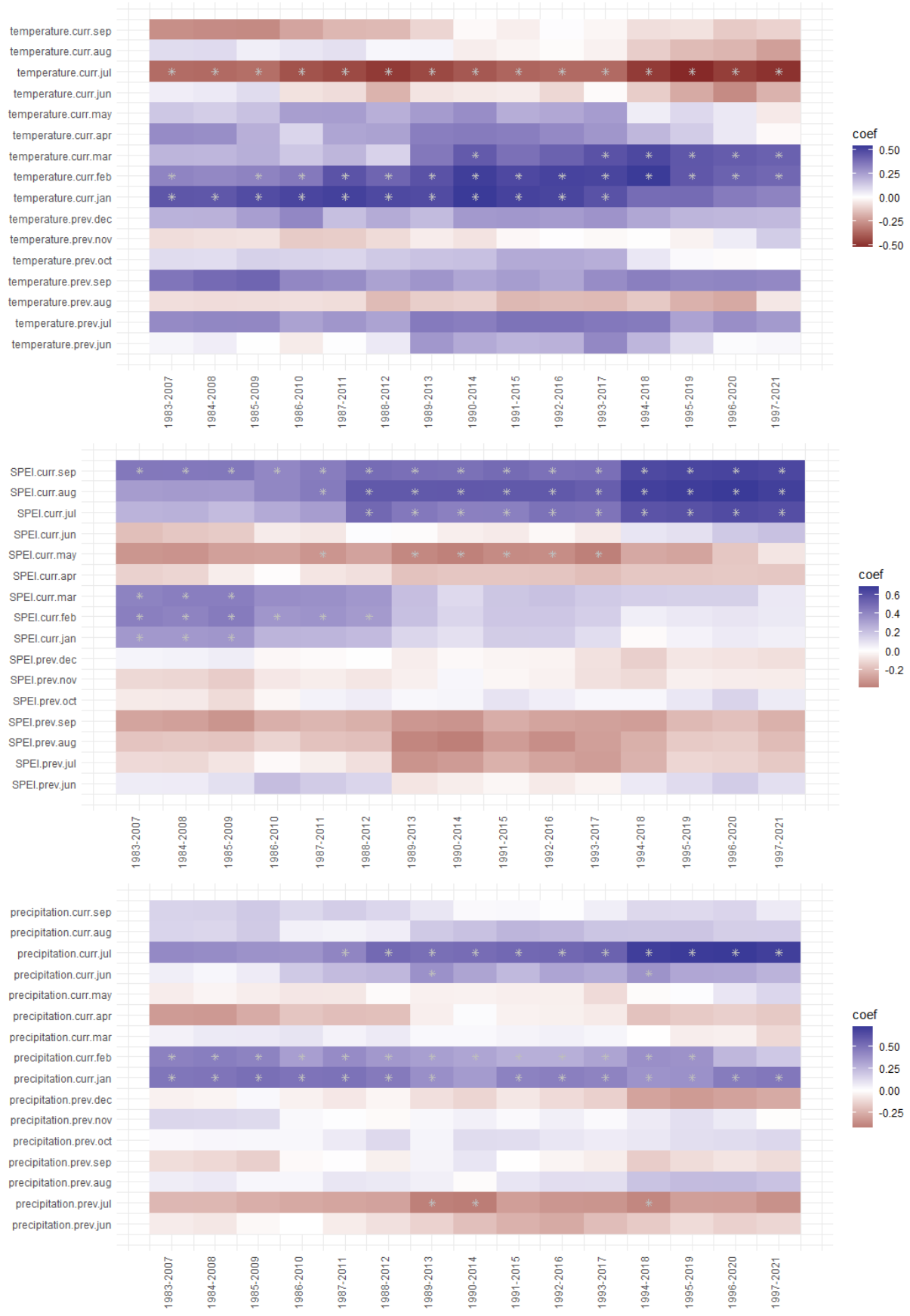

Figure 17: Correlograms of moving window growth correlations with temperature, SPEI and precipitation throughout 1983 to 2021 for Johannahoeve 1. Months in which these climatic variables correlated significantly are marked with a star.

3.4b Johannahoeve 2

Unlike the nearby Johannahoeve 1, ring widths of the black cherries in Johannahoeve 2 correlated less to strongly to summer temperatures, to the point of insignificance. Significant correlation with mean maximum temperatures was only observed during the winter month of December in figure 18. This also applied to the months of January, February and March between 1986 and 2017 when these months are viewed in specific years of figure 19. Though not visible in figure 18, figure 19 shows that the 1993-2017 period and onwards also saw significantly larger ring widths in years with higher mean maximum September temperatures in their respective preceding years.

While the mean maximum temperature may not have seen significantly less growth in the years with higher mean maximum temperatures in the summer months, the drought index and precipitation did retain significant correlations with growth in the summer months. These are August and September for SPEI and July for precipitation, according to figure 18. In figure 19, this effect was limited to the month September specific year ranges, starting from the 1994 -2018 period. Positive correlation was also observed for the month March in the 1986 to 2013 period, and February for the 1988-2011 period. Ring widths were significantly larger in years with dryer May months in two isolated periods, those being 1983-2007 and 1986-2010.

Observed ring widths were frequently larger in the years with more February precipitation from 1986 to 2019, gradually shifting towards February in later years. The precipitation with September precipitation started correlating even higher with observed ring widths, starting from the 1994-2018 period.

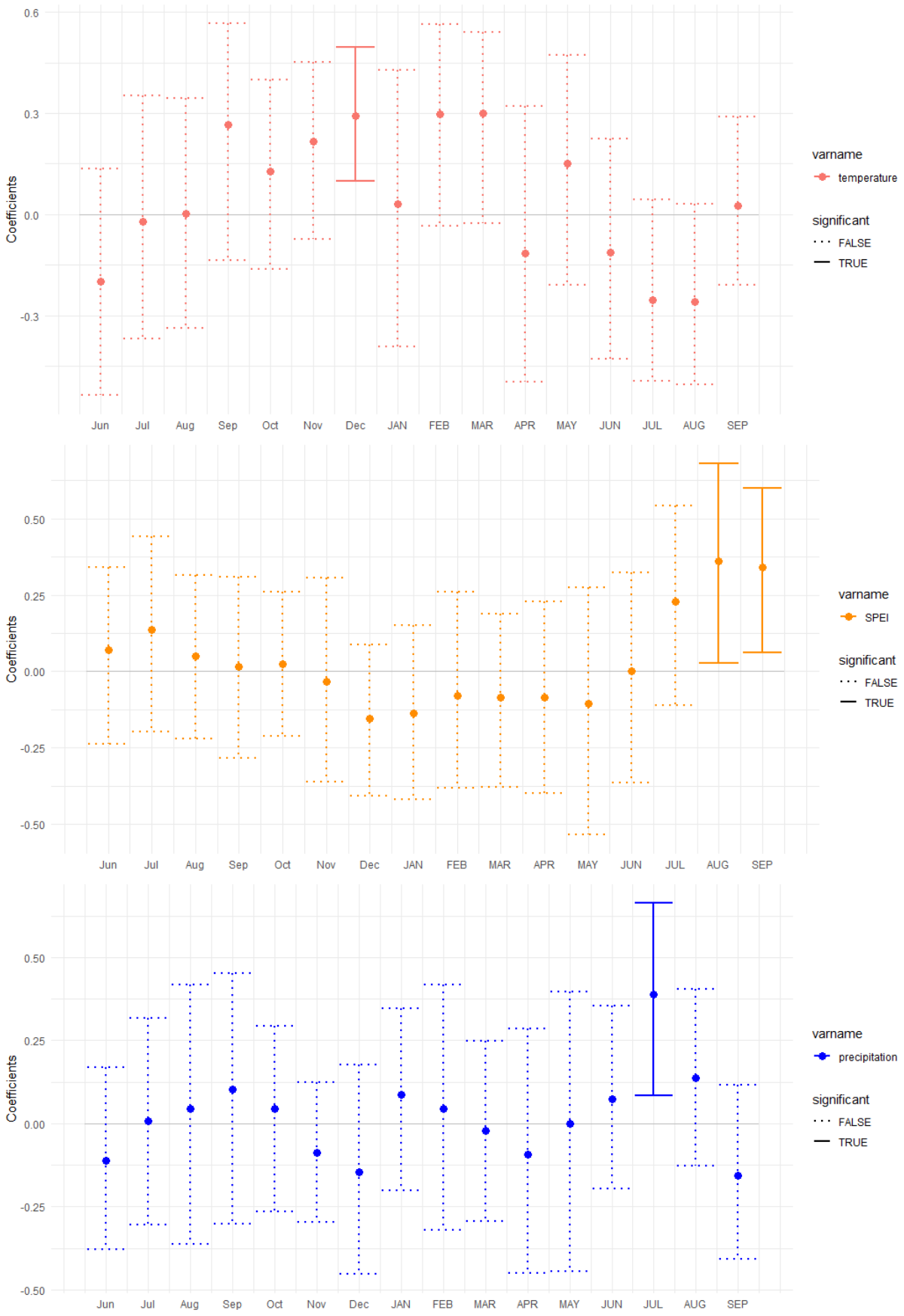

Figure 18: Plots of the correlation values between temperature (red), SPEI (orange) and precipitation per month with the ring-width series of Johannahoeve 2.

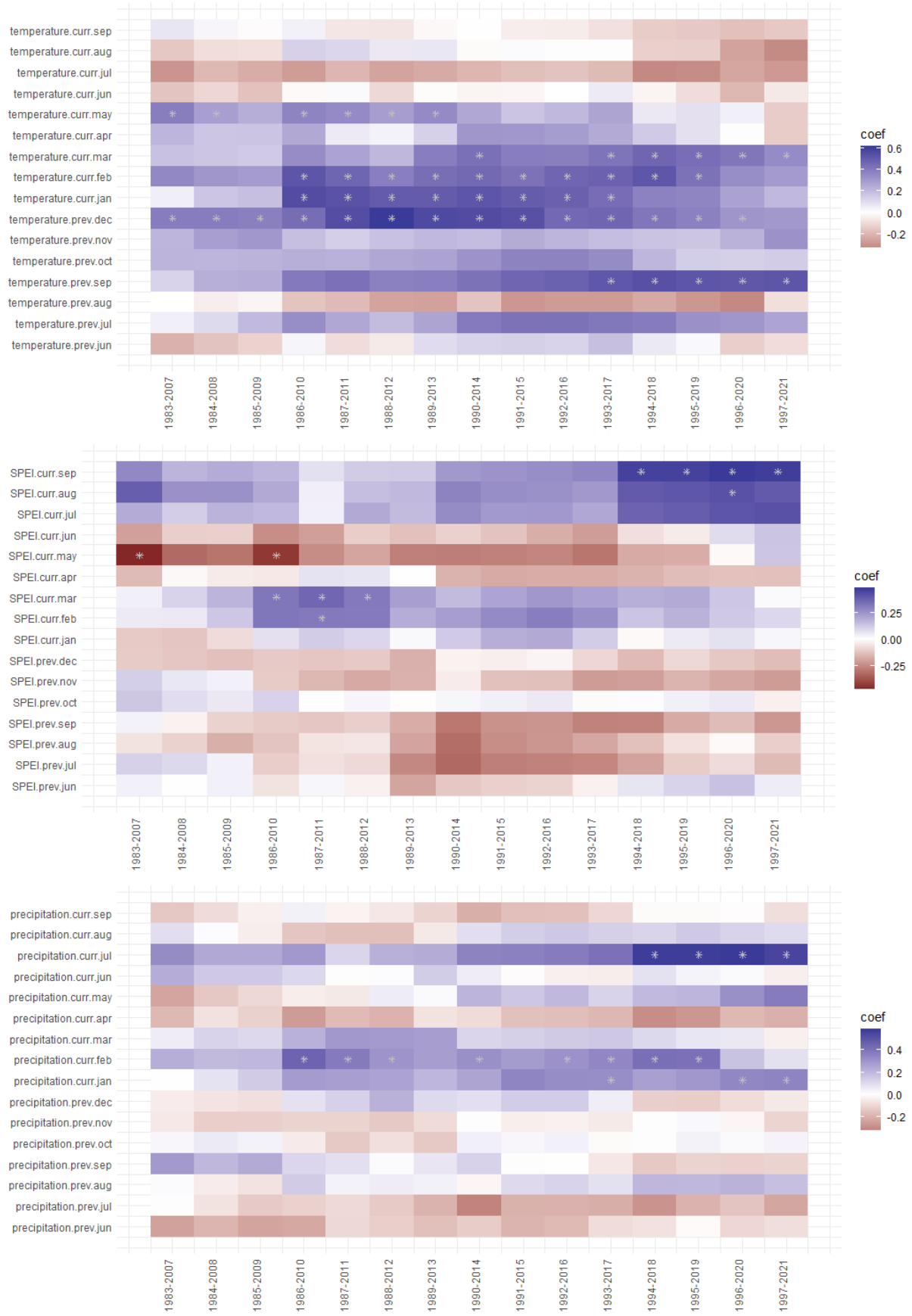

Figure 19: Correlograms of moving window growth correlations with temperature, SPEI and precipitation throughout 1983 to 2021 for Johannahoeve 2. Months in which these climatic variables correlated significantly are marked with a star.

3.4c Oerle

Ring widths from Oerle correlated negatively with high mean maximum temperature during the summer months, and significantly so when the mean maximum temperature was high in July of the previous year. The moving window growth correlations of figure 21 were different from that of other sites in that negative correlations were much more frequent and occurred outside of summer months as well. Incidentally, high mean maximum temperatures in the November months of the 1987-2011 period and the 1982-2016 period even had significantly negative correlations with ring widths during these periods. Negative correlation with July of the previous year was strongest and only significant during the 1988-2021 period. Positive correlation with mean maximum temperatures still occurred during the late winter months, but only significantly so for March in the 1992-2016 period.

Ring widths were larger in the years with more moist August months and preceding moist September, November and December months according to figure 20. The importance of moisture in the preceding August and September for growth in a year was only replicated for the early years of the black cherries, constituting the 1987-2012 period. With time, these correlations shifted towards October, November and December moisture. Growth always positively correlated with moist August and September months in their respective growth years, only starting to become insignificant for both months in the latest evaluated period of 1997-2021.

Correlations of the ring widths with the drought index of SPEI did not align with the correlations of precipitation values. In figure 20, this only occurred for precipitation in the previous September. In other months, precipitation correlated positively with ring width size where SPEI correlated negatively, significantly so in May. Ring widths were also larger in years with high precipitation in the preceding October. Unlike in figure 20, figure 21 saw growth correlate negatively with precipitation in the most recent September months of the 1985-2021 period. The adjacent month of August saw a positive correlation in contrast, for the 1998-2020 period. Precipitation in spring also tended to correlate to higher growth, significantly so in April of the 1989-2013 period and in May of the 1990-2014 and 1996-2021 periods. Precipitation correlated to larger ring widths in most consistently when it was high in September of the previous year, though this was no longer significantly so since the 1995-2019 period, the correlation with the preceding precipitation might be declining.

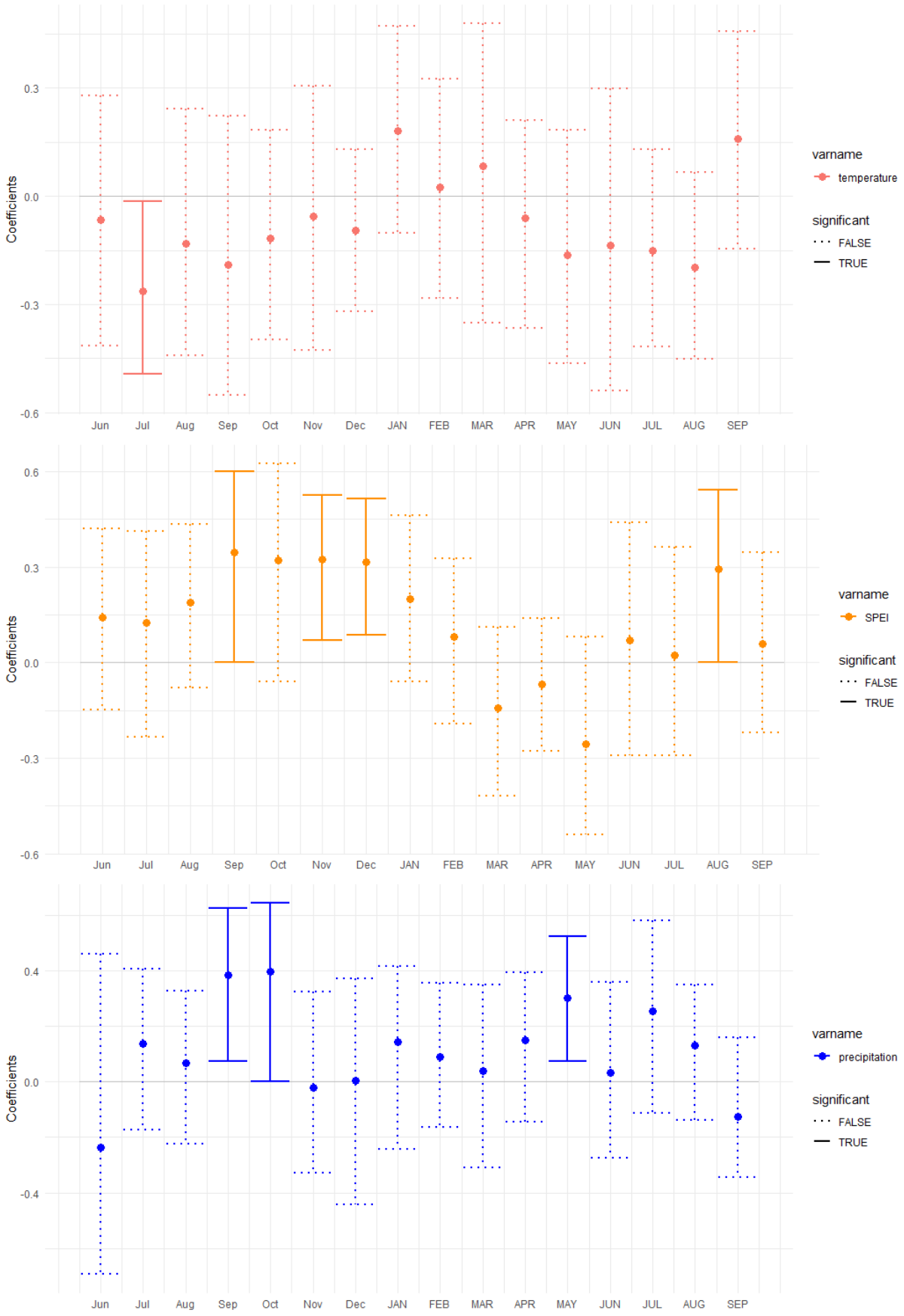

Figure 20: Plots of the correlation values between temperature (red), SPEI (orange) and precipitation per month with the ring-width series of Oerle.

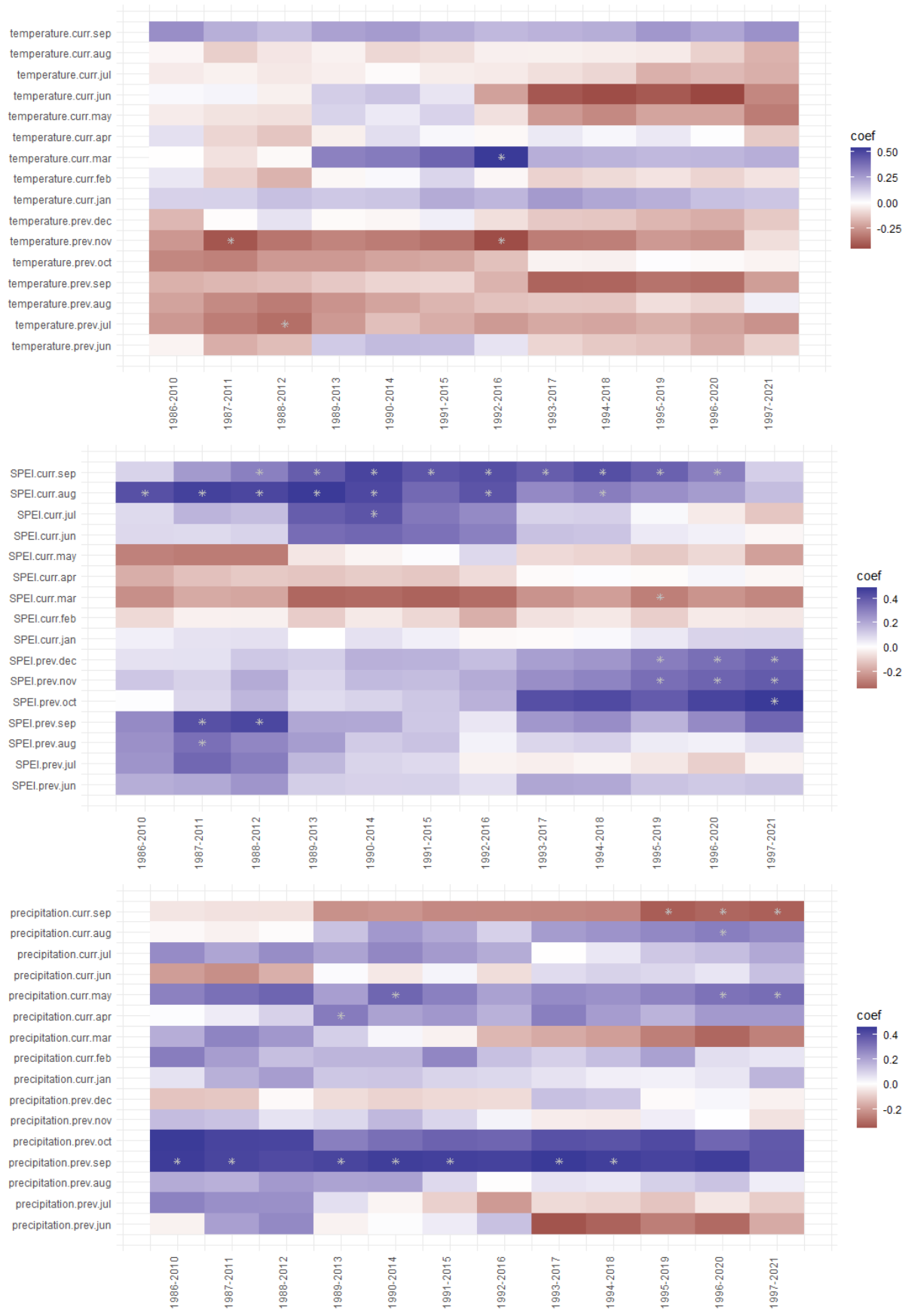

Figure 21: Correlograms of moving window growth correlations with temperature, SPEI and precipitation throughout 1986 to 2021 for Oerle. Months in which these climatic variables correlated significantly are marked with a star.

3.4d Leersum

In Leersum, ring width most prominently correlated to the climatic conditions in the summer. In Figure 22, temperature only correlated significantly with the ring widths in August, regardless of this month being the August of the preceding year or the same year of the ring width. This is replicated in Figure 23, though the correlation coefficients of mean maximum August temperatures in the year of the ring width declined into insignificance since the 1988-2012 period. While these correlation coefficients declined, a positive correlation emerged for the mean maximum temperatures in the winter: first in January and then also appearing in December, February and January. In the latest evaluated time period of 1997-2021, this correlation with high mean maximum winter temperatures only occurred for December.

The ring widths correlated significantly with high monthly SPEI values only in the months August and September according to figure 22. In Figure 23, this was replicated for the 1983-2011 period, with September SPEI values also correlating significantly with ring larger ring widths in the 1979-2003 and 1987-2012 periods. Ring width sizes also correlated significantly with SPEI values in a broad autumn and winter period, going from the preceding October to December starting with the 1979-2003 period, expanding towards the preceding august and March of the ring width year at it's extremes. These winter moisture correlations with ring width size disappear in the 1993-2021 period, even turning into negative, though still insignificant, correlations for the January months of the latest 1995-2021 period.

Yearly ring widths correlated positively with July precipitation both in figure 22 and 2021. Figure 23 reveals that this correlation coefficient between the ring widths and July precipitation declined into insignificance in the 1988-2021 period.

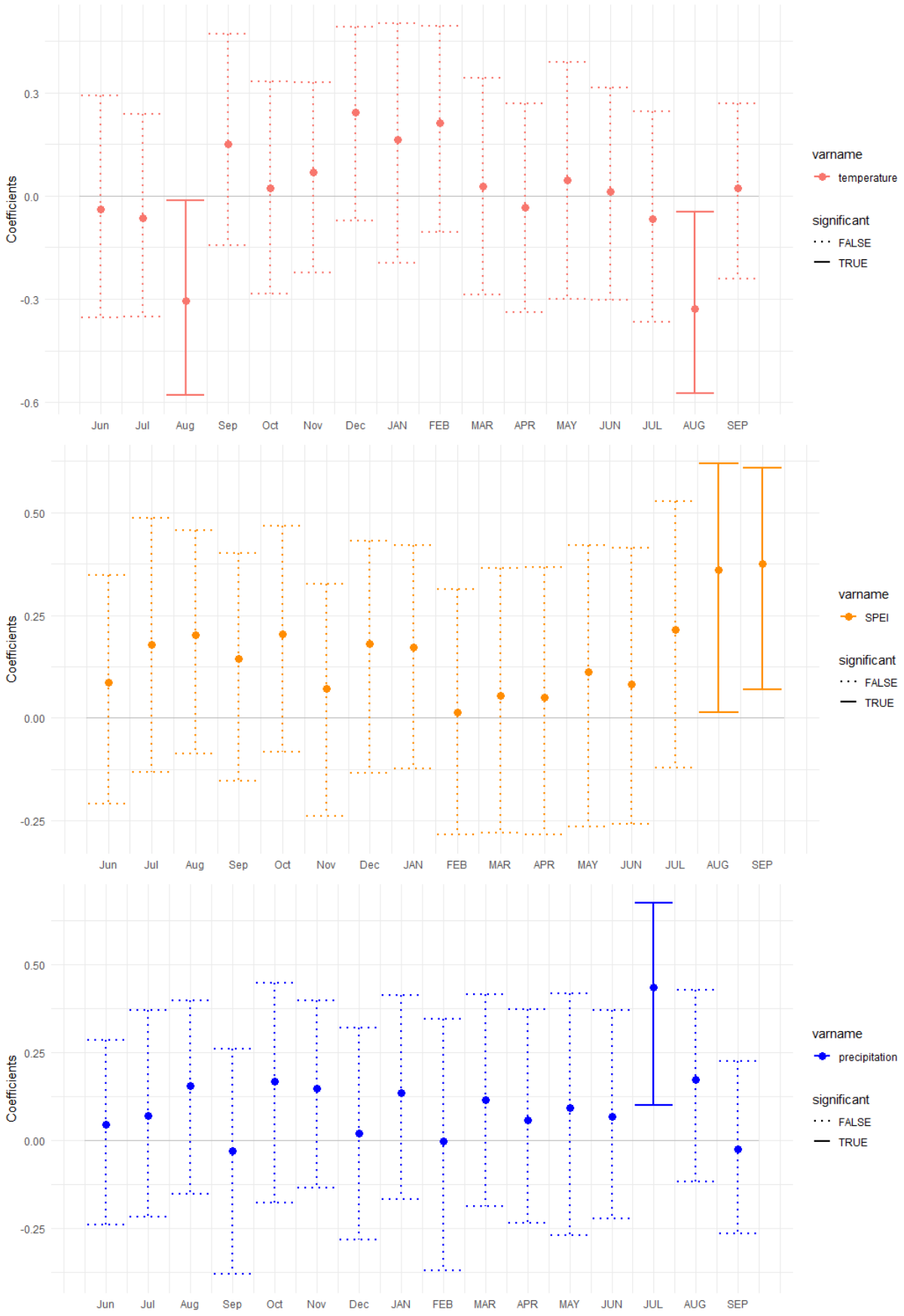

Figure 22: Plots of the correlation values between temperature (red), SPEI (orange) and precipitation per month with the ring-width series of Leersum.

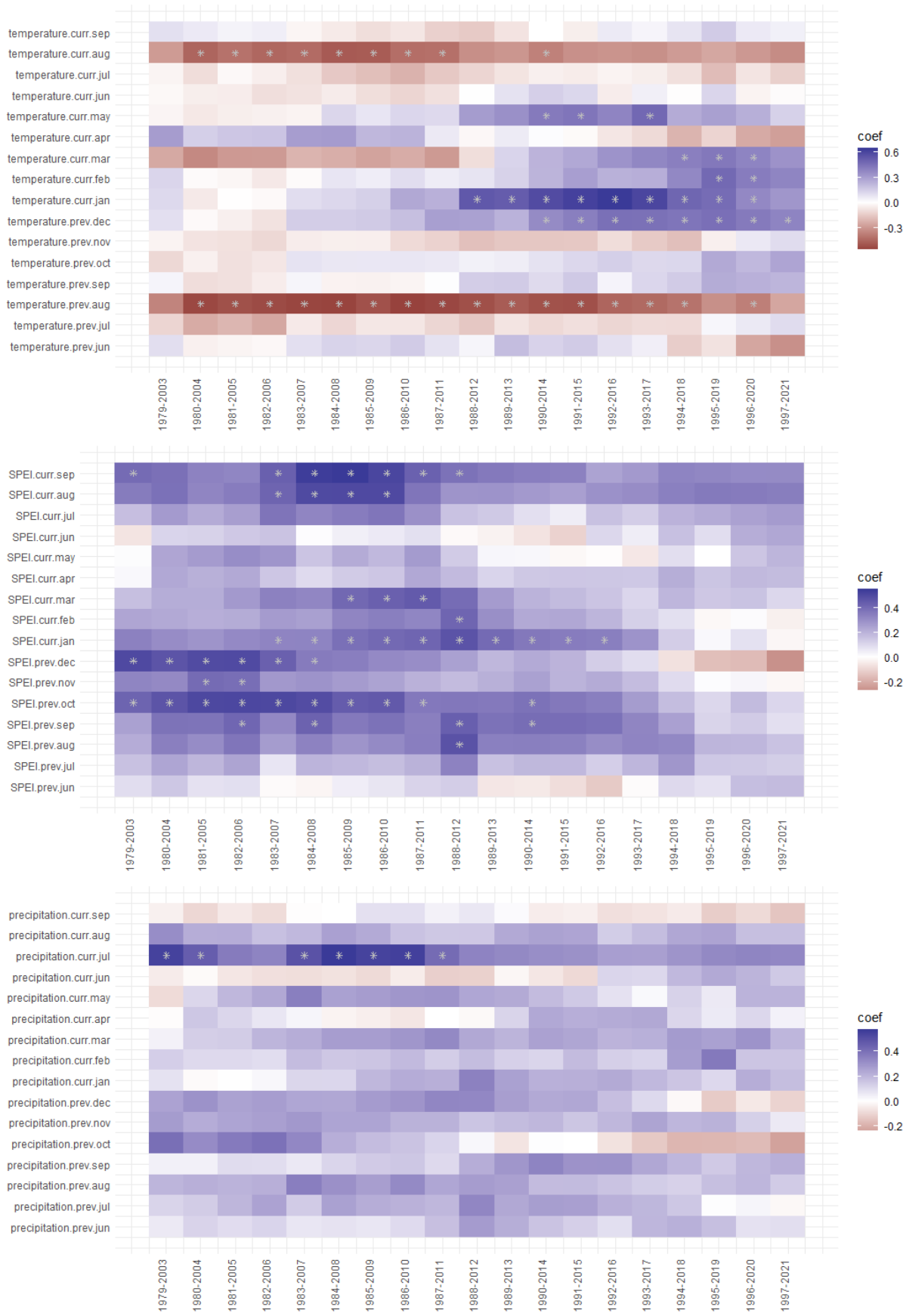

Figure 23: Correlograms of moving window growth correlations with temperature, SPEI and precipitation throughout 1979 to 2021 for Leersum. Months in which these climatic variables correlated significantly are marked with a star.

3.4e Canopy positions

To visualize the relative correlation values of each climate factor with the ring width chronologies for each site and canopy position, correlograms have been made and were gathered in figure 24. In addition to the mean maximum temperature, mean medium temperature and mean minimum temperature are also displayed.
These correlograms also divided the trees of each site in their respective canopy positions. Since this effectively cut the sample size in half, none of the correlation coefficients were high enough to achieve significance. At the sample sizes of 10, the correlation coefficients would have to have reached 0.648 or higher to achieve significance in a spearman correlation.

The correlation coefficients of Johannahoeve 1 were generally stronger for trees in the dominant canopy position for every climate condition.
In Johannahoeve 2, the climatic conditions have stronger correlations for July precipitation and temperatures in February and March, but not for the SPEI index in July.
In Oerle, the correlation of May precipitation was stronger for the dominant group, but the same precipitation correlated more strongly for the codominant group in September. Negative correlation with SPEI values in August to October in the dominant group was only replicated in August and October, but not September, where the correlation has become positive. The temperature correlations were strongest in July for the dominant group, but in September for the codominant group.
In Leersum correlation coefficients with climatic conditions were generally stronger for the codominant group, barring the August temperatures.

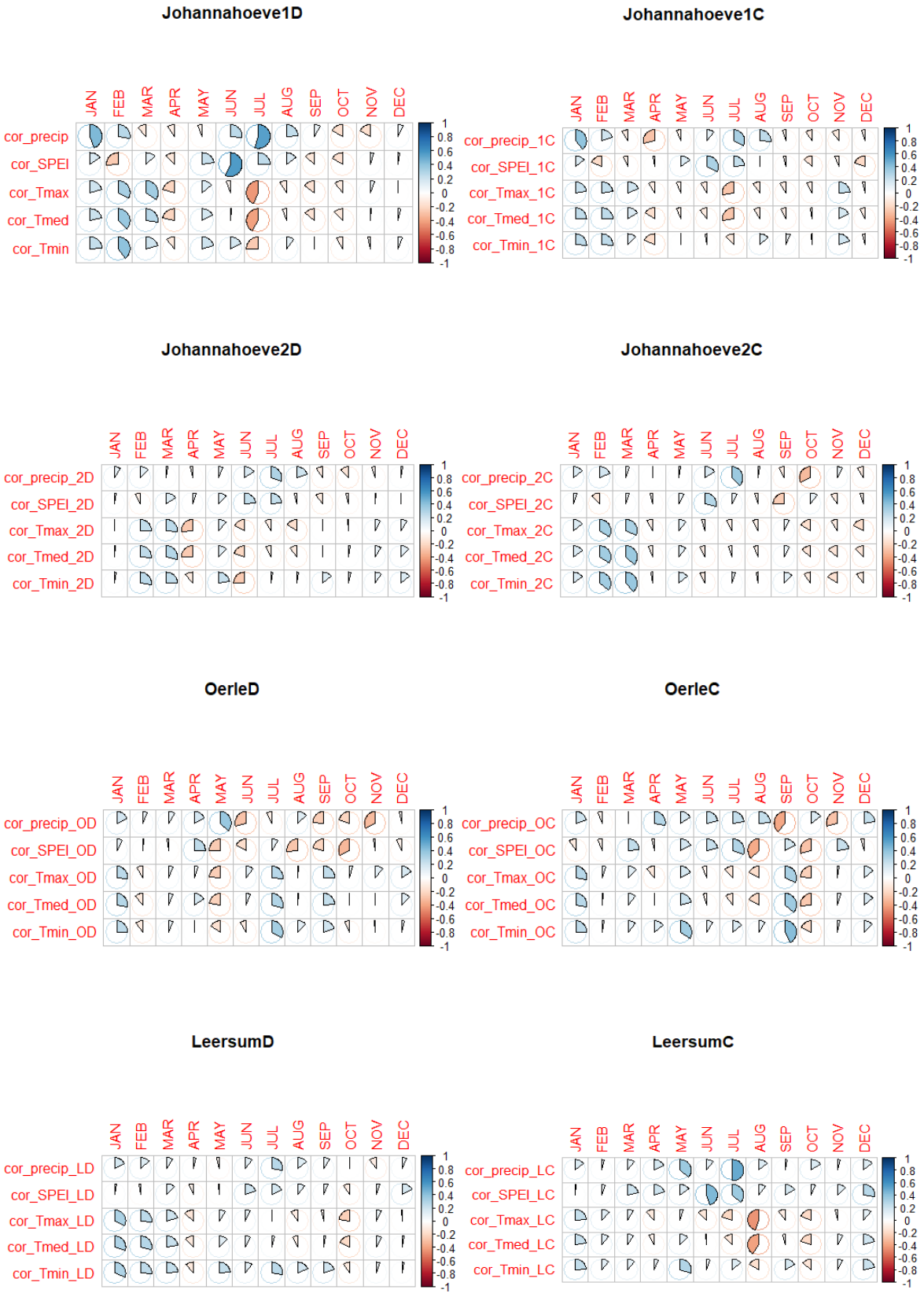

Figure 24: Correlograms of each climate factor correlated to detrended standard ring width chronologies, for each month on each site and canopy position. Positive correlations are shown in blue, whereas negative correlations are shown in red. The higher the correlation, the bigger the blue pie is. The farther below zero the correlation, the bigger the red pie is.

3.5 Linear models

Linear models were performed with the tree diameter at breast height as response variable and forest basal area and light intensity (called *Lichtintensiteit* in the models) as predictor variables, to see whether these predictors could have a moderating effect besides the climatic influences. Where applicable, the study sites were included in the models as factors.

```
Call:
lm(formula = Misc$DBH ~ Misc$Basal.area + Sites_vector, data = Misc)

Residuals:
     Min       1Q   Median       3Q      Max
-11.5515  -3.5326   0.0022   3.4211  10.2991

Coefficients:
                Estimate Std. Error t value Pr(>|t|)
(Intercept)      23.6612     2.8281   8.366 1.94e-11 ***
Misc$Basal.area  -0.3874     0.1051  -3.686 0.000516 ***
Sites_vectorL-   15.0635     1.6991   8.866 2.98e-12 ***
Sites_vectorO-    6.9574     1.9276   3.609 0.000656 ***
---
Signif. codes:  0 ‘***’ 0.001 ‘**’ 0.01 ‘*’ 0.05 ‘.’ 0.1 ‘ ’ 1

Residual standard error: 5.12 on 56 degrees of freedom
  (20 observations deleted due to missingness)
Multiple R-squared:  0.6133,     Adjusted R-squared:  0.5925
F-statistic:  29.6 on 3 and 56 DF,  p-value: 1.344e-11
```

The first model, including the forest basal area and study sites, explained a lot of the variance in DBH with an R squared of 0.5925. The measured DBH of the black cherries was modelled to be significantly lower in forests with a higher basal area. The sites were also modelled to be a significant factor. Oerle and especially Leersum had significantly higher DBH values than the reference factor, which in this case was Johannahoeve 1.

```
Call:
lm(formula = BAI.stat_5$mean ~ Misc$Basal.area + Sites_vector,
    data = BAI.stats)

Residuals:
      Min        1Q    Median        3Q       Max
-0.010571 -0.004535 -0.002305  0.003132  0.017966

Coefficients:
                 Estimate Std. Error t value Pr(>|t|)
(Intercept)     0.0126319  0.0040087   3.151  0.00275 **
Misc$Basal.area -0.0003845  0.0001469  -2.617  0.01169 *
Sites_vectorL-   0.0078599  0.0023142   3.396  0.00135 **
Sites_vectorO-   0.0007864  0.0028022   0.281  0.78015
---
Signif. codes:  0 ‘***’ 0.001 ‘**’ 0.01 ‘*’ 0.05 ‘.’ 0.1 ‘ ’ 1

Residual standard error: 0.00693 on 50 degrees of freedom
  (16 observations deleted due to missingness)
Multiple R-squared:  0.2307,     Adjusted R-squared:  0.1846
F-statistic: 4.999 on 3 and 50 DF,  p-value: 0.00414
```

In the second model, the response variable is replaced by the mean basal area growth of 2017-2021. The direction of change and significance are retained in this model, except for Oerle, which did not have a significantly different BAI compared to Johannahoeve 1. The R-squared of this model is just 0.1846.

```
Call:
lm(formula = Misc$DBH ~ Misc$Lichtintensiteit + Sites_vector,
    data = Misc)

Residuals:
    Min      1Q  Median      3Q     Max
-15.238  -3.991  -1.185   2.562  18.263

Coefficients:
                     Estimate Std. Error t value Pr(>|t|)
(Intercept)           24.1120     4.3642   5.525 2.76e-06 ***
Misc$Lichtintensiteit -0.4346     0.2584  -1.682 0.101082
Sites_vectorL-         9.6458     2.2325   4.321 0.000112 ***
---
Signif. codes:  0 ‘***’ 0.001 ‘**’ 0.01 ‘*’ 0.05 ‘.’ 0.1 ‘ ’ 1

Residual standard error: 7.023 on 37 degrees of freedom
  (40 observations deleted due to missingness)
Multiple R-squared:  0.3856,     Adjusted R-squared:  0.3524
F-statistic: 11.61 on 2 and 37 DF,  p-value: 0.0001218
```

The third model, including light, explains less variance than the model including the forest basal area. Light and the sites as factors result in an R-squared of 0.3524. Extra exposure to light would cause a decrease in DBH of the black cherries in this model, but the effect was insignificant. DBH was significantly higher in Leersum than in the reference site Johannahoeve 1. Johannahoeve 2 and Oerle were excluded from this model due to lack of light measurements there.

```
Call:
lm(formula = BAI.stat_5$mean ~ Misc$Lichtintensiteit + Sites_vector,
    data = BAI.stats)

Residuals:
      Min        1Q    Median        3Q       Max
-0.012989 -0.004883 -0.002434  0.004251  0.015898

Coefficients:
                      Estimate Std. Error t value Pr(>|t|)
(Intercept)           0.0188291  0.0053578   3.514  0.00134 **
Misc$Lichtintensiteit -0.0007922  0.0003265  -2.427  0.02105 *
Sites_vectorJ2         0.0019448  0.0087358   0.223  0.82525
Sites_vectorL-         0.0021028  0.0026913   0.781  0.44035
---
Signif. codes:  0 ‘***’ 0.001 ‘**’ 0.01 ‘*’ 0.05 ‘.’ 0.1 ‘ ’ 1

Residual standard error: 0.007874 on 32 degrees of freedom
  (34 observations deleted due to missingness)
Multiple R-squared:  0.1889,     Adjusted R-squared:  0.1129
F-statistic: 2.484 on 3 and 32 DF,  p-value: 0.07852
```

The fourth model is the same as the third model, but with the response variable DBH replaced again by the mean basal area growth of the 2017-2021 period. This model yields a different result, with light still reducing the value of the response variable (mean basal area increment), but this time significantly. The site vector also included Johannahoeve 2, despite this site not having light measurements taken. Both Johannahoeve 2 and Leersum did not significantly differ in their BAI in comparison to the reference site of Johannahoeve 1. The model had an insignificant F-statistic, which means this model performed worse than a model without independent variables.

```
Call:
lm(formula = Misc$DBH ~ Misc$Basal.area + Misc$Lichtintensiteit,
    data = Misc)

Residuals:
    Min      1Q  Median      3Q     Max
-7.4844 -4.2324 -0.8591  4.1531  7.3179

Coefficients:
                     Estimate Std. Error t value Pr(>|t|)
(Intercept)           39.9424     4.9365   8.091 3.13e-07 ***
Misc$Basal.area       -0.7190     0.1687  -4.261 0.000527 ***
Misc$Lichtintensiteit  0.5758     0.3031   1.900 0.074553 .
---
Signif. codes:  0 ‘***’ 0.001 ‘**’ 0.01 ‘*’ 0.05 ‘.’ 0.1 ‘ ’ 1

Residual standard error: 5.236 on 17 degrees of freedom
  (60 observations deleted due to missingness)
Multiple R-squared:  0.5172,     Adjusted R-squared:  0.4604
F-statistic: 9.105 on 2 and 17 DF,  p-value: 0.002052
```

The fifth model included both the forest basal area and light, but not the sites as factor. With 60 observations excluded, the site would become a constant: Leersum. Based only on data from this site, the model had an R squared of 0.4604, explaining less variance than the first model. Light is once again an insignificant factor, but would in this model increase DBH at higher light levels. The forest basal area in contrast, still significantly decreases DBH.

```
Call:
lm(formula = BAI.stat_5$mean ~ Misc$Lichtintensiteit + Misc$Basal.area,
    data = BAI.stats)

Residuals:
      Min        1Q    Median        3Q       Max
-0.013502 -0.004938 -0.001617  0.005847  0.015948

Coefficients:
                      Estimate Std. Error t value Pr(>|t|)
(Intercept)           0.0271685  0.0074970   3.624   0.0021 **
Misc$Lichtintensiteit -0.0001157  0.0004603  -0.251   0.8046
Misc$Basal.area       -0.0005525  0.0002562  -2.156   0.0457 *
---
Signif. codes:  0 ‘***’ 0.001 ‘**’ 0.01 ‘*’ 0.05 ‘.’ 0.1 ‘ ’ 1

Residual standard error: 0.007951 on 17 degrees of freedom
  (50 observations deleted due to missingness)
Multiple R-squared:  0.2894,     Adjusted R-squared:  0.2058
F-statistic: 3.462 on 2 and 17 DF,  p-value: 0.0548
```

The sixth model, which is the same as the fifth model, but with the DBH replaced again by the mean basal area increment of the 2016-2021 period, also showed the forest basal area, but not light, as a significant effect. This model differs from the fifth model in that the negative estimate for light means that greater exposure to light would decrease the basal area increment of the black cherries in this model, rather than increase it. The model had an insignificant F-statistic, which means this model performed worse than a model without independent variables.

The scatterplots of these values in Figure 25 show DBH decreasing at both higher forest basal area and higher light levels. Of the separate model fits, the plot with light intensity appeared to have a greater slope. However, it is also visible that the fit of the light intensity variable is weaker. The scatterplots show different data points due to incomplete measurements.

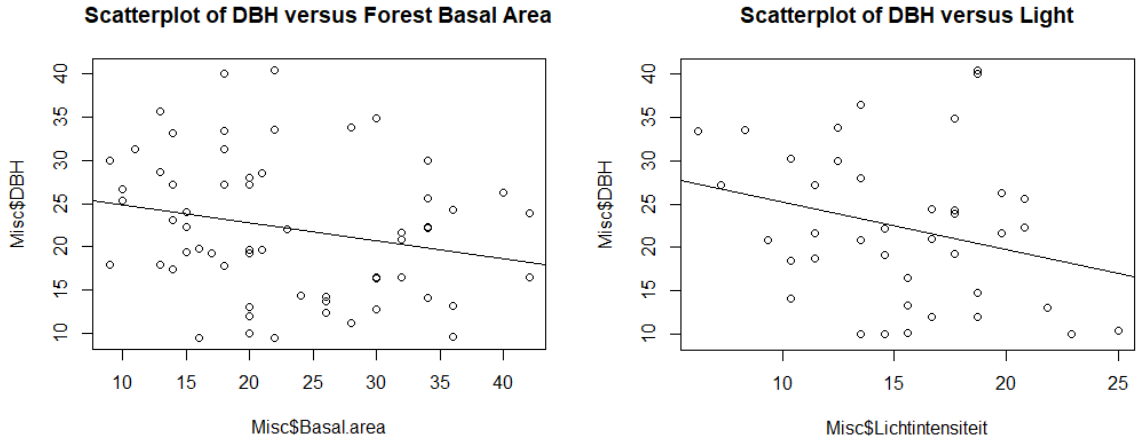

Figure 25: scatterplots of BAI versus forest basal area (left) and light intensity (right) respectively.

3.6 Mixed Models

When comparing the mean growth values, the soil appeared to make a significant difference. A one-way ANOVA supported this notion when the means across three different grain sizes were compared. Since the values of grain size, as well as the soil types, were each unique to a single site (with Johannahoeve being counted as one), the results of this test identical to the same test with the soil type as a categorical variable. Since Johannahoeve only featured one soil type, but two sites, replacing the grain size by sites as the grouping factors, resulted in a more significant difference between the means.

```
            Df Sum Sq Mean Sq F value    Pr(>F)
M50_Factor   2 0.1167 0.05835   14.35 5.05e-06 ***
Residuals   77 0.3131 0.00407
---
Signif. codes:  0 ‘***’ 0.001 ‘**’ 0.01 ‘*’ 0.05 ‘.’ 0.1 ‘ ’ 1
```

```
             Df Sum Sq Mean Sq F value   Pr(>F)
Sites_vector  3   2326   775.2   20.87 5.81e-10 ***
Residuals    76   2823    37.1
---
Signif. codes:  0 ‘***’ 0.001 ‘**’ 0.01 ‘*’ 0.05 ‘.’ 0.1 ‘ ’ 1
```

The spread of these means became visible in the plots of figure 26, from the post-hoc Tukey test. Trees growing on plots with higher values of M50, meaning larger grain sizes, deviated towards smaller mean growth, whereas trees growing on plots with lower values of M50 deviated towards comparatively larger mean growth. However, the difference in means between an M50 of 210 and an M50 of 310 is insignificant. According to the post-hoc test, the difference in mean growth on plots was only significant when the one plot has a grain size double that of the other.
While the F-test was identical with the soil type as a categorical variable, the post-hoc Tukey differed in its parameters. The outcome was the same however, with only the Hd21 soil-type significantly differing from the rest. This corresponded with the mean growth in the Johannahoeve differing significantly with the mean growth in Oerle and Leersum. The different means between grain sizes corresponded with these sites in the same way.

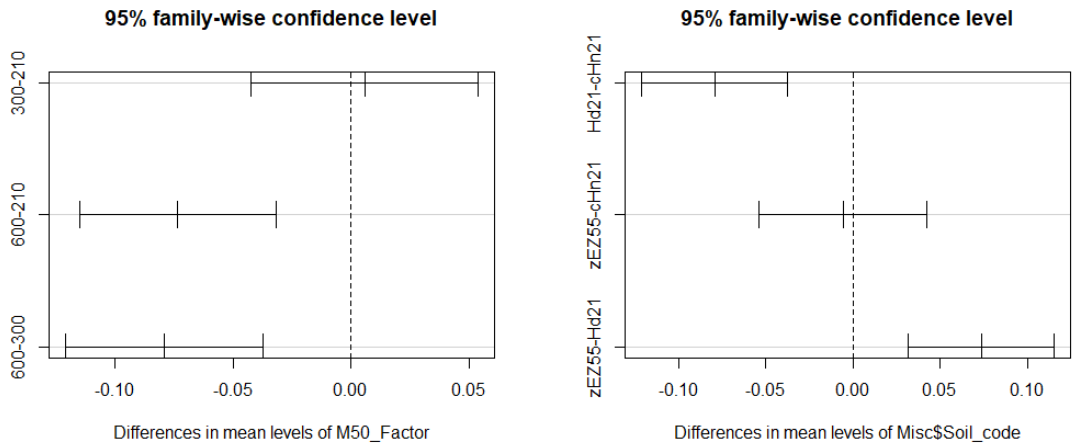

Figure 26: Plots of the post-hoc Tukey-test of the ANOVAs grouped by grain size (left) and soil type (right)

This effect is also replicated in figure 27 when the same ANOVA was performed with the sites, rather than the soil, as a grouping factor. The means of Oerle and Leersum and of Johannahoeve 1 and 2 differed not much more or less than zero, whereas any other combination saw larger differences in the means.

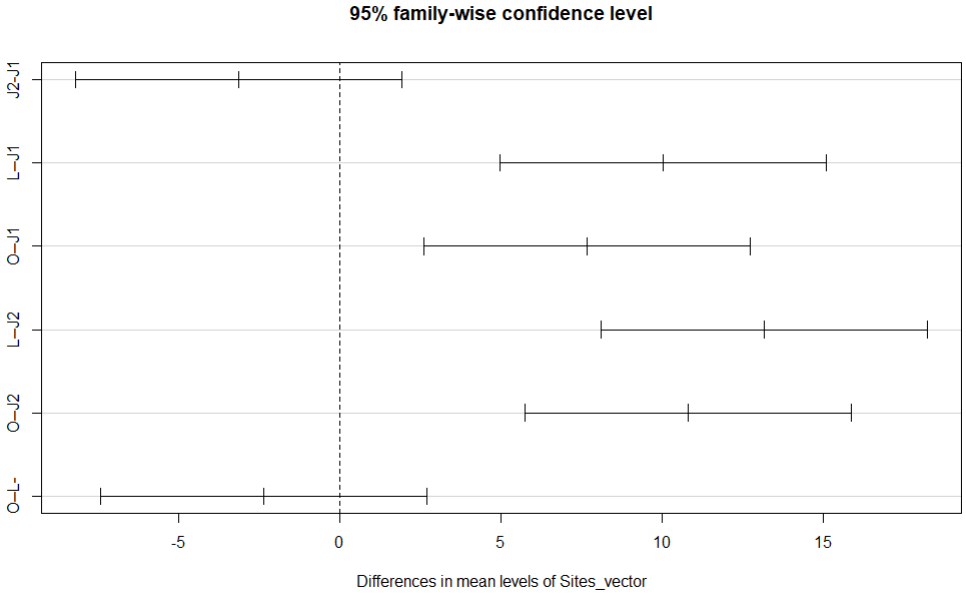

Figure 27: Plot of the post-hoc Tukey-test of the Anova grouped by Site

A linear mixed model has been performed with the site as the grouping variable and light and stand basal area as fixed effect variables. This model assumed that an increase in basal area or light would result in a change in mean diameter growth in a opposite direction. The size of this effect may, however, vary depending on the site.

```
Linear mixed model fit by REML. t-tests use Satterthwaite's method
[lmerModLmerTest]
Formula: value ~ variable + (1 | Sites_vector)
   Data: Molten_data

REML criterion at convergence: 1216.7

Scaled residuals:
     Min       1Q   Median       3Q      Max
-1.67160 -0.78108 -0.05002  0.66036  2.32829

Random effects:
 Groups       Name        Variance Std.Dev.
 Sites_vector (Intercept) 10.91    3.303
 Residual                 50.88    7.133
Number of obs: 180, groups:  Sites_vector, 4

Fixed effects:
                   Estimate Std. Error      df t value Pr(>|t|)
(Intercept)          20.908      1.834   3.770  11.402 0.000465 ***
variableBasal_area    1.831      1.265 176.628   1.447 0.149727
variableLight        -7.603      1.503 176.605  -5.059 1.05e-06 ***
---
Signif. codes:  0 ‘***’ 0.001 ‘**’ 0.01 ‘*’ 0.05 ‘.’ 0.1 ‘ ’ 1

Correlation of Fixed Effects:
            (Intr) vrblB_
variblBsl_r -0.274
variablLght -0.231  0.257
```

The mixed model shows a reverse understanding of the linear models. Instead of light, basal area was an insignificant positive predictor for DBH, whereas light became a significant negative predictor for DBH in the mixed model.

```
Linear mixed model fit by REML. t-tests use Satterthwaite's method
[lmerModLmerTest]
Formula: value ~ variable + (1 | Sites_vector)
   Data: Molten_data

REML criterion at convergence: 971

Scaled residuals:
    Min      1Q  Median      3Q     Max
-2.2015 -0.3984 -0.1301  0.7652  3.1709

Random effects:
 Groups       Name        Variance Std.Dev.
 Sites_vector (Intercept)  7.711   2.777
 Residual                 25.145   5.015
Number of obs: 160, groups:  Sites_vector, 4

Fixed effects:
                    Estimate Std. Error       df t value Pr(>|t|)
(Intercept)          -0.2138     1.5133   3.4665  -0.141    0.895
variableBasal_area   24.1010     0.9363 155.8421  25.742   <2e-16 ***
variableLight        13.9246     1.1079 156.9222  12.568   <2e-16 ***
---
Signif. codes:  0 ‘***’ 0.001 ‘**’ 0.01 ‘*’ 0.05 ‘.’ 0.1 ‘ ’ 1

Correlation of Fixed Effects:
            (Intr) vrblB_
variblBsl_r -0.248
variablLght -0.216  0.288
```

A repeat of this mixed model, in which the dependent variable is replaced by the mean basal area increment of each tree of the years 2017 to 2021, yielded different results yet again. Limited to these years, both the forest basal area and light were predictors of higher basal area increment in this model.

3.7 Site comparisons

Unconstrained ordination of the detrended ring-width series In figure 28, subsequently grouped by site, revealed that the investigated black cherries grew differently depending on what site it grew. The two sites in the Johannahoeve, however, appeared not to be too distant from each other in terms of their variance in ring width history, forming a group. Cherries from Oerle and Leersum formed their own groups distinct from the other sites. Cherries within Oerle showed most of its variance to be across the second component axis, whereas all other sites vary strongest across the first component axis. When the PCGA ranks were tested for differences between sites, Oerle and Leersum were both confirmed to vary distinctly from each site, whereas the Johannahoeve sites are confirmed to have similar variance.

Table 9: P-values of pairwise comparison Wilcoxon rank sum exact tests of pca ranks grouped by site.

```
Pairwise comparisons using Wilcoxon rank sum exact test

data:  All_pcga$rank and Sites_vector
```

	J1	J2	L
J2	0.27663		
L	8.2e-06	8.3e-06	
O	0.00478	0.03907	0.00042

```
P value adjustment method: holm
```

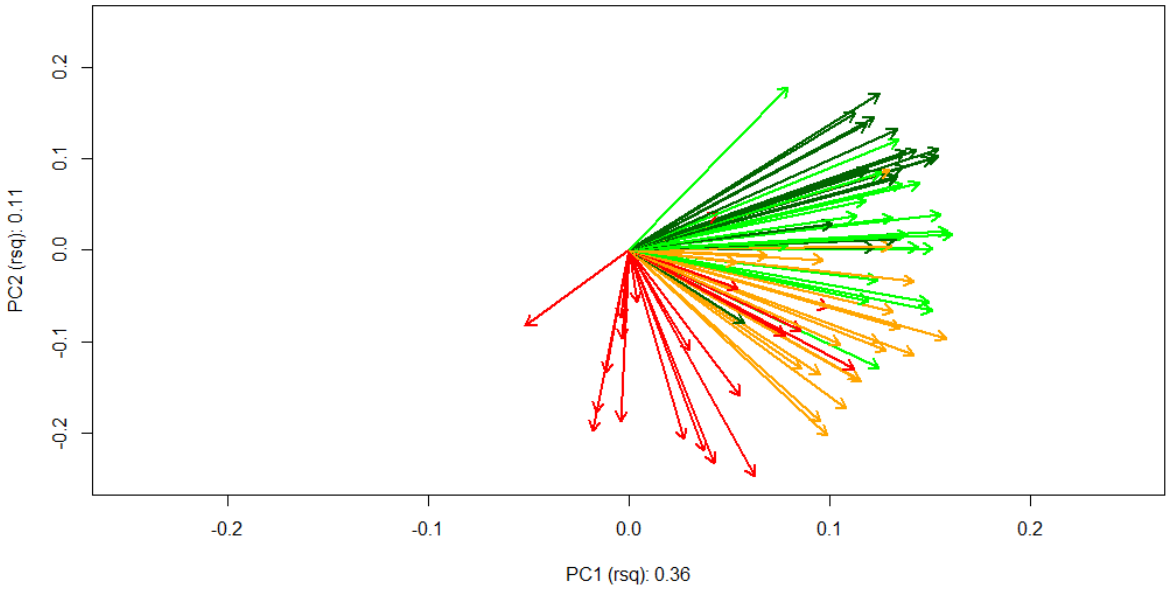

Figure 28: Unconstrained ordination of the detrended ring-with series colour-coded by site. Dark green represents trees from Johannahoeve 1. Light green represents trees from Johannahoeve 2. Gold represents trees from Leersum. Red represents trees from Oerle.

A simple comparison between sites was made by displaying the mean growth values in boxplots, grouped by site, as in Figure 29. The boxplots show a clear distinction between the Johannahoeve sites on the one hand and Leersum and Oerle on the other hand. The medians of the second group exceeded the maximum growth values found in Johannahoeve 2. While Johannahoeve 1 still displays overlap with the upper 4th quartile when it comes to undetrended radial growth values, the basal area increment does not exceed the upper 3rd quartile of Leersum and Oerle. These overlaps were replicated when grouping the same increment data by local soil type.

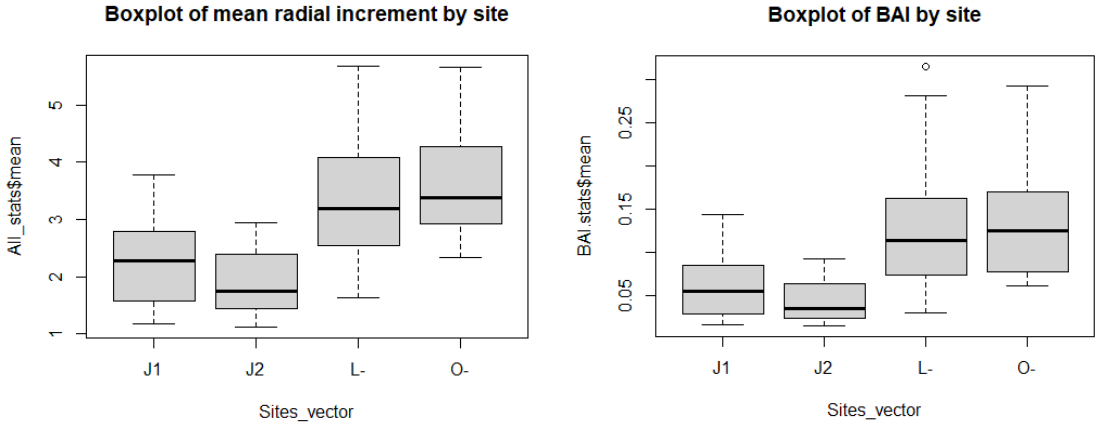

Figure 29: Boxplots displaying the distribution of mean radial increment in mm (left) and mean Basal Area Increment (Right) grouped by site.

4 Discussion

4.1 Interpretation of results

4.1a Climate

The correlations with climatic variables (figures 16 to 24) show that monthly weather conditions can be quite influential, but not equally important for every site. The climatic conditions are most influential during the late summer, where the growing season approaches its end. The significant correlations of the climate conditions in the summer months with growth, suggest that the summer conditions could determine when the growing season ends. During this study, black cherry has been observed shedding still-green foliage as early as 15th of June. Black cherries can shed their leaves during the growing season when in drought stress to reduce water loss through transpiration (Ryan, 2011). Should the summer months be too hot and dry, the black cherries could prevent damage by ending their growing seasons somewhat prematurely. This mechanism would allow good recovery in the following year, but reduces or eliminates radial growth in the remainder of the year.

Even though correlations with precipitation were only significant in specific months, like July for Leersum in figure 22: black cherries without access to groundwater remain dependent on it throughout the year. This is visible through the many positive correlations with precipitation in winter and autumn months for precipitation and SPEI. Even if groundwater cannot be reached, autumn precipitation could provoke a hormonal response in the black cherry to produce primordial leaf buds, which are more likely to survive the warmer winters (Pan et al., 1997), thus also resulting in significantly positive correlations of tree ring widths and winter temperatures of the year, as observed in this study.

All combined, it appears that black cherry is able to deal well with droughts in the Netherlands so far. Regardless of when just one occurs, or three in a row, the black cherries are able to return to the growth rates that were attained before these droughts. But that does not make the black cherry invincible. It should be noted that in this sampling design, only black cherry individuals were sampled that lived to see the year 2022, adding a risk of survivorship bias. Mortality has undoubtedly taken place in the investigated sites before sampling took place. One of the trees selected for sampling in Johannahoeve 2 even died before the sampling took place, most likely by windthrow, prompting sampling of an extra tree. With only surviving dominants and codominants sampled, there is no indication of whether mortality increased during drought years compared to other years. Black cherry growth can definitely be impaired by the ever more frequent droughts as they grow more extreme. The survivors are at least not impaired in their vitality thus far.

4.1b Soil

Both the ring-width series (figure 5 & 6) and the resistance indices calculated from them (figure 12 to 15) are in line with the growth behaviour expected from the hypothesis. Black cherries in the Netherlands indeed suffer some growth reductions when drought years occur. While the resistance index tended to be lower in the Johannahoeve sites, the recovery index was higher on these two sites. This dichotomy between the two xeric sites on the one hand, and the two mesic sites on the other (figure 29) suggest that the soil is one of the most important of the investigated factors in determining mean growth. While the ANOVA was not constructed using only data from drought years, the significant influence of grain size fortifies the importance of the soil towards radial growth in general. The dichotomy between the index values during drought years then becomes logical, since between the investigated sites, the dichotomy of soil types is also a dichotomy of grain sizes, and thus water holding capacities. During a drought on a sandy soil without groundwater access, the water holding capacity logically becomes a limiting factor, resulting in growth dependency on climate, which is also visible through the larger coefficients of climate correlations on the xeric sites compared to the mesic sites. The null hypothesis that radial growth is equal on the xeric sandy soils and the on mesic sandy soils has thus been rejected by this study.

The main hypothesis of the introduction, which points towards abiotic conditions as the driver of resistance and biotic conditions as the driver of recovery has not been not rejected. This is on the basis of the significant differences in resistance between sites and the dichotomy of xeric and mesic sites with regards to recovery. The driver of resistance remains unclear, since the geographical position of the tree does not reflect purely abiotic or biotic drivers. The recovery, however, differs significantly between xeric and mesic sites, pointing towards soil moisture, an abiotic factor, being the main driver of recovery.

4.1c Shade and competition

The linear models have also shown that it is difficult to identify an effect of biotic conditions on radial growth. If present, it is likely drowned out by the abiotic conditions. Grouping the sites in a mixed model resulted in very different coefficients and significances. The difference points towards a greater importance of the growing sites, which largely correspond to differences in soil. The Lloret indices of Oerle were also often so different from those in the other sites that it would appear Oerle did not experience droughts simultaneously with the other sites, as the different SPEI-values between the sites suggest. Precipitation data confirms this, for example, for the year 2017, where the Eindhoven weather station saw less precipitation than De Bilt weather station until July (KNMI, 2022b). Oerle reacted differently to climatic variation than other sites. Ring widths from Oerle correlated negatively with high temperatures outside of summer months (figure 21) more often than the other sites, for example. These differences could possibly be explained by the one feature that sets Oerle apart from the other investigated sites. The heterogenous forest structure and its resulting forest climate may have shielded the black cherries during drought years, improving their resistance, and decreasing their recovery, since there is little growth loss to recover from. Something which could also explain the slightly higher resistance of codominant individuals (Appendix 7). As a trade-off, growth reduction is experienced in other years than drought years by the competitive pressure in this forest climate. Something black cherry is known to be susceptible to (Marquis, 1990).

Conversely, the basal area measurements, a proxy variable for competition intensity on the site, do

not support the notion that Oerle is a more competitive environment. When averaged (table 2) the basal area of Oerle is the lowest of all investigated sites.

Light intensity cannot be adduced to support any claims about competitiveness here, since light measurements have not taken place in Oerle. A mistake in the sampling design also meant that no light measurements could be taken from Johannahoeve 2 either. Here, interception was supposed to be measured in the summer to allow the maximum interception by fully grown leaves. But as this site had stem discs taken instead of cores, the crown was already opened by the felled trees, preventing representative light interception values from being obtained. For these reasons, only half of the sites have light interception measurements, weakening the power of the linear and mixed models in which it was included.
Canopy positions could thus make for a more suitable proxy to deduce shade levels, since codominant trees and trees in less favourable positions are more shaded than dominant trees by definition. When viewed through this lens, the insignificant differences in Lloret indices between the canopy positions (table 6) are line with the insignificance of light levels most linear models and the first mixed model, but not the fourth linear model and second mixed model.

Alternative explanations are possible for the strange performance of basal area as a measure of competition. Oerle had, for example, a comparatively low stem density. While not recorded specifically, stem density appeared much higher in Johannahoeve 1. Stem density was high here because in this even-aged stand, all the trees were still in the late pole stage, where trees are relatively thin and compete in height to reach or stay in the crown. This is in contrast to Oerle, which is not mono-aged and which is relatively open underneath the crown, which includes potentially older trees of other species. The measured basal area was highest in Leersum, even though most of the black cherries stood next to an empty field of grass, letting more light reach the forest floor and crowns than in Oerle. This portrays the larger diameter of the black cherries in Leersum compared to other sites, rather than the severity of the competition for light, for which stem density would likely have made a more suitable proxy variable, given that none of the sites have recently been subject to forest management. It should also be noted that the investigated black cherries are still young enough to react to openings in the forest canopy (Auclair & Cottam., 1971; Marquis, 1990), meaning that the black cherry adapts to its new situation, rather than suffer from the change.

The null hypothesis that there is no difference in radial growth on a shade gradient is rejected by this study on the basis of the basal area in the linear models and light in the mixed models. But care should be taken when generalizing this result, since these models with, which notably have conflicting results, are on the basis of incomplete forest basal area measurements and lacking measurements of light in the year 2022, compared alternatively to a DBH that is the result of growth years with and without drought and unknown historical stand dynamics or to the mean basal area increment restricted to the latest five year period towards 2021. Models like the first mixed model suggest light could be detrimental to diameter growth, possibly through increased evapotranspiration. But this seems unlikely since the model that is limited to the BAI values of the most recent rings, of which three out of five formed during drought years, point towards light having a beneficial effect on radial growth despite the droughts.
Should the null hypothesis be based on the indices of resistance, recovery and resilience, rather than radial growth, the hypothesis would not be rejected on the basis of the statistically equal reaction to drought by both the dominant and codominant canopy positions.

4.2 Comparison to existing knowledge

Growth behaviour of the black cherries in relation to the soil humidity fits the general expectation for angiosperms during drought. Resistance and especially resilience is determined in large part by the soil humidity, rather than the intensity of the drought, as DeSoto et al. (2020) suggest.
With regards to the soil humidity, black cherries in the Netherlands appear to share the preference for mesic soil moisture that is also found in North America (Marquis, 1990).

The variation of the Ring-Width index is about equal to that of black cherries on riparian sites of Pennsylvania between 1984 and 1995, which varied between 0.5 and 1.40 (Abrams et al., 1998). The Ring-width chronologies are different in that those of Pennsylvania rarely reached, before the sampling date of 1996, an RWI of 1 or above since 1988, indicating a decline. This is especially true for the Pennsylvanian cherries on mesic sites. The black cherries of the Netherlands, investigated in this study, saw both positive and negatives extremes occur immediately after each other. This holds true for every Dutch site investigated and also holds true for the mesic valleys and xeric ridges of Pennsylvania. The dry-mesic barrens are more similar to the Dutch ring-width chronologies. Since Dutch black cherries did not experience this decline in their first twenty years, as is visible in figure 6 and figure 30, it is unlikely to be an age-related trend.

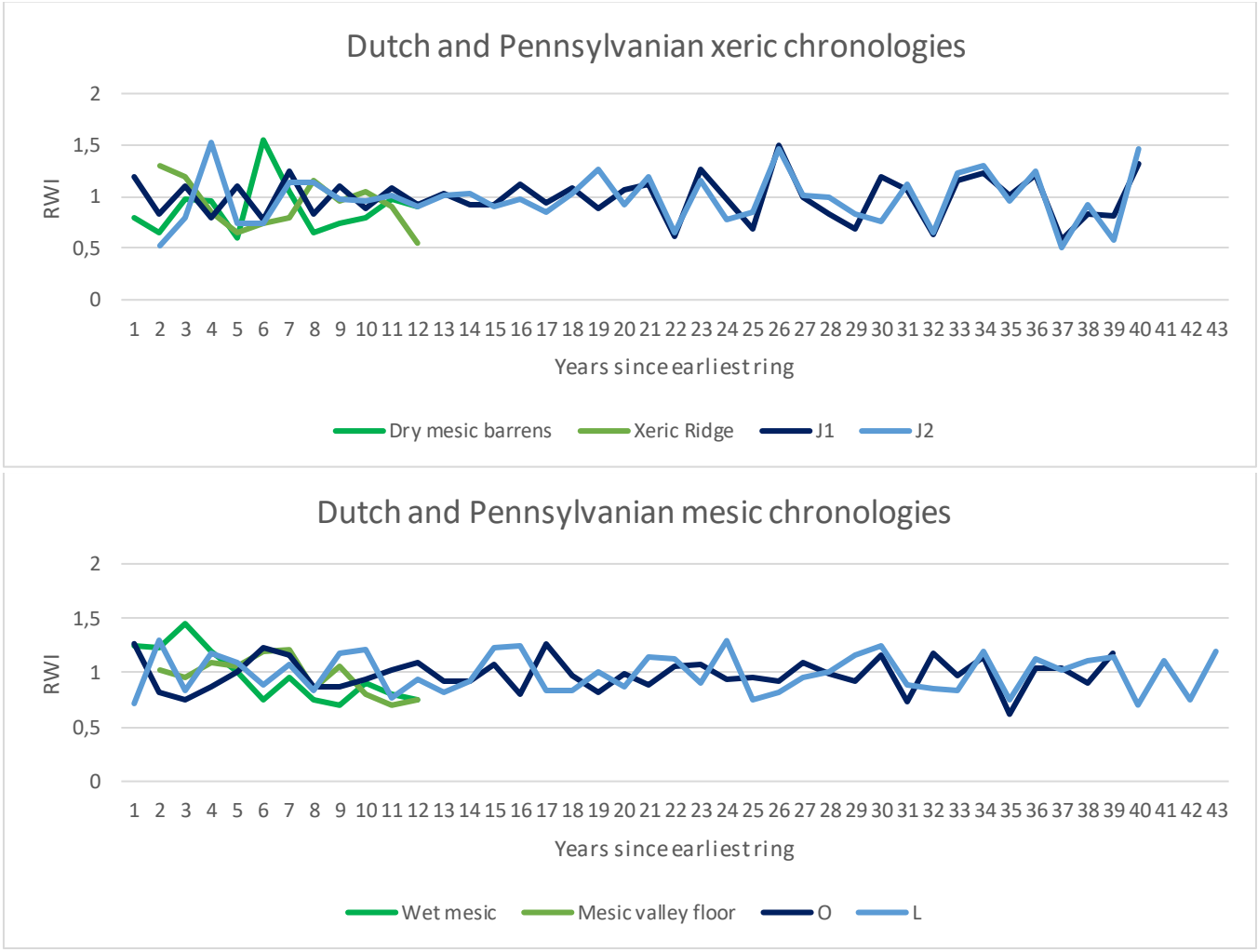

Figure 30: The RWI chronologies of this study and the approximated RWI chronologies from Abrams et al. (1998) plotted together, grouped by soil moisture. Dutch chronologies are plotted in variants of blue. Pennsylvanian chronologies are plotted in variants of green.

While the climates and even the decennia of these chronologies are far removed from each other, it suggests the possibility of recovery rates being larger in the Netherlands than in Pennsylvania for the black cherry. Alternatively, it could be an effect of an unusually high frequency of droughts for Pennsylvania at four droughts in ten years (Abrams et al. 1998).
Black cherries in the Netherlands seem to benefit more from precipitation than its American counterparts. The correlation between RWI and precipitation there ranged from 0.12 to 0.38 (Abrams et al., 1998) and 0.2 for a study of 1993 black cherries in West Virginia (Pan et al., 1997), while the RWI of the black cherries from Johannahoeve 1 had a correlation exceeding 0.5, with Johannahoeve 2 and Oerle having a correlation of around 0.3. These Dutch values are limited to July, however, rather than the whole summer, and only concern the median of the site, rather than the extremes.
In contrast to precipitation, the negative correlation between the temperatures and RWI was farther below zero for the Pennsylvanian black cherries than the Dutch ones. For the Pennsylvanian cherries, this correlation ranged from -0.54 tot -0.46 (Abrams et al., 1998). For the Dutch cherries, this ranged from almost -0.4 for Johannahoeve 1, to just under 0 at -0.05 for Leersum. Since the Pennsylvanian black cherries are much younger at only twelve to twenty years old at the time of their sampling (Abrams et al., 1998), it could be possible that the Pennsylvanian black cherries were growing in younger stands or clearances, where the forest structure is less stratified than in the Dutch stands of 2022. If these younger stands or clearances were less able to moderate moisture loss, that could explain such strongly negative correlations because of a greater sensitivity to high temperatures and therefore evapotranspiration. The black cherries of the West Virginia study, for example are older, featuring trees stemming from the 1940's, while correlating negatively with July temperatures at about -0.15 (Pan et al., 1997).
Correlations between the RWI and drought indices were similar in the Netherlands to those in Pennsylvania. Correlations varied a lot here depending on the soil humidity. Correlations were smaller at the mesic sites both in Pennsylvania and the Netherlands, whereas correlations were larger on the xeric sites. Note that the drought index used in the US study (Abrams et al., 1998) is the Palmer Drought Severity Index (PDSI) instead of the Standardized Precipitation Evapotranspiration Index (SPEI). This means that these values are not directly comparable, although they are both indicative of drought severity.
The correlations compared here, differ in that none of the Pennsylvanian climate-growth correlations are significant. Insofar as variation in the climatic indicators of precipitation, drought and temperature determines the growth rates of black cherry, these indicators were not the decisive factors when the whole growth histories of the black cherries are concerned in Pennsylvania. In the Netherlands and West Virginia however, all climate variables were influential at some point in the year for every site. This raises the question of what causes the differences between the Pennsylvanian and other sites. Plausible causes can be found in the age differences, sample sizes and forest structures and the climate. Since climate extremes become more frequent in the Netherlands, the current climate is beginning to resemble the climate that Pennsylvania had in the late 20th century. Dutch black cherries smaller sensitivity to heat, but larger sensitivity to precipitation, might be a result of growing in less species diverse sites, which might be less able to moderate extreme heat and to retain moisture. It could also result from a difference in soils despite the qualifications as mesic and xeric soils or even forest management, if it took place in the Pennsylvanian sites. The given background information in the studies of Abrams et al. (1998) Pan et al. (1997) and of this study do not overlap enough to find a definitive cause.

5. Conclusions

Prunus serotina radial growth on fully drained sandy soils in the Netherlands declines during drought years. *Prunus serotina* is nevertheless well able to recover from such drought years, often experiencing better growth immediately after a drought than immediately before this drought. The time period needed for this recovery is minimal. This is despite growth in a year frequently being dependent the temperature, precipitation and moisture of both the current and previous year. Radial growth is better on mesic sandy soils than on xeric sandy soils. While grain size appears to be among the most important of the investigated mechanisms on the investigated sites, other factors that were not investigated are likely more influential in determining radial growth in the general life history of the investigated trees. Among those could be competition mechanisms, since the less relevant competition by basal area is of significant influence. While shade might still be helpful in protecting against desiccation depending on the model, canopy positions make little difference in *Prunus serotina's* growth response to drought.

6 References

Abrams, M. D., Kloeppel, B. D., & Kubiske, M. E. (1992). Ecophysiological and morphological responses to shade and drought in two contrasting ecotypes of *Prunus serotina*. *Tree physiology*, *10*(4), 343-355.

Abrams, M. D., Ruffner, C. M., & Morgan, T. A. (1998). Tree-ring responses to drought across species and contrasting sites in the ridge and valley of central Pennsylvania. *Forest Science*, *44*(4), 550-558.

Auclair, A. N., & Cottam, G. (1971). Dynamics of black cherry (*Prunus serotina* Erhr.) in southern Wisconsin oak forests. *Ecological Monographs*, *41*(2), 153-177.

Auclair, A. N. (1975). Sprouting response in *Prunus serotina* Erhr.: Multivariate analysis of site, forest structure and growth rate relationships. *American Midland Naturalist*, 72-87.

Beguería S, Vicente-Serrano SM, Reig F, Latorre B. (2014). Standardized precipitation evapotranspiration index (SPEI) revisited: parameter fitting, evapotranspiration models, tools, datasets and drought monitoring. *International Journal of Climatology* 34(10): 3001-3023.

Bunn, A., & Korpela, M. (2020). An introduction to dplR. *Washington University: Seattle, WA, USA*.

Buras, A. (2022). dendRolAB: Analytical tools for tree-ring data. R package version 0.3.

Buras, A., Ovenden, T., Rammig, A., & Zang, C. S. (2022). Refining the standardized growth change method for pointer year detection: accounting for statistical bias and estimating the deflection period. *Dendrochronologia*, 125964.

Bussotti, F., Pollastrini, M., Holland, V., & Brueggemann, W. (2015). Functional traits and adaptive capacity of European forests to climate change. *Environmental and Experimental Botany*, *111*, 91-113.

Cailleret, M., Jansen, S., Robert, E. M., Desoto, L., Aakala, T., Antos, J. A., ... & Martínez-Vilalta, J. (2017). A synthesis of radial growth patterns preceding tree mortality. *Global change biology*, *23*(4), 1675-1690.

CBS, PBL, RIVM, WUR (2020). Jaarlijkse hoeveelheid neerslag in Nederland, 1910-2019 (indicator 0508, versie 08 , 24 april 2020). Retrieved February 2nd 2022 from https://www.clo.nl/indicatoren/nl0508-jaarlijkse-hoeveelheid-neerslag-in-nederland Centraal Bureau voor de Statistiek (CBS), Den Haag; PBL Planbureau voor de Leefomgeving, Den Haag; RIVM Rijksinstituut voor Volksgezondheid en Milieu, Bilthoven; en Wageningen University and Research, Wageningen.

Closset-Kopp, D., Saguez, R., & Decocq, G. (2011). Differential growth patterns and fitness may explain contrasted performances of the invasive *Prunus serotina* in its exotic range. *Biological Invasions*, *13*(6), 1341-1355.

DeSoto, L., Cailleret, M., Sterck, F., Jansen, S., Kramer, K., Robert, E. M., ... & Martinez-Vilalta, J. (2020). Low growth resilience to drought is related to future mortality risk in trees. *Nature communications*, *11*(1), 1-9.

Foundation for Statistical Computing. (2021). R: A language and Environment for Statistical Computing. Vienna, Austria. *htttps://www.R-project.org*

Grissino-Mayer, H. D. (2001). Evaluating crossdating accuracy: a manual and tutorial for the computer program COFECHA.

Het Kadaster. (2022). *Topotijdreis: 200 jaar topografische kaarten*. Retrieved July 26th, 2022 from: https://www.topotijdreis.nl

Holmes, R. L. (1983). Computer-assisted quality control in tree-ring dating and measurement.

Hough, A. F. (1960). Silvical characteristics of black cherry (*Prunus serotina*). *Station Paper NE-139. Upper Darby, PA: US Department of Agriculture, Forest Service, Northeastern Forest Experiment Station. 26 p.*, *139*.

KNMI. (2022a). *KNMI - Klimaatviewer*. Retrieved February 2, 2022, from KNMI.nl: https://www.knmi.nl/klimaat-viewer

KNMI. (2022b). *KNMI - Maand- en jaarwaarden*. Opgehaald van knmi.nl: https://www.knmi.nl/nederland-nu/klimatologie/maandgegevens

Krejza, J., Cienciala, E., Světlík, J., Bellan, M., Noyer, E., Horáček, P., ... & Marek, M. V. (2021). Evidence of climate-induced stress of Norway spruce along elevation gradient preceding the current dieback in Central Europe. *Trees*, *35*(1), 103-119.

McDowell, N., Pockman, W. T., Allen, C. D., Breshears, D. D., Cobb, N., Kolb, T., ... & Yepez, E. A. (2008). Mechanisms of plant survival and mortality during drought: why do some plants survive while others succumb to drought?. *New phytologist*, *178*(4), 719-739.

Nyssen, B., Den Ouden, J., Verheyen, K., & Vanhellemont, M. (2016). Integrating black cherry in forest management in the Netherlands and Belgium. In *Introduced tree species in European forests: opportunities and challenges* (pp. 362-372). European Forest Institute.

Nyssen, B., Koopmans, B., & Den Ouden, J. (2019). *Beslisboom Amerikaanse vogelkers: Bestrijden, uitfaseren, integreren en bos weerbaar maken*. Provincie Gelderland.

Nyssen. (2011). De Amerikaanse vogelkers *(Prunus serotina*) als bosboom.

Marquis, D. A. (1990*). Prunus serotina* Ehrh. black cherry. *Silvics of North America*, *2*, 594-604.

Matthews, S. N., Iverson, L. R., Peters, M. P., Prasad, A. M., & Subburayalu, S. (2014). Assessing and comparing risk to climate changes among forested locations: implications for ecosystem services. *Landscape ecology*, *29*(2), 213-228.

Morin, X., Fahse, L., Jactel, H., Scherer-Lorenzen, M., García-Valdés, R., & Bugmann, H. (2018). Long-term response of forest productivity to climate change is mostly driven by change in tree species composition. *Scientific Reports*, *8*(1), 1-12.

Okx, J. P. (2015). Bodemkundige Informatie Systeem (BIS) Nederland.

Ouyang, Y. (2021). New insights on evapotranspiration and water yield in crop and forest lands under changing climate. *Journal of Hydrology*, *603*, 127192.

Pairon, M., Petitpierre, B., Campbell, M., Guisan, A., Broennimann, O., Baret, P. V., ... & Besnard, G. (2010). Multiple introductions boosted genetic diversity in the invasive range of black cherry (*Prunus serotina*; Rosaceae). *Annals of Botany*, *105*(6), 881-890.

Pan, C., Tajchman, S. J., & Kochenderfer, J. N. (1997). Dendroclimatological analysis of major forest species of the central Appalachians. *Forest Ecology and Management*, *98*(1), 77-87.

Ryan, M. G. (2011). Tree responses to drought. *Tree Physiology*, *31*(3), 237-239.

Rijkswaterstaat. (2018). *Actueel Hoogtebestand 3 (AHN3) | Data Overheid*. Retrieved August 8th 2022 from data.overheid.nl: https://data.overheid.nl/dataset/11513-actueel-hoogtebestand-nederland-3--ahn3-#panel-resources

Thuiller, W., Lavorel, S., Sykes, M. T., & Araújo, M. B. (2006). Using niche-based modelling to assess the impact of climate change on tree functional diversity in Europe. *Diversity and Distributions*, *12*(1), 49-60.

Sevanto, S., Mcdowell, N. G., Dickman, L. T., Pangle, R., & Pockman, W. T. (2014). How do trees die? A test of the hydraulic failure and carbon starvation hypotheses. *Plant, cell & environment*, *37*(1), 153-161.

Van der Maaten-Theunissen, M., Trouillier, M., Schwarz, J., Skiadaresis, G., Thurm, E. A., & van der Maaten, E. (2021). pointRes 2.0: New functions to describe tree resilience. Dendrochronologia, 70, 125899.

Vanhellemont, M., Van der Putten, W. H., & Verheyen, K. (2010). Invasieve exoten in bossen. In *Bosecologie en bosbeheer* (pp. 469-476). Acco.

Wei, T., Simko, V. (2021). R package 'corrplot': Visualization of a Correlation Matrix (Version 0.92). Available from
https://github.com/taiyun/corrplot

Zang, C., and F. Biondi. 2015. treeclim: an R package for the numerical calibration of proxy-climate relationships. *Ecography* 38:431–436.

Zweifel, R., Zimmermann, L., Zeugin, F., & Newbery, D. M. (2006). Intra-annual radial growth and water relations of trees: implications towards a growth mechanism. *Journal of experimental botany*, *57*(6), 1445-1459.

7 Appendix

7.1 Detrended mean chronologies

.

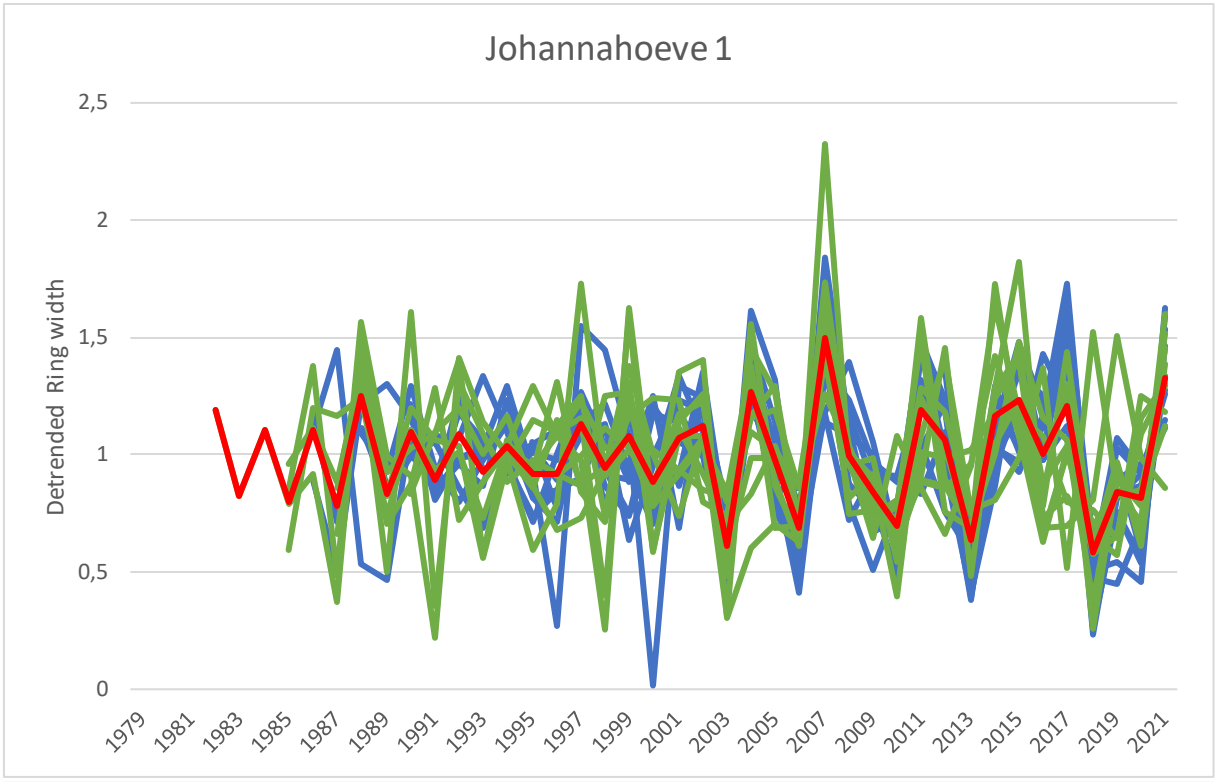

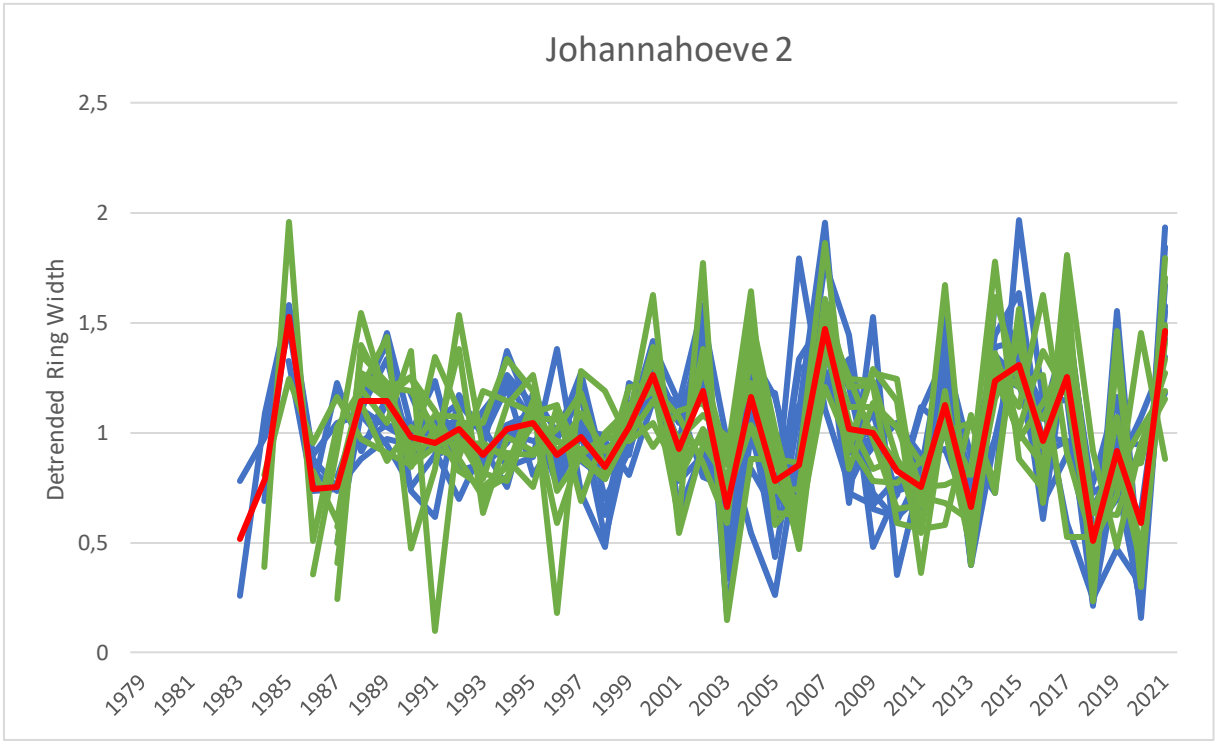

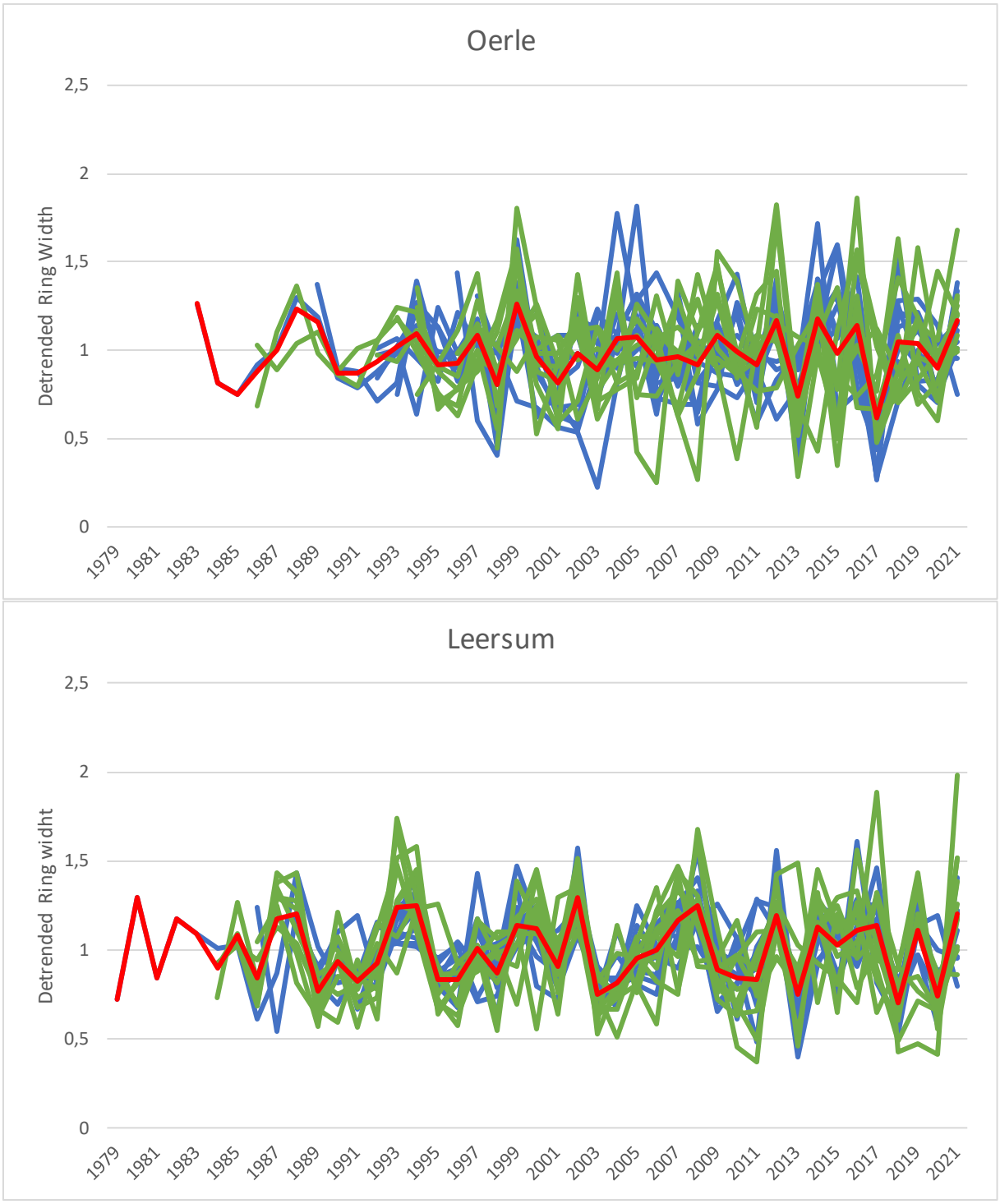

Appendix 1: The ring width chronologies after detrending. Clockwise from top-left: Johannahoeve 1, Johannahoeve 2, Leersum and Oerle.

7.2 Satellite images of study sites

Appendix 2: A satellite image, courtesy of Google Maps (October 2022) of the study stands in Johannahoeve, roughly outlined in red. The bottom outline is Johannahoeve 1. The Top outline is Johannahoeve 2.

Appendix 3: A satellite image, courtesy of Google Maps (October 2022) of the studied stand of Oerle, roughly outlined in red.

Appendix 4: A satellite image, courtesy of Google Maps (October 2022) of the studied forest edge nearby Leersum, roughly outlined in red.

7.3 Comparative figures of Lloret indices

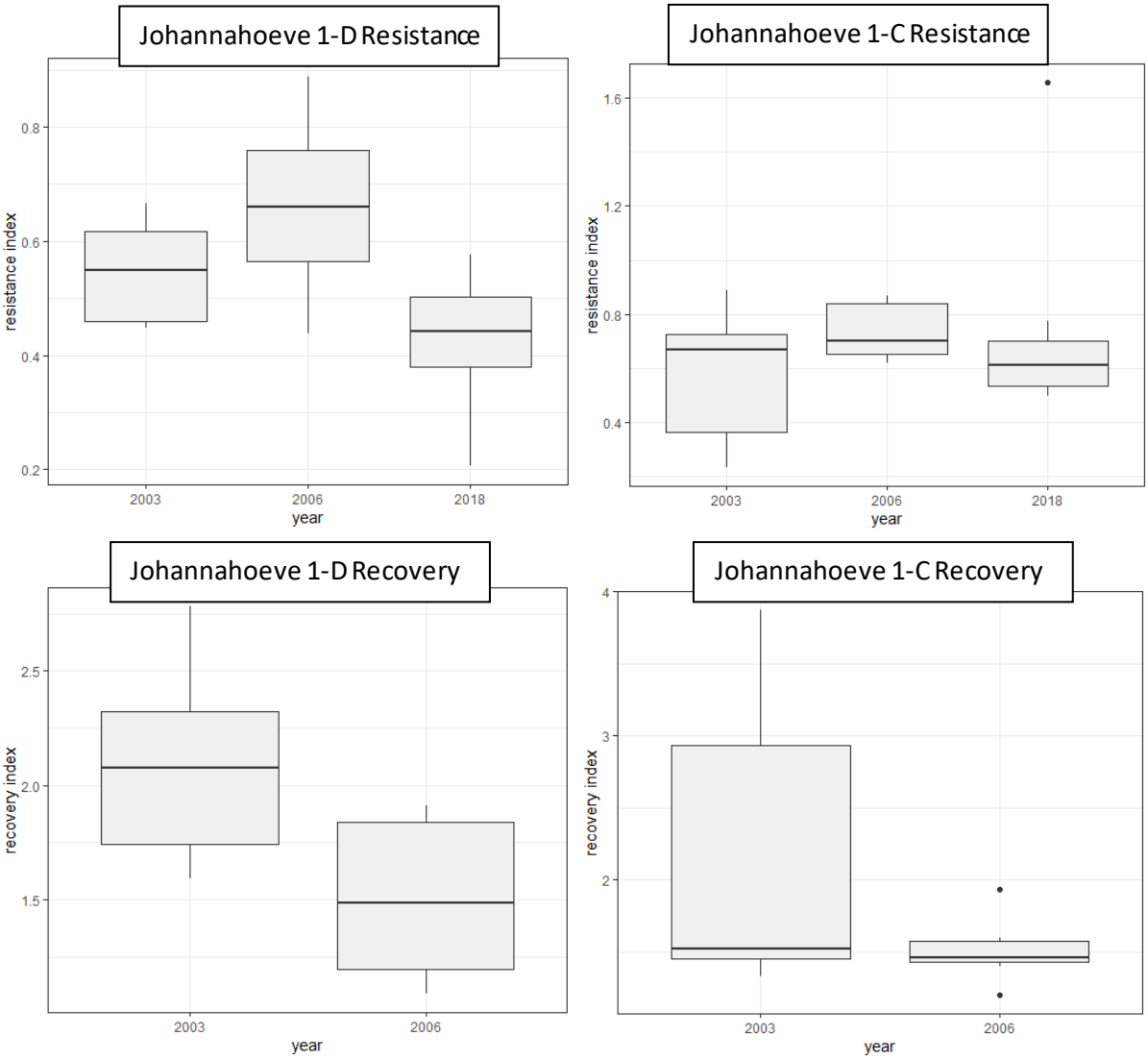

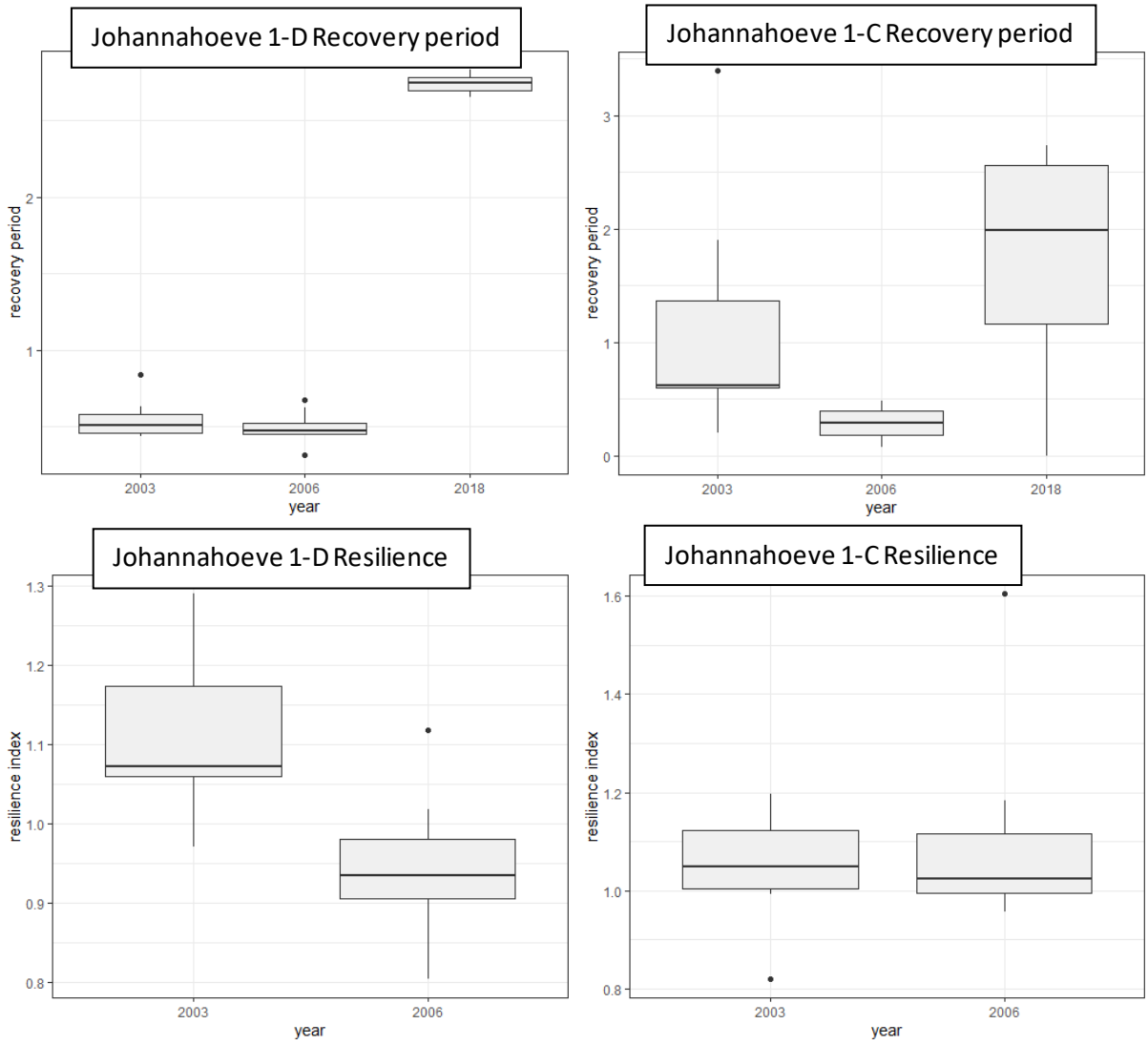

Appendix 5: The boxplots of the Lloret indices of Johannahoeve 1, divided by canopy position compared side-by side. The dominant plots are displayed on the left, whereas the codominant plots are displayed on the right. Note that scales are not equal, but automatically adjusted by pointRes.

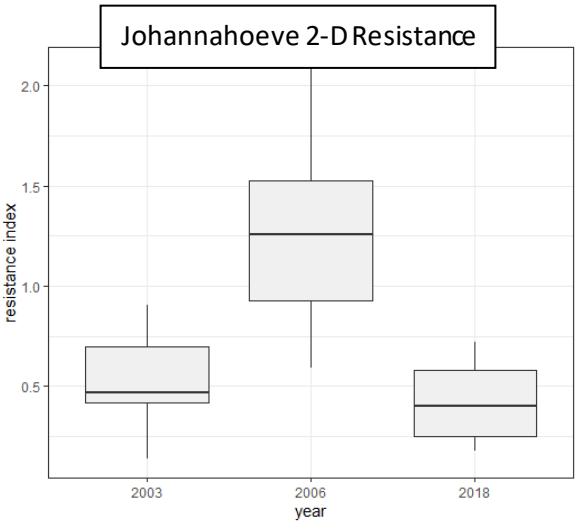
Johannahoeve 2-D Resistance
resistance index
2.0
1.5
1.0
0.5
2003
2006
2018
year

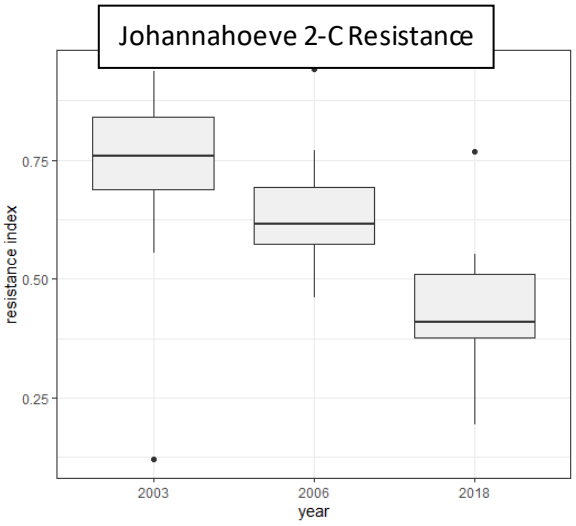
Johannahoeve 2-C Resistance
resistance index
0.75
0.50
0.25
2003
2006
2018
year

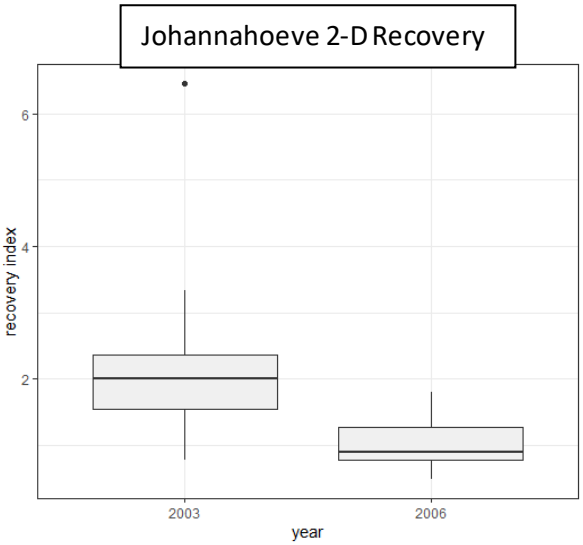
Johannahoeve 2-D Recovery
recovery index
6
4
2
2003
2006
year

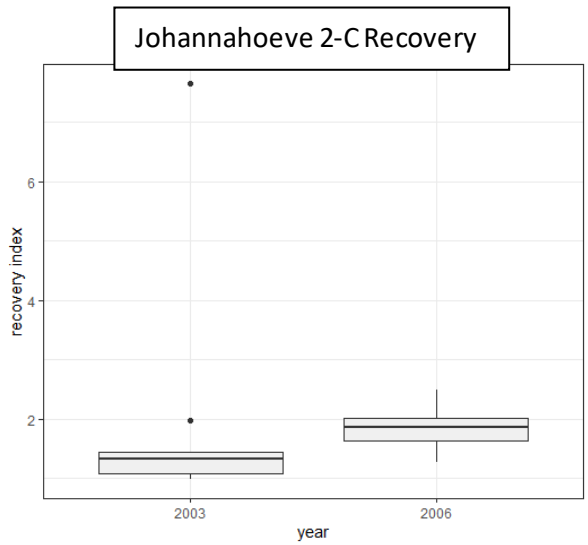
Johannahoeve 2-C Recovery
recovery index
6
4
2
2003
2006
year

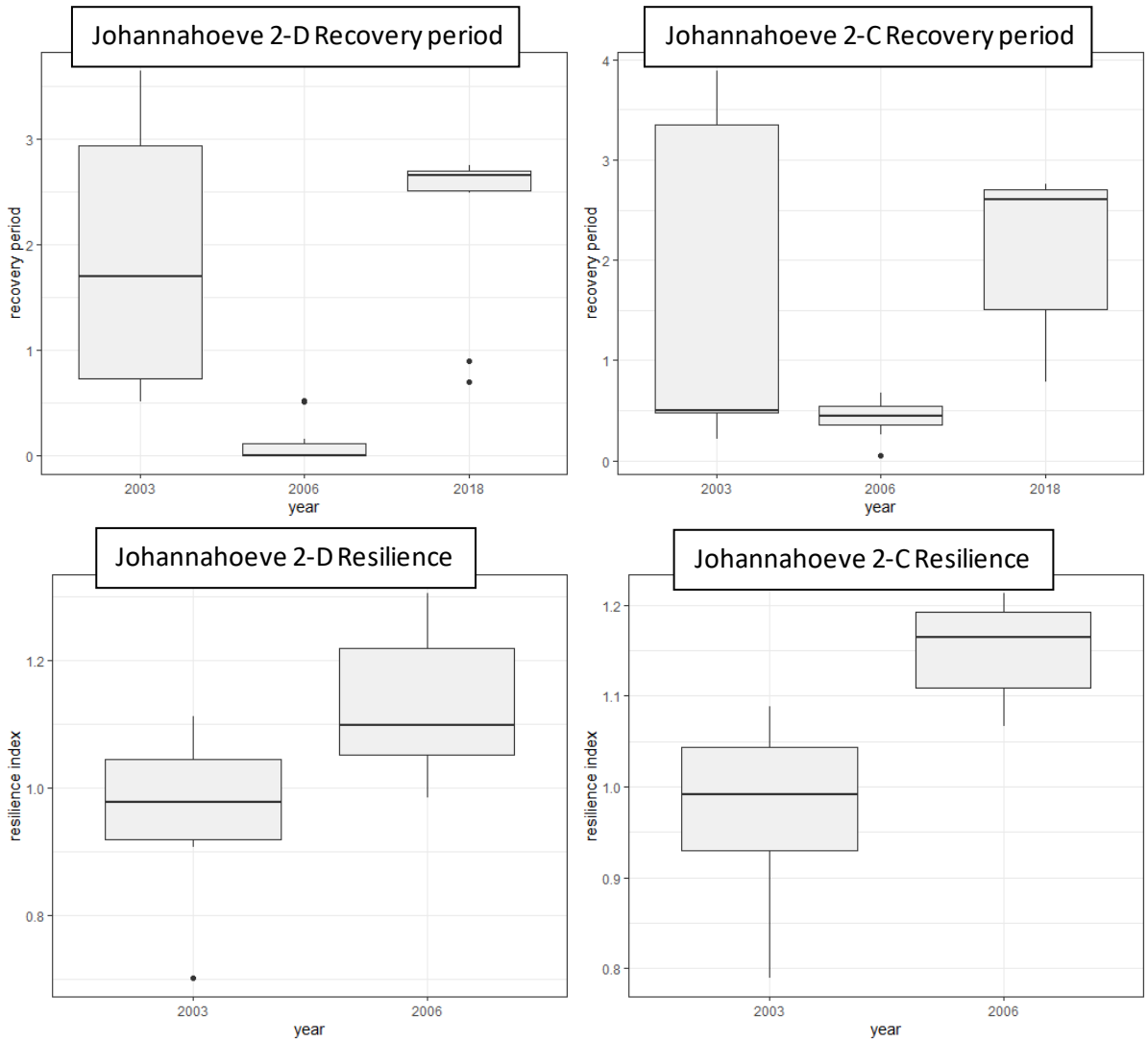

Appendix 6: The boxplots of the Lloret indices of Johannahoeve 2, divided by canopy position compared side-by side. The dominant plots are displayed on the left, whereas the codominant plots are displayed on the right. Note that scales are not equal, but automatically adjusted by pointRes.

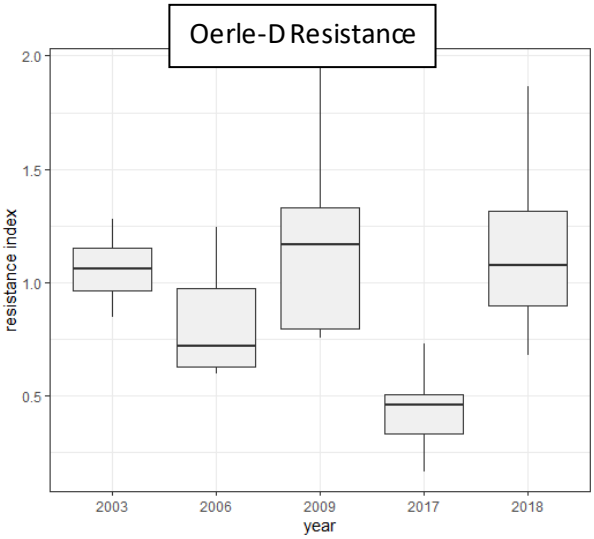
Oerle-D Resistance
resistance index
2.0
1.5
1.0
0.5
2003
2006
2009
2017
2018
year

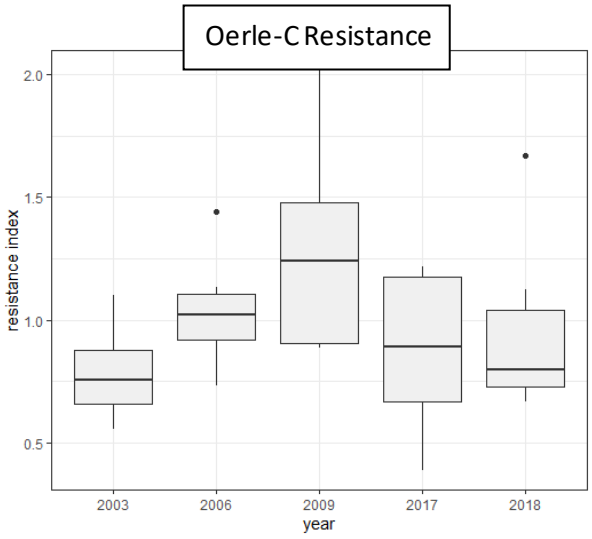
Oerle-C Resistance
resistance index
2.0
1.5
1.0
0.5
2003
2006
2009
2017
2018
year

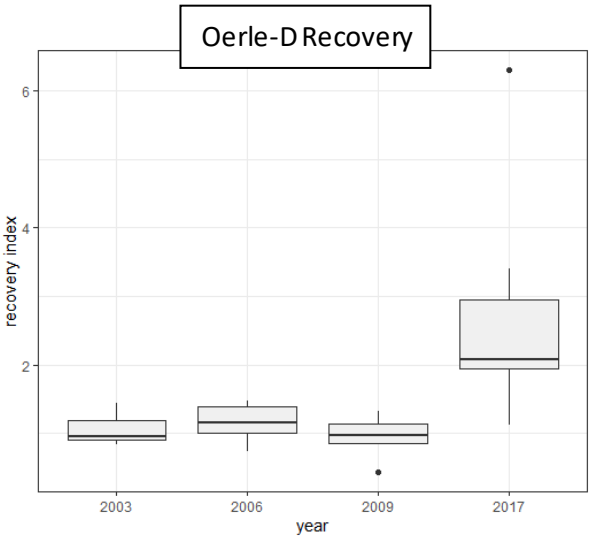
Oerle-D Recovery
recovery index
6
4
2
2003
2006
2009
2017
year

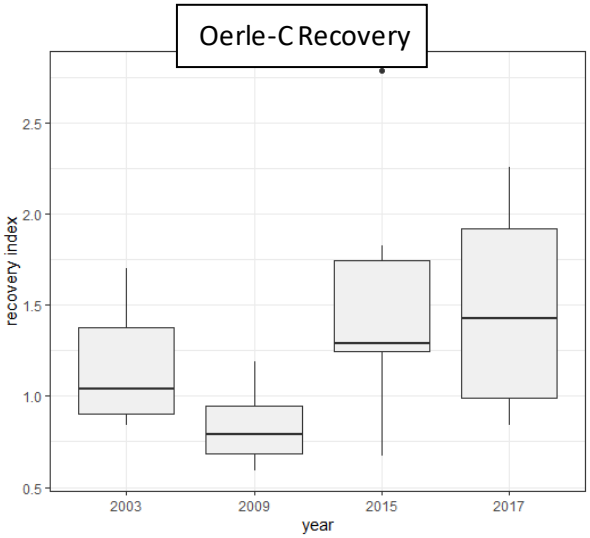
Oerle-C Recovery
recovery index
2.5
2.0
1.5
1.0
0.5
2003
2009
2015
2017
year

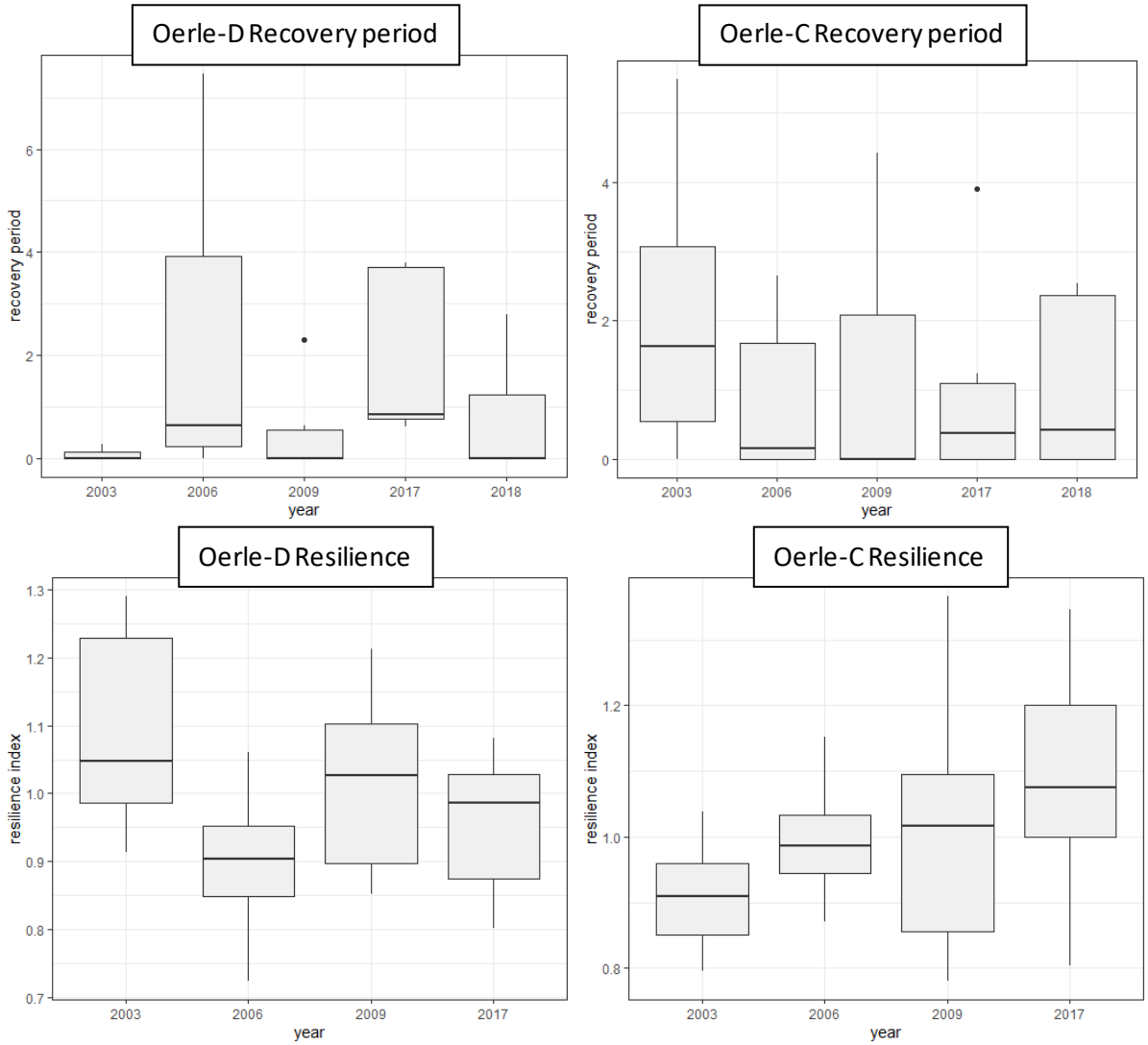

Appendix 7: The boxplots of the Lloret indices of Oerle, divided by canopy position compared side-by side. The dominant plots are displayed on the left, whereas the codominant plots are displayed on the right. Note that scales are not equal, but automatically adjusted by pointRes.

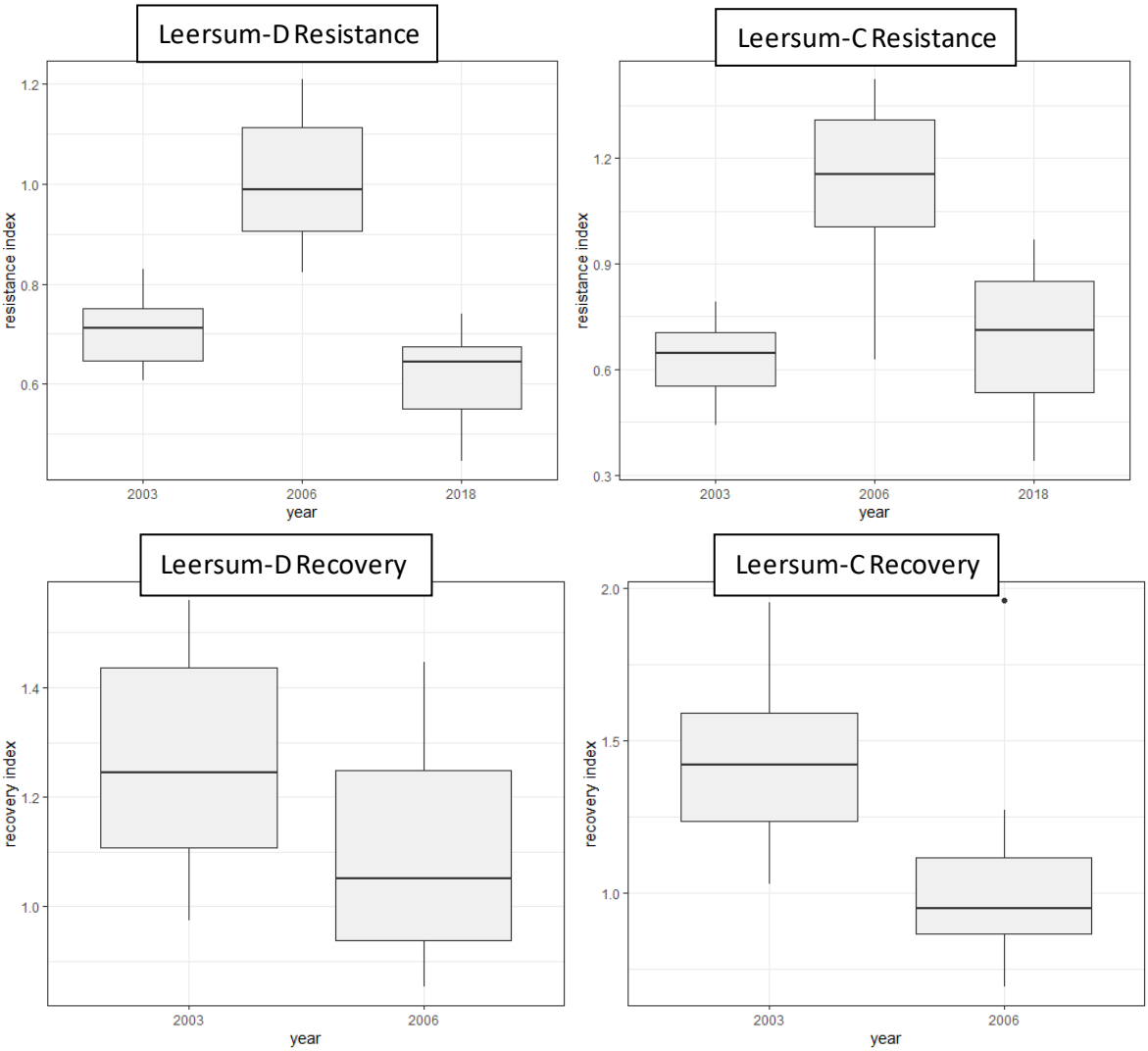
Leersum-D Resistance
resistance index
1.2
1.0
0.8
0.6
2003
2006
2018
year
Leersum-C Resistance
resistance index
1.2
0.9
0.6
0.3
2003
2006
2018
year
Leersum-D Recovery
recovery index
1.4
1.2
1.0
2003
2006
year
Leersum-C Recovery
recovery index
2.0
1.5
1.0
2003
2006
year

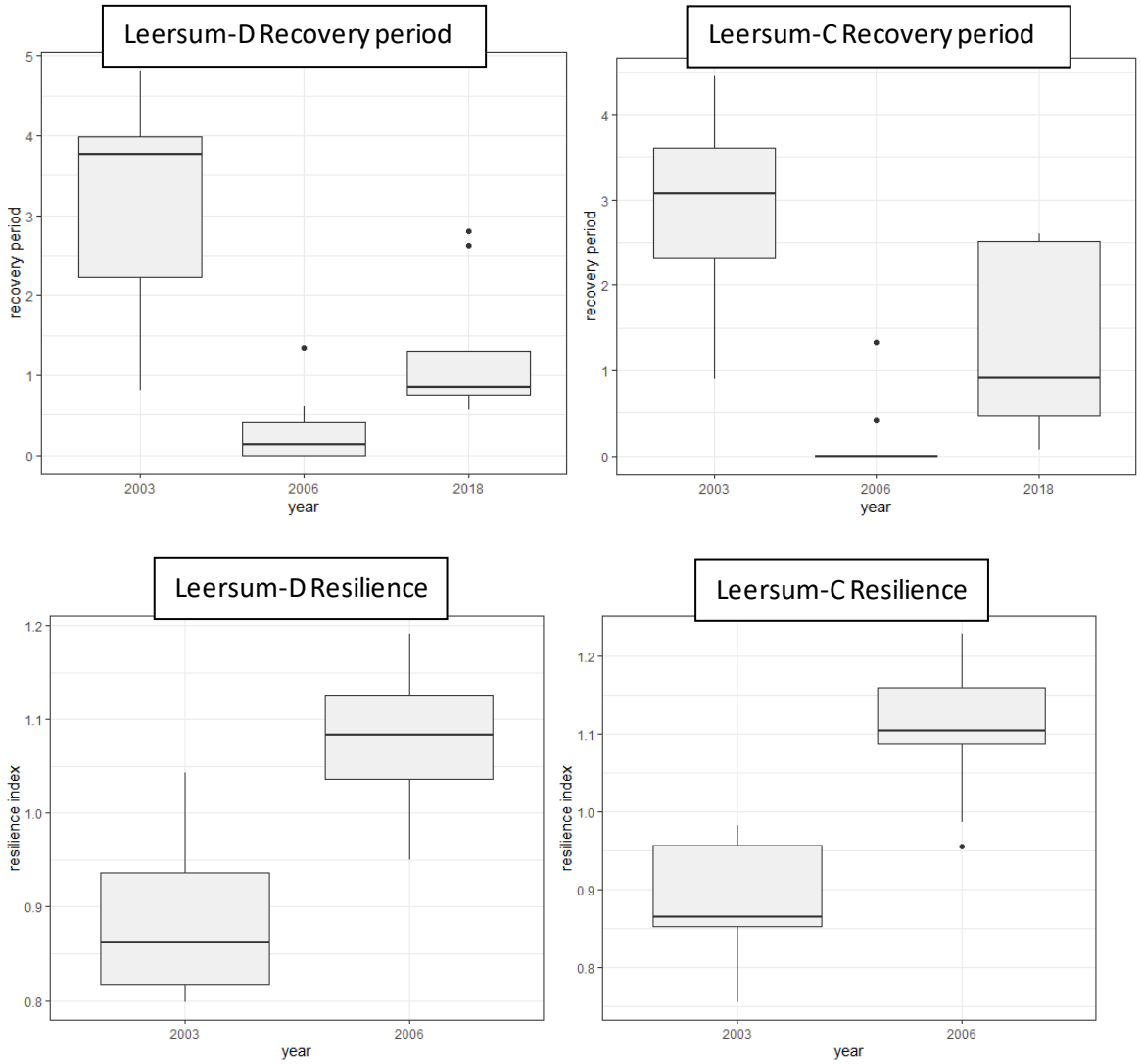

Appendix 8: The boxplots of the Lloret indices of Leersum, divided by canopy position compared side-by side. The dominant plots are displayed on the left, whereas the codominant plots are displayed on the right.

7.4 Tree curve and measurement characteristics

Group	# Years	segments	Flags	Correlation with master	Mean msmt	Max msmt	Std dev	Auto corr	Mean sens	Max value	RBAR	EPS	Interseries Correlation
J1-D	607	63	16	0.614	3.21	9.73	1.383	0.204	0.450	1.20	0.461	0.945	0.6584615
J1-C	609	66	28	0.525	1.52	4.51	0.852	0.419	0.456	3.05			
J2-D	691	74	29	0.568	2.25	7.3	1.149	0.296	0.468	2.10	0.426	0.937	0.6387097
J2-C	713	80	19	0.623	1.45	4.90	0.827	0.453	0.451	2.09			
O-D	556	61	42	0.473	3.92	12.81	1.891	0.441	0.416	1.91	0.149	0.777	0.2243913
O-C	575	62	53	0.454	3.13	17.90	2.228	0.696	0.410	2.83			
L-D	644	69	20	0.606	4.14	10.57	1.532	0.383	0.338	1.61	0.453	0.943	0.6454926
L-C	689	75	30	0.593	2.48	6.53	1.205	0.510	0.391	2.59			

Appendix 8: Descriptive statistics for each group as retrieved from the COFECHA quality control output

The RBAR of all measurements together is 0.248

The Expressed Population Signal value of all measurements together is 0.964

The interseries correlation of all measurements together is 0.482

7.5 Gleichläufigkeit of individual sites/ canopy position groups

Johannahoeve 1D

	J1-03	J1-04	J1-07	J1-08	J1-09	J1-01	J1-02	J1-05	J1-10	J1-06
J1-03	NA	0.8387097	0.8387097	0.7878788	0.7575758	0.7575758	0.7575758	0.8076923	0.7575758	0.7000000
J1-04	NA	NA	0.8064516	0.7419355	0.6451613	0.6451613	0.6451613	0.7307692	0.7096774	0.6000000
J1-07	NA	NA	NA	0.6774194	0.7096774	0.7741935	0.8387097	0.8846154	0.6451613	0.6666667
J1-08	NA	NA	NA	NA	0.6666667	0.6764706	0.6285714	0.6923077	0.6285714	0.7000000
J1-09	NA	NA	NA	NA	NA	0.6969697	0.7575758	0.6923077	0.7575758	0.7000000
J1-01	NA	NA	NA	NA	NA	NA	0.7941176	0.7692308	0.7647059	0.6333333
J1-02	NA	NA	NA	NA	NA	NA	NA	0.8076923	0.6000000	0.6333333
J1-05	NA	NA	NA	NA	NA	NA	NA	NA	0.6923077	0.7307692
J1-10	NA	NA	NA	NA	NA	NA	NA	NA	NA	0.7000000

Johannahoeve 1C

	J1-12	J1-11	J1-13	J1-15	J1-16	J1-17	J1-20	J1-14	J1-18	J1-19
J1-12	NA	0.72	0.6153846	0.6129032	0.6129032	0.5161290	0.6451613	0.6296296	0.6774194	0.7096774
J1-11	NA	NA	0.5200000	0.6800000	0.6000000	0.5600000	0.6800000	0.6800000	0.7600000	0.6400000
J1-13	NA	NA	NA	0.6923077	0.5769231	0.6538462	0.6538462	0.6153846	0.6538462	0.7307692
J1-15	NA	NA	NA	NA	0.5294118	0.6111111	0.6944444	0.7777778	0.7647059	0.8611111
J1-16	NA	NA	NA	NA	NA	0.5882353	0.7352941	0.7037037	0.6470588	0.6176471
J1-17	NA	NA	NA	NA	NA	NA	0.6388889	0.5925926	0.5294118	0.6944444
J1-20	NA	NA	NA	NA	NA	NA	NA	0.7777778	0.8529412	0.7222222
J1-14	NA	NA	NA	NA	NA	NA	NA	NA	0.7037037	0.8148148
J1-18	NA	NA	NA	NA	NA	NA	NA	NA	NA	0.7352941

Johannahoeve 2D

	J2-02	J2-03	J2-04	J2-05	J2-09	J2-10	J2-06	J2-01	J2-07	J2-08
J2-02	NA	0.5757576	0.7575758	0.7027027	0.6129032	0.6470588	0.8108108	0.6285714	0.8055556	0.7647059
J2-03	NA	NA	0.6969697	0.7575758	0.5806452	0.7575758	0.6060606	0.7272727	0.6969697	0.7575758
J2-04	NA	NA	NA	0.6969697	0.7741935	0.7575758	0.7272727	0.8484848	0.8181818	0.6969697
J2-05	NA	NA	NA	NA	0.7419355	0.7647059	0.7368421	0.7142857	0.8333333	0.8235294
J2-09	NA	NA	NA	NA	NA	0.7096774	0.7419355	0.6774194	0.7741935	0.6451613
J2-10	NA	NA	NA	NA	NA	NA	0.7352941	0.7058824	0.7647059	0.7647059
J2-06	NA	NA	NA	NA	NA	NA	NA	0.6571429	0.8888889	0.8529412
J2-01	NA	NA	NA	NA	NA	NA	NA	NA	0.7714286	0.7058824
J2-07	NA	NA	NA	NA	NA	NA	NA	NA	NA	0.8823529

Johannahoeve 2C

	J2-13	J2-11	J2-14	J2-15	J2-16	J2-17	J2-19	J2-20	J2-21	J2-12
J2-13	NA	0.7058824	0.5294118	0.5714286	0.7297297	0.6176471	0.5294118	0.6060606	0.6470588	0.4571429
J2-11	NA	NA	0.7058824	0.7941176	0.7058824	0.6764706	0.5882353	0.7272727	0.8235294	0.7647059
J2-14	NA	NA	NA	0.7352941	0.5882353	0.7352941	0.6470588	0.6666667	0.7058824	0.8235294
J2-15	NA	NA	NA	NA	0.5714286	0.5882353	0.6764706	0.6363636	0.8529412	0.7714286
J2-16	NA	NA	NA	NA	NA	0.5588235	0.5294118	0.5151515	0.5294118	0.5714286
J2-17	NA	NA	NA	NA	NA	NA	0.5588235	0.8181818	0.6764706	0.6764706
J2-19	NA	NA	NA	NA	NA	NA	NA	0.4848485	0.7058824	0.6470588
J2-20	NA	NA	NA	NA	NA	NA	NA	NA	0.6666667	0.6060606
J2-21	NA	NA	NA	NA	NA	NA	NA	NA	NA	0.7647059

Oerle D

	O-09	O-10	O-02	O-06	O-04	O-01	O-03	O-07	O-08	O-05
O-09	NA	0.5357143	0.6250000	0.7857143	0.5862069	0.6666667	0.7241379	0.5862069	0.6250000	0.5600000
O-10	NA	NA	0.7142857	0.6071429	0.8214286	0.6250000	0.5357143	0.5357143	0.6666667	0.6000000
O-02	NA	NA	NA	0.6071429	0.8275862	0.4166667	0.6206897	0.6206897	0.6250000	0.5600000
O-06	NA	NA	NA	NA	0.7142857	0.7500000	0.7142857	0.5000000	0.5416667	0.6400000
O-04	NA	NA	NA	NA	NA	0.5833333	0.6551724	0.6551724	0.5416667	0.7200000
O-01	NA	NA	NA	NA	NA	NA	0.7500000	0.4583333	0.5416667	0.7500000
O-03	NA	NA	NA	NA	NA	NA	NA	0.5862069	0.6250000	0.6400000
O-07	NA	NA	NA	NA	NA	NA	NA	NA	0.5833333	0.6400000
O-08	NA	NA	NA	NA	NA	NA	NA	NA	NA	0.5416667

Oerle C

	O-14	O-15	O-17	O-19	O-13	O-16	O-11	O-12	O-20	O-18
O-14	NA	0.6086957	0.6086957	0.5217391	0.5217391	0.5652174	0.4782609	0.3913043	0.6086957	0.4782609
O-15	NA	NA	0.8518519	0.5185185	0.6296296	0.5555556	0.7037037	0.5600000	0.7037037	0.5185185
O-17	NA	NA	NA	0.6666667	0.6296296	0.6296296	0.7037037	0.5600000	0.7037037	0.6666667
O-19	NA	NA	NA	NA	0.5185185	0.5714286	0.5517241	0.5600000	0.4137931	0.7037037
O-13	NA	NA	NA	NA	NA	0.6296296	0.7777778	0.6400000	0.7037037	0.5925926
O-16	NA	NA	NA	NA	NA	NA	0.6428571	0.4800000	0.6428571	0.5185185
O-11	NA	NA	NA	NA	NA	NA	NA	0.7600000	0.6857143	0.5185185
O-12	NA	NA	NA	NA	NA	NA	NA	NA	0.7200000	0.5600000
O-20	NA	NA	NA	NA	NA	NA	NA	NA	NA	0.5185185

Leersum D

	L-03	L-04	L-05	L-06	L-07	L-08	L-09	L-10	L-01	L-02
L-03	NA	0.7741935	0.7878788	0.7142857	0.6666667	0.6000000	0.7272727	0.7586207	0.8484848	0.7878788
L-04	NA	NA	0.6129032	0.7500000	0.6451613	0.7000000	0.6774194	0.7241379	0.6451613	0.7419355
L-05	NA	NA	NA	0.6428571	0.7575758	0.5666667	0.6969697	0.7586207	0.6969697	0.7575758
L-06	NA	NA	NA	NA	0.6071429	0.6071429	0.6071429	0.6071429	0.7142857	0.7500000
L-07	NA	NA	NA	NA	NA	0.6333333	0.6969697	0.7241379	0.6969697	0.7575758
L-08	NA	NA	NA	NA	NA	NA	0.5333333	0.6206897	0.7000000	0.6333333
L-09	NA	NA	NA	NA	NA	NA	NA	0.8620690	0.6285714	0.6363636
L-10	NA	NA	NA	NA	NA	NA	NA	NA	0.6551724	0.7241379
L-01	NA	NA	NA	NA	NA	NA	NA	NA	NA	0.6363636

Leersum C

	L-11	L-12	L-13	L-14	L-15	L-16	L-17	L-18	L-19	L-20
L-11	NA	0.6969697	0.6060606	0.6129032	0.6969697	0.5151515	0.7575758	0.7575758	0.7272727	0.6060606
L-12	NA	NA	0.6764706	0.8064516	0.6571429	0.5714286	0.6666667	0.7297297	0.8648649	0.7500000
L-13	NA	NA	NA	0.5806452	0.6764706	0.5294118	0.6764706	0.6176471	0.6470588	0.7058824
L-14	NA	NA	NA	NA	0.7419355	0.6451613	0.6774194	0.7741935	0.7096774	0.7741935
L-15	NA	NA	NA	NA	NA	0.5714286	0.7142857	0.6571429	0.6285714	0.8000000
L-16	NA	NA	NA	NA	NA	NA	0.5142857	0.5714286	0.5428571	0.7142857
L-17	NA	NA	NA	NA	NA	NA	NA	0.7777778	0.6944444	0.7500000
L-18	NA	NA	NA	NA	NA	NA	NA	NA	0.7567568	0.6388889
L-19	NA	NA	NA	NA	NA	NA	NA	NA	NA	0.7222222